Title
A NUMERICAL STUDY OF THE REGGE PARAMETERS IN POTENTIAL SCATTERING

Author
Ahmadzadeh, Akbar.

Publication Date
1964-10-30

UCRL-11096

University of California

Ernest O. Lawrence Radiation Laboratory

A NUMERICAL STUDY OF THE REGGE PARAMETERS IN POTENTIAL SCATTERING

Berkeley, California

DISCLAIMER

UCRL-11096
UC-34 Physics
TID-4500 (19th Ed.)

UNIVERSITY OF CALIFORNIA

Lawrence Radiation Laboratory
Berkeley, California

AEC Contract No. W-7405-eng-48

A NUMERICAL STUDY OF THE REGGE PARAMETERS IN POTENTIAL SCATTERING

Akbar Ahmadzadeh
(Thesis)

October 30, 1963

Printed in USA. Price $2.75. Available from the
Office of Technical Services
U. S. Department of Commerce
Washington 25, D.C.

CONTENTS

Abstract		v
I.	Introduction	1
II.	Established Properties of the Regge Parameters:	
	A. Reality and Analyticity	8
	B. Threshold and Asymptotic Behavior	13
III.	Dispersion Relations of the Regge Parameters	18
IV.	Relativistic-Looking Trajectories	22
V.	Modification of the Khuri Series	24
VI.	Regge Parameters and the Partial-Wave S Matrix for a Singe Yukawa Potential	38
Acknowledgments		40
References		41

A NUMERICAL STUDY OF THE REGGE PARAMETERS IN POTENTIAL SCATTERING

Akbar Ahmadzadeh

Lawrence Radiation Laboratory
University of California
Berkeley, California

October 30, 1963

ABSTRACT

The threshold and asymptotic behavior of the Regge parameters are discussed and some examples given. It is shown that the position and residue of the first trajectory of a single attractive Yukawa potential satisfy the dispersion relation expected when there are no intersections with other trajectories. An example is given of a repulsive Yukawa potential where the position of the pole does not satisfy such a dispersion relation. The Regge parameters for the first few trajectories of a single attractive Yukawa potential are given in the form of figures. Examples are given of a simple superposition of attractive and repulsive Yukawa potentials for which the trajectories are similar to the relativistic case.

By modifying the background integral, the Regge formula is rewritten to include the Born term and to make the background integral less significant. The Khuri series for the partial-wave amplitude has been modified to explicitly single out the Born term. In deriving this modified series it is shown that one needs weaker asymptotic conditions on the partial-wave amplitude than those used by Khuri. The convergence of this series has been investigated for the case of a single Yukawa potential. It is found that the modified series converges considerably faster than the Khuri series.

I. INTRODUCTION

The notion of complex angular momenta was first introduced by Sommerfeld in connection with the problem of scattering of radio waves by the earth,[1] and the idea was later utilized by Regge to prove the Mandelstam representation in potential scattering.[2-4] The point is that, under certain conditions on the potential, the partial-wave series can be converted into a sum of contributions from poles in the complex angular-momentum plane plus a background integral. The position, in the angular-momentum plane, of these so-called Regge poles changes as the energy is varied, and the pole farthest to the right determines the asymptotic behavior of the scattering amplitude for fixed energy and large (nonphysical) momentum transfers. The importance of Regge poles in the relativistic case was first realized in connection with this asymptotic behavior and the number of subtractions[5] in the Mandelstam representation. It was later shown by Froissart[6] and Gribov[7] that, in the relativistic case and based on the Mandelstam representation, the analytic continuation in complex angular momentum can be uniquely defined.

Aside from the clarification given to the asymptotic behavior of scattering amplitudes, there are certain other aspects of the Regge-pole idea that are particularly appealing in the theory of strong interactions. We mention two of these aspects.

A. Regge Poles and Composite Particles

Ever since Yukawa's theory was advanced, it has been known that the range of the strong interaction forces is of the same order of magnitude as the size of the particles involved, so that when two

particles are close enough to interact, their combined size is about the same as that of one particle. In contrast to the strong interactions, the electromagnetic forces allow for bound states considerably larger than the size of each constituent. For example, the hydrogen atom is larger than a proton or an electron by several orders of magnitude. Through collision with another particle, the hydrogen atom can be broken into an electron and a proton. One is thus led to consider the hydrogen atom as composite, and the proton and the electron as elementary particles. Let us now consider a pionization process, $p + x \rightarrow p + \pi^{o} + x$. By considering this process to be analogous with the above ionization process, one is then led to the absurd conclusion that the proton before the collision is composite, and the proton after the collision is elementary! But as long as one does not introduce the "elementary" notion, the proton can always be considered as a composite state of any number of particles which, together, have the same quantum numbers as the proton.

Only by analogy with electrodynamics and in connection with Lagrangian renormalization was the idea of "bare" and "dressed" protons introduced. This concept then led to consideration of a physical proton as a "bare" proton with a cloud of pions (as well as of baryons, antibaryons, etc.) surrounding it. In the S matrix theory of strong interactions,[8] any one particle can be considered as a bound state of any number of particles that combine to give the same quantum numbers. In particular, the proton can be considered as predominantly a bound state of a proton and a pion; this pion in turn can be considered as a bound state of two other particles (e.g., $\Sigma + \bar{\Sigma}$), and so on.

Now, for example, the $I = 1/2$ even-parity spin-5/2 resonance state of the pion-nucleon system has the same quantum numbers as the proton, the only difference being the mass and the angular momentum. Once the proton is considered as a bound state, the Regge-pole hypothesis is a natural way of putting such a resonance and bound state on an equal footing--in direct analogy with the potential case.

B. The Pomeranchuk Trajectory

To express the hypothesis of maximal strength of strong interactions (i.e., saturation of unitarity) and (or) the Pomeranchuk theorem (constancy of the total cross sections at very high energies), Chew and Frautschi[9] and, independently, Gribov[10] found it natural to hypothesize the existence of the Pomeranchuk trajectory, the applications of which have already shown qualitative success in high-energy diffraction scattering. It led, for example, to the successful prediction of the f^o particle.[11]

From the above and similar arguments, the Regge-pole hypothesis is expected to play an important role in the theory of strong interactions. Furthermore, a considerable degree of similarity exists between the potential and the relativistic cases. Because of this similarity, a study of Regge poles in potential scattering appears interesting.

For certain potentials--among these the Coulomb[12] and the square-well[13] potential--the problem can be solved analytically, but each of these potentials has its shortcomings. The Coulomb case produces an infinite number of bound states and no resonances. For the square-well potential, there are spurious singularities in momentum transfer, and the trajectories increase indefinitely. For

a superposition of Yukawa potentials, certain general theorems have been proved, but a solution in closed form is not possible. Nevertheless, the Yukawa potential is the most interesting and useful to study in detail. Restricting ourselves to a single Yukawa potential, we have a well-defined problem without the above-mentioned shortcomings of the Coulomb and square-well potentials.

By direct integration of the Schrödinger equation, we have calculated the Regge parameters for the first few trajectories. The numerical calculations were carried out with the help of the IBM 7094 computer of the Lawrence Radiation Laboratory. The program used is a modified version of the FORTRAN TREGGE program written by Burke and Tate.[14] Once the Regge parameters are calculated, we examine certain properties attributed to them. Let us now explain the type of questions to which we shall apply our numerical results.

The partial-wave amplitude for a superposition of Yukawa potentials

$$V(r) = \int_{m_1}^{\infty} \sigma(\mu) \frac{e^{-\mu r}}{r} d\mu \qquad (1)$$

has been studied by Regge et al.[2-4] They have shown that the amplitude $A(\ell,s)$ (where ℓ is the angular momentum, and $s = k^2$ is the energy) can be continued in the complex ℓ plane and, in the $\mathrm{Re}\ \ell > -1/2$ region, $A(\ell,s)$ is meromorphic in ℓ. In the complex s-plane, $A(\ell,s)$ has a right-hand cut from $s = 0$ to ∞ and a left-hand cut from $s = -m_1^2/4$ to $s = -\infty$, where m_1 is the lower limit of the integral in Eq. (1). They have also shown that for $s < 0$ the $\ell = \alpha_i(s)$ poles of $A(\ell,s)$ lie on the real ℓ axis.

Throughout this paper, we are concerned only with the subclass of potentials (1) that can be expanded in a power series,

$$V(r) = \sum_{n=0}^{\infty} C_n r^{n-1} .$$

It follows from the proof by Mandelstam[15] and Froissart[16] that $A(\ell,s)$ is also meromorphic in the left-half ℓ plane. On the other hand, the proof by Regge et al.[4] that $\alpha_i(s)$ are real for $s < 0$ has no obvious generalization to include the region $\mathrm{Re}\ \ell < -1/2$, since this proof rests on the integrability of the wave function.

A third property of $A(\ell,s)$, shown by Zemach,[17] is that $A(\ell,s)$ has no multiple poles in ℓ for $\mathrm{Re}\ \ell > -1/2$. This proof again rests on the integrability of the wave function and has no obvious generalization in the left-half plane; consequently for $\mathrm{Re}\ \ell < -1/2$ it is not known under what conditions multiple poles can be excluded.

Based on the meromorphy of $A(\ell,s)$, reality of $\alpha_i(s)$, and absence of the multiple poles, Taylor was able to show that the Regge parameters $\alpha_i(s)$ and $b_i(s)$ [where $b_i(s)$ are the reduced residues] are real analytic functions of s with only the right-hand cut.[18] However, from the Coulomb limit[15] it follows that for sufficiently large values of $|s|$, all trajectories lie in the region $\mathrm{Re}\ \ell < -1/2$. Thus, to our knowledge there is no proof that any given trajectory is free of anomalous branch points. Nevertheless, our numerical study shows that the leading trajectory, $\alpha_1(s)$, for a single attractive Yukawa potential is indeed real analytic in s with only a right-hand cut. That multiple poles in $A(\ell,s)$ and corresponding anomalous branch points of $\alpha_i(s)$ in s for the region $\mathrm{Re}\ \ell < -1/2$ do occur

in general is shown by the example of a single repulsive Yukawa potential.

The threshold behavior of the Regge parameters in the relativistic case of two spinless particles has been investigated by Barut and Zwanziger,[19] starting from the Mandelstam representation. As they have pointed out, the same threshold behavior holds in the nonrelativistic case with potentials (1). Starting from a formula by Regge et al.,[4] we obtain the threshold behavior of all Regge parameters for both the right- and the left-half planes.

For high enough energies, one needs consider the behavior of the potential near the origin only. Thus, in potential (1), if the limit of $rV(r)$ is finite as r aproaches zero, then the Regge parameters at high energies approach the Coulomb case, and in this way one can determine the asymptotic behavior of the poles and residues. In particular, one finds that the reduced residues need subtractions in their dispersion relations.

Regge trajectories for certain cases of a single Yukawa potential already exist in the literature.[20,21] One peculiarity of single Yukawa potentials is that $\mathrm{Re}\ \alpha(s)$ increases very little above the threshold and the trajectory moves quickly towards the left. This is in contrast to the relativistic ase (e.g., the Pomeranchuk trajectory) in which $\mathrm{Re}\ \alpha$ increases considerably from the threshold value. We have attempted to find a simple sum of attractive and repulsive Yukawa potentials which produces relativistic looking trajectories.

The question has often been raised: Is it possible to write the scattering amplitude solely in terms of Regge parameters, thus eliminating the background integral? A major step in this direction

has been taken by Khuri.[22] Based on a rather restrictive assumption concerning the asymptotic behavior of $A(\ell,s)$ for large $|\ell|$, Khuri has found an extension of Regge's formula in which the background integral is entirely removed.[22] He has also proposed a series representation of the partial-wave amplitude in terms of the Regge parameters. We examine the rate of convergence of the Khuri series for a single Yukawa potential, and show that, even if the series is mathematically convergent, it is not useful at high energies. We also modify the series starting from somewhat weaker assumptions and examine the rate of convergence of the modified series.

In the following section we give a short review of certain results of Regge et al.[2,3,4] and Taylor.[18] We also give the threshold and asymptotic behavior of the Regge parameters. Section III deals with the dispersion relations satisfied by the Regge parameters. In Section IV we discuss a simple superposition of Yukawa potentials which produce relativistic-looking trajectories. Khuri's extension of Regge's formula is treated in Section V. Finally, in Section VI we give the Regge parameters for several trajectories and also give the S matrix for the first three partial waves.

II. ESTABLISHED PROPERTIES OF THE REGGE PARAMETERS

A. Reality and Analyticity

In this section, for the sake of completeness, we review briefly certain results of Regge et al.[2,3,4] and Taylor[18] that are of interest to us in the subsequent sections. No attempt has been made to make the arguments rigorous; we only give plausibility arguments.

The radial Schrödinger equation

$$\frac{d^2\psi}{dr^2} + \left[k^2 - V(r) - \frac{\ell(\ell+1)}{r^2}\right]\psi = 0 \tag{2}$$

together with the boundary conditions near the origin

$$\psi \sim r^{\ell+1} \tag{3}$$

defines the analytic continuation of the physical scattering solution. Asymptotically, this solution is of the form

$$\psi(r) \underset{r\to\infty}{\sim} \frac{f(\ell,k)e^{ikr} - f(\ell,-k)e^{-ikr}}{2ik} \tag{4}$$

where $f(\ell,k)$ and $f(\ell,-k)$ are the so-called Jost functions. In terms of the Jost functions the S matrix is defined as

$$S(\ell,k) = \frac{f(\ell,k)}{f(\ell,-k)}e^{i\pi\ell} \quad . \tag{5}$$

For the class of potentials (1), Bottino et al.[4] have shown that $f(\ell,k)$ is holomorphic in the ℓ plane for $\mathrm{Re}\,\ell > -1/2$, and in the k plane it has a cut on the positive imaginary axis from $k = im_1/2$ to $k = i\infty$ and a kinematic branch point at $k = 0$. Similarly, $f(\ell,-k)$ is analytic for positive imaginary k. Furthermore, it turns out that $S(\ell,k)$ can be continued in the gap

from $k = 0$ to $k = im_1/2$ and also that

$$f^*(\ell,k) = f(\ell^*, k^* e^{-i\pi}) . \tag{6}$$

Thus $f(\ell,k)$ is real for real ℓ and negative imaginary k and $f(\ell, -k)$ is real for real ℓ and positive imaginary k .

The poles in $\ell = \alpha(k)$ of the S matrix are then the implicit solutions of the equation

$$f(\ell, -k) = 0 . \tag{7}$$

From Eq. (7), we have

$$f(\ell, -k) = \left[\frac{\partial f(\ell, -k)}{\partial \ell}\right]_{\ell=\alpha(k)} \left[\ell - \alpha(k)\right] + \frac{1}{2}\left[\frac{\partial^2 f(\ell, -k)}{\partial \ell^2}\right]_{\ell=\alpha(k)} \left[\ell - \alpha)k)\right]^2 + \cdots = 0 . \tag{8}$$

If the first derivative does not vanish, we have

$$\ell - \alpha(k) \simeq \frac{f(\ell, -k)}{\left[\frac{\partial f(\ell, -k)}{\partial \ell}\right]_{\ell=\alpha(k)}} , \quad \text{for} \quad \ell \simeq \alpha(k) . \tag{9}$$

Now since $f(\ell, -k)$ and consequently $\partial f(\ell,k)/\partial \ell$ are analytic in k , then $\alpha(k)$ is also analytic in the upper half k plane. Then in the k^2 plane, $\alpha(k^2)$ has only the right-hand cut. Furthermore, if $\alpha(k^2)$ is real for $k^2 < 0$, then $\alpha(k^2)$ is a real analytic function.

In the k^2 plane we denote $f(\ell,k)$ by $f_+(\ell,k^2)$ and $f(\ell, -k)$ by $f_-(\ell,k^2)$. It turns out that whereas $f_+(\ell,k^2)$ has a left-hand cut in k^2, $f_+[\alpha(k^2), k^2]$ does not.[18] Defining the modified residue as

$$B(k^2) = \frac{f_+(\alpha(k^2), k^2)}{\left\{\dfrac{\partial f_-[\alpha(k^2), k^2)]}{\partial \ell}\right\}} , \tag{10}$$

$B(k^2)$ has only a right-hand cut in k^2. It is also real for $k^2 < 0$, as can be seen from Eqs. (2), (3), and (4), which are all real. The residue of the S matrix,

$$\beta(k^2) = B(k^2) \exp[i \pi \alpha(k^2)] , \tag{11}$$

is also analytic with only the right-hand cut. However, $\beta(k^2)$ is not real, because of the factor $\exp[i \pi \alpha(k^2)]$. The reduced residue, defined as

$$b(k^2) = \frac{\beta(k^2)}{2i(k^2)^{\alpha(k^2)+\frac{1}{2}}} = \frac{B(k^2)}{2ik(-k^2)^{\alpha(k^2)}} , \tag{12}$$

also turns out to be a real analytic function. We wish to emphasize that the reality and analyticity properties of the Regge parameters mentioned above are rigorously valid for the class of potentials (1) in the right-half ℓ plane. In the above arguments it has been assumed that (a) the partial-wave S matrix is meromorphic in ℓ, (b) no multiple poles of $S(\ell,k)$ occur, and (c) $\alpha(k^2)$ is real for $k^2 < 0$. These conditions have been shown to hold for the region $\mathrm{Re}\ \ell > -\frac{1}{2}$.

As already mentioned, at high enough energies all trajectories approach their Coulomb limit and finally end at negative integers as $|k^2| \to \infty$. Consequently, no trajectory lies entirely to the right of $\mathrm{Re}\ \ell = -\frac{1}{2}$. Mandelstam[15] and Froissart[16] have shown that the amplitude is also meromorphic in ℓ for $\mathrm{Re}\ \ell < -\frac{1}{2}$. On the other hand, both the proof of Bottino et al.[4] that $\alpha(k^2)$ is real for $k^2 < 0$ and Zemach's[17] proof that multiple poles do not occur rest on the integrability of the wave function and have no obvious generalizations in the left-half plane. It is not known under what conditions multiple poles in the region $\mathrm{Re}\ \ell < -\frac{1}{2}$ do not occur. We later give an example of a single repulsive Yukawa potential in which $\alpha(k^2)$ is complex below the threshold as a consequence of two trajectories in the complex angular-momentum plane intersecting at the same energy.

It has been shown by Bottino et al. that[4]

$$Z(\ell,k) \equiv -ik^{2\ell+1}\ \frac{S(\ell,k) - \exp[2i\pi(\ell + \frac{1}{2})]}{S(\ell,k) - 1} \tag{13}$$

is continuous in the gap $G' = \{\, k \mid k = i\,\eta, \quad |\eta| < m_1/2 \,\}$, and that

$$Z(\ell,k) = Z(\ell,\ k\ e^{\pm i\pi}) \tag{14}$$

and also

$$S^*(\ell,k) = S^{-1}(\ell^*,\ k^*\ e^{-i\pi})\ . \tag{15}$$

Now let us consider

$$Y(\ell,k) = -i\, Z(\ell,k) \exp[-i\pi(\ell + \tfrac{1}{2})]$$

$$= \frac{k^{2\ell+1} \exp[-i(\ell + \frac{1}{2})] \left\{ \exp[2i\pi(\ell + \frac{1}{2})] - S(\ell,k) \right\}}{S(\ell,k) - 1} \tag{16}$$

$$= Y(\ell, k\ e^{\pm i\pi}) \ .$$

It follows from (15) and (16) that, for k in the gap G and for real ℓ, $Y(\ell,k)$ is real and $Y(\ell,k^2)$ is a real analytic function of ℓ and k^2 with only a left-hand cut in k^2 starting at $k^2 = -m_1^2/4$. In terms of $Y(\ell,k)$, the S matrix can be written as

$$S(\ell,k) = \frac{Y(\ell,k) + k^{2\ell+1} \exp[i\pi(\ell + \frac{1}{2})]}{Y(\ell,k) + k^{2\ell+1} \exp[-i\pi(\ell + \frac{1}{2})]} \ . \tag{17}$$

The poles of the S matrix are the solutions $\ell = \alpha(k)$ of

$$Y(\ell,k) + k^{2\ell+1} \exp[-i\pi(\ell + \tfrac{1}{2})] = 0 \ , \tag{18}$$

which is the nonrelativistic analogue of Barut and Zwanziger's formula.[19] Near a pole we have

$$S(\ell,k) \simeq \frac{2\, i\, k^{2\alpha+1} \sin \pi(\alpha + \frac{1}{2})}{\left\{ \frac{\partial Y(\ell=\alpha(k),\, k)}{\partial \ell} + 2\, \ell n(k\, e^{-i\pi/2}) k^{2\alpha+1} \exp[-i\pi(\alpha+\frac{1}{2})] \right\} [\ell - \alpha(k)]}, \tag{19}$$

and it follows from Eq. (11) that $\partial Y[\ell=\alpha(k^2),\, k^2]/\partial\ell$ has only a right-hand cut in k^2. We shall use these results in connection with the threshold behavior.

B. Threshold and Asymptotic Behavior

The threshold behavior of the residues for the left-half plane has not been given so far. However, they follow easily from Barut and Zwanziger's expansion,[19] and here for the sake of completeness we give a full set of threshold behaviors.

For $\mathrm{Re}\ \ell > -\frac{1}{2}$ and near the threshold, since $Y(\ell,k)$ is even in k, we have

$$Y_\ell(\alpha - \alpha_0) + s\, Y_s + s^{\alpha+\frac{1}{2}} \exp[-i\pi(\alpha + \tfrac{1}{2})] + O(s^2) = 0 , \tag{20}$$

where $s = k^2$, $Y_\ell = \dfrac{\partial Y(\ell = \alpha_0,\ s = 0)}{\partial \ell}$, $Y_s = \dfrac{\partial Y(\ell = \alpha_0,\ s = 0)}{\partial s}$,

and $\alpha_0 = \alpha(s = 0)$. Therefore, we have

$$\alpha = \alpha_0 - Y_\ell^{-1} \left\{ sY_s + s^{\alpha_0 + \frac{1}{2}} \exp[-i\pi(\alpha_0 + \tfrac{1}{2})] \right\} + O(s^2) \tag{21}$$

and

$$\left.\begin{aligned}
&\mathrm{Re}\ \alpha = \alpha_0 - Y_\ell^{-1}\, s^{\alpha_0+\frac{1}{2}} \cos \pi(\alpha_0 + \tfrac{1}{2}) + O(s) , && s > 0 \\
&\mathrm{Re}\ \alpha = \alpha_0 - Y_\ell^{-1}(-s)^{\alpha_0+\frac{1}{2}} + O(s) , && s < 0 \\
&\mathrm{Im}\ \alpha = Y_\ell^{-1}\, s^{\alpha_0+\frac{1}{2}} \sin \pi(\alpha_0 + \tfrac{1}{2}) , && s > 0 \\
&\mathrm{Im}\ \alpha = 0 , && s < 0
\end{aligned}\right\} \text{for } \alpha_0 > -\tfrac{1}{2} . \tag{22}$$

For $\mathrm{Re}\ \ell > -\frac{1}{2}$ and near $s = 0$, it follows from Eq. (19) that

$$\beta(s) \simeq 2i\, Y_\ell^{-1}\, s^{\alpha_0+\frac{1}{2}} \sin \pi(\alpha_0 + \tfrac{1}{2}) , \tag{23}$$

$$B(s) \simeq -2\, Y_\ell^{-1}\, s^{\alpha_0+\frac{1}{2}} \sin \pi(\alpha_0 + \tfrac{1}{2}) \exp[-i\pi(\alpha_0 + \tfrac{1}{2})] \tag{24}$$

and

$$b(s) \simeq Y_\ell^{-1} \sin \pi(\alpha_0 + \tfrac{1}{2}) \, . \tag{25}$$

Therefore we have

$$\left.\begin{aligned} \text{Re } B(s) &\simeq -Y_\ell^{-1} \, s^{\alpha_0+\frac{1}{2}} \sin \pi(2\alpha_0 + 1) \, , && s > 0 \\ \text{Re } B(s) &\simeq -2Y_\ell^{-1} \, (-s)^{\alpha_0+\frac{1}{2}} \sin \pi(\alpha_0 + \tfrac{1}{2}) \, , && s < 0 \\ \text{Im } B(s) &\simeq 2Y_\ell^{-1} \sin^2 \pi(\alpha_0 + \tfrac{1}{2}) \, s^{\alpha_0+\frac{1}{2}} \, , && s > 0 \\ \text{Im } B(s) &= 0 \, , && s < 0 \end{aligned}\right\} \text{for } \alpha_0 > -\tfrac{1}{2} \, . \tag{26}$$

To investigate the threshold behavior in the region $\text{Re } \ell < -\frac{1}{2}$ we rewrite Eq. (17) in the form

$$S(\ell,s) = \frac{\left\{ R(\ell,s) + s^{-(\ell+\frac{1}{2})} \exp[-i\pi(\ell + \tfrac{1}{2})] \right\} \exp[i\pi(2\ell + 1)]}{R(\ell,s) + s^{-(\ell+\frac{1}{2})} \exp[i\pi(\ell + \tfrac{1}{2})]} \, , \tag{27}$$

where $R(\ell,s) = Y^{-1}(\ell,s)$. We assume that $S(\ell,s)$ and $Y(\ell,s)$ have the same analytic properties as before. Near a pole we have

$$S(\ell,s) \simeq \frac{-2i \, s^{-(\ell+\frac{1}{2})} \sin \pi(\ell + \tfrac{1}{2}) \exp[2i\pi(\ell + \tfrac{1}{2})]}{R(\ell,s) + s^{-(\ell+\frac{1}{2})} \exp[i\pi(\ell + \tfrac{1}{2})]} \, . \tag{28}$$

Again the poles of $S(\ell,s)$ are the solutions $\ell = \alpha(s)$ of

$$R(\ell,s) + s^{-(\ell+\frac{1}{2})} \exp[i\pi(\ell + \tfrac{1}{2})] = 0 \, , \tag{29}$$

and near the threshold we obtain

$$R_\ell(\alpha - \alpha_0) + s \, R_s + s^{-(\alpha_0+\frac{1}{2})} \exp[i\pi(\alpha_0 + \tfrac{1}{2})] + O(s^2) = 0 \, , \tag{30}$$

where $R_\ell = \partial R(\ell = \alpha_0,\ s = 0)/\partial \ell$ and $R_s = \partial R(\ell = \alpha_0,\ s = 0)/\partial s$.

Therefore, provided that α_0 is real, we have

$$\left.\begin{aligned}
&\text{Re } \alpha = \alpha_0 - R_\ell^{-1}\, s^{-(\alpha_0+\frac{1}{2})} \cos \pi(\alpha_0 + \tfrac{1}{2}) + 0(s)\ , && s > 0\\
&\text{Re } \alpha = \alpha_0 - R_\ell^{-1}\, (-s)^{-(\alpha_0+\frac{1}{2})} + 0(s)\ , && s < 0\\
&\text{Im } \alpha = -R_\ell^{-1}\, s^{-(\alpha_0+\frac{1}{2})} \sin \pi(\alpha_0 + \tfrac{1}{2})\ , && s > 0\\
&\text{Im } \alpha = 0\ , && s < 0
\end{aligned}\right\} \text{for } \alpha_0 < -\tfrac{1}{2}\ . \qquad (31)$$

Also for the residues we obtain

$$\left.\begin{aligned}
\beta(s) &\simeq -2i\, R_\ell^{-1}\, s^{-(\alpha_0+\frac{1}{2})} \sin \pi(\alpha_0 + \tfrac{1}{2}) \exp[2i\pi(\alpha_0 + \tfrac{1}{2})]\\
B(s) &\simeq 2\, R_\ell^{-1}\, s^{-(\alpha_0+\frac{1}{2})} \exp[i\pi(\alpha_0 + \tfrac{1}{2})] \sin \pi(\alpha_0 + \tfrac{1}{2})\\
b(s) &\simeq -R_\ell^{-1}\, s^{-(2\alpha_0+1)} \sin \pi(\alpha_0 + \tfrac{1}{2}) \exp[2i\pi(\alpha_0 + \tfrac{1}{2})]
\end{aligned}\right\} \text{for } \alpha_0 < -\tfrac{1}{2}\ . \qquad (32)$$

giving

$$\left.\begin{aligned}
&\text{Re } B(s) \simeq R_\ell^{-1}\, s^{-(\alpha_0+\frac{1}{2})} \sin \pi(2\alpha_0 + 1), && s > 0\\
&\text{Re } B(s) \simeq 2\, R_\ell^{-1}\, (-s)^{-(\alpha_0+\frac{1}{2})} \sin \pi(\alpha_0 + \tfrac{1}{2})\ , && s < 0\\
&\text{Im } B(s) \simeq 2\, R_\ell^{-1}\, s^{-(\alpha_0+\frac{1}{2})} \sin^2 \pi(\alpha_0 + \tfrac{1}{2})\ , && s > 0\\
&\text{Im } B(s) = 0\ , && s < 0\\
&\text{Re } b(s) \simeq -R_\ell^{-1}\, s^{-(2\alpha_0+1)} \cos \pi(2\alpha_0+1) \sin \pi(\alpha_0+\tfrac{1}{2}), && s > 0\\
&\text{Re } b(s) \simeq -R_\ell^{-1}\, (-s)^{-(2\alpha_0+1)} \sin \pi(\alpha_0 + \tfrac{1}{2})\ , && s < 0\\
&\text{Im } b(s) \simeq -R_\ell^{-1}\, s^{-(2\alpha_0+1)} \sin \pi(2\alpha_0+1) \sin \pi(\alpha_0+\tfrac{1}{2}), && s > 0\\
&\text{Im } b(s) = 0\ , && s < 0
\end{aligned}\right\} \text{for } \alpha_0 < -\tfrac{1}{2}. \qquad (33)$$

This completes the threshold behavior of the Regge parameters.

Now let us consider the asymptotic behavior of these parameters. Since we have assumed that in Eq. (1) $\lim_{r\to 0} r\,V(r)$ is finite, the potential behaves as $1/r$ near the origin. As $|s|$ approaches ∞, one needs consider only the behavior of the potential near the origin, so the Regge parameters should approach asymptotically the Coulomb limit. For a Coulomb potential $V = -g/r$ the S matrix is[12]

$$S(\ell,s) = \frac{\Gamma\left(\ell + 1 - \frac{i\,g}{2\sqrt{s}}\right)}{\Gamma\left(\ell + 1 + \frac{i\,g}{2\sqrt{s}}\right)} \quad . \tag{34}$$

The positions of the poles are given by[12]

$$\alpha_n(s) = -n + \frac{i\,g}{2\sqrt{s}} \quad , \qquad n = 1, 2, \cdots, \tag{35}$$

while the residues are[12]

$$\beta_n(s) = \frac{(-1)^n/(n-1)!}{\Gamma\left(-n + 1 + \frac{i\,g}{\sqrt{s}}\right)} \xrightarrow[|s|\to\infty]{} \frac{i\,g}{\sqrt{s}} \quad . \tag{36}$$

Therefore for potential (1) at high energies one obtains Eqs. (35) and (36), where

$$g = -\lim_{r\to 0} \int_{m_1}^{\infty} \sigma(\mu)\, e^{-\mu r}\, d\mu \quad . \tag{37}$$

Also we have

$$B_n(s) \underset{|s|\to\infty}{\sim} i(-1)^n \frac{g}{\sqrt{s}} \tag{38}$$

and

$$b_n(s) \underset{|s|\to\infty}{\sim} (s)^{n-1} \frac{g}{2} \quad . \tag{39}$$

We shall use these asymptotic values when we consider the dispersion relations for the Regge parameters in the next section. It is interesting to note that from the asymptotic formulas (35) and (36) as well as the threshold formulas (22) and (23) one gets

$$\beta(s) \simeq 2\, i\ \mathrm{Im}\,\alpha(s)\ . \tag{40}$$

We shall see in our later examples that, although expression (40) holds both near the threshold and at large $|s|$, at intermediate energies it is far from correct.

III. DISPERSION RELATIONS OF THE REGGE PARAMETERS

In this section we examine the dispersion relations of the Regge parameters for some examples of a single Yukawa potential. As seen from the arguments of Section II, none of the trajectories is completely contained in the right-half ℓ plane, and to our knowledge it is not known under what conditions in the region Re $\ell < -\frac{1}{2}$ the Regge parameters are free from singularities other than the right-hand cut.

In the absence of branch points due to trajectory intersections, one expects $\alpha_n(s)$ to satisfy the following dispersion relation:

$$\text{Re } \alpha_n(s) = -n + \frac{P}{\pi} \int_0^\infty \frac{\text{Im } \alpha_n(s')ds'}{s' - s} . \qquad (41)$$

The real and imaginary parts of $\alpha(s)$ have been calculated numerically from the Schrödinger equation for the case of a single attractive Yukawa potential $V(r) = -ge^{-r}/r$. By substituting Im α in Eq. (41) and integrating numerically, the left-hand side of Eq. (41) is compared with the actual values of Re α from the Schrödinger equation. Figures 1 and 2 show Re α vs s for the first trajectory of an attractive Yukawa potential $V = -1.8\ e^{-r}/r$ and $V = -5\ e^{-r}/r$. Figure 3 shows the corresponding Im $\alpha_1(s)$. The cross marks on the curves for Re α are the result of the dispersion relation. From the agreement we conclude that in these examples $\alpha_1(s)$ does indeed satisfy the dispersion relation (41), so the trajectories in question must be free from intersections on the physical sheet.

From the arguments of Section II, it follows that for nonintersecting trajectories, $B_n(s)$ satisfies a dispersion relation

$$\text{Re } B_n(s) = \frac{P}{\pi} \int_0^\infty \frac{\text{Im } B_n(s')ds'}{s' - s} \quad . \tag{42}$$

Notice that no subtraction is needed.

In contrast to $B_n(s)$, $b_n(s)$ does not vanish at large s. In particular, since $b_1(s) \to g/2 = \text{constant}$ we have

$$\text{Re } b_1(s) = \frac{g}{2} + \frac{P}{\pi} \int_0^\infty \frac{\text{Im } b_1(s)}{s' - s} ds' \, , \tag{43}$$

where we have made the subtraction at ∞. It also follows from Eq. (39) that for higher-order trajectories we need more subtraction. From the point of view of a dispersion relation, it is more useful to work with the modified residue $B_n(s)$ rather than the reduced residue $b_n(s)$, since the former vanishes both near the threshold and at infinity.

Figures 4 and 6 show $\text{Re } B_1(s)$ for $V = -5\, e^{-r}/r$ and $V = -1.8\, e^{-r}/r$ respectively. Figures 5 and 7 are the corresponding $\text{Im } B_1(s)$. The marks on the curves for $\text{Re } B_1(s)$ show the result of the dispersion relation. The agreement obtained here is expected when one observes the corresponding results for the trajectory; it supports the accuracy of the numerical calculation of the residues.

Figures 10 and 13 show $\text{Im } b_1(s)$ for the first trajectory of $V = -5\, e^{-r}/r$ and $V = -1.8\, e^{-r}/r$ respectively. The corresponding $\text{Re } b_1(s)$ are given in Figs. 8 and 11. Again the marks show the result of dispersion relation (43).

For $s < 0$, to avoid a build up of truncation errors, the asymptotic solution $\psi \sim e^{ikr}$ is integrated inwards and matched to the solution $\psi \sim r^{\ell+1}$ near the origin. [For details see refer-

ence 14.] Thus for $s < 0$ the residues have so far not been calculated directly from the Schrödinger equation. We have, therefore, calculated $b_1(s)$ for $s < 0$ using the dispersion relation and Im $b_1(s)$ for $s > 0$. The result is given in Figs. 9 and 12.

We conclude this section by giving an example of an anomalous trajectory. For a single repulsive Yukawa potential $V = 1.8\, e^{-r}/r$ the first trajectory is plotted in Fig. 14. The energy is given as a running parameter. For $s < 0$, it is seen from this figure that $\alpha_1(s)$ is not real. That $\alpha(s)$ becomes complex before reaching the threshold is due to the branch point at $s = -3.1$. Figure 15 shows $\alpha(s)$ in this neighborhood, and it can be seen that $\alpha(s)$ is double-valued. There are two trajectories that cross at $s = -3.1$.

We now proceed to show that for $V = 1.8\, e^{-r}/r$ the singularities of $\alpha_1(s)$ are not confined to the real s axis. In the absence of complex branch points, $\alpha_1(s)$ should satisfy a dispersion relation with a cut from $s = -3.1$ to $s = +\infty$. The imaginary part of α_1 is plotted in Fig. 16. By inspection of this curve, one can easily convince oneself that, since Im $\alpha_1(s)$ has a very large negative slope at $s = 0$, if $\alpha_1(s)$ satisfied a dispersion relation, Re α_1 would have a sharp minimum at $s = 0$. But from Fig. 14 we see that Re $\alpha_1(s)$ has a maximum there. Of course there is an ambiguity of the sign of Im $\alpha_1(s)$ for $s < 0$. The reason for this ambiguity is that Im $\alpha_1(s)$ vanishes at $s = 0$, and in the Cauchy integral we have the ambiguity of closing the contour in two different ways, as shown in Fig. 17. However, even if we choose Im α_1 to be negative for $s < 0$, an actual integration shows that we can not reproduce Re $\alpha_1(s)$.

It follows that $\alpha_1(s)$ must have branch points at complex s values. Examples of a repulsive Yukawa potential for which $\alpha_1(s)$ is complex below the threshold have already been pointed out by Lovelace and Masson[20] and by Burke and Tate.[23]

IV. RELATIVISTIC-LOOKING TRAJECTORIES

Some Regge trajectories for a single Yukawa potential, calculated by different authors, already exist in the literature.[20,21] In all these example, Re α increases beyond the threshold value by an amount considerably less than that required to explain observed resonances.[9] In the case of the Pomeranchuk trajectory for example, at the threshold we have

$$\alpha(t = 4\, m_\pi^2) \simeq \alpha(t = 0) = 1 , \tag{44}$$

where t is the total energy in the barycentric system. At the position of the f^o particle[11] we have

$$\text{Re}\ \alpha(t = 80\, m_\pi^2) = 2 . \tag{45}$$

Therefore, if f^o is on the Pomeranchuk trajectory, as is believed to be the case, Re α must increase at least by one unit beyond its value at the threshold. For the single Yukawa potential with $g = 10$, where α is approximately 1 at the threshold, we have $(\text{Re}\ \alpha)_{max} - \alpha_{threshold} \simeq 0.25$. Therefore, it is desirable to find a simple superposition of Yukawa potentials for which Re α increases significantly so as to produce a relativistic-looking trajectory. The simplest superposition, as suggested by Chew,[24] is the combination of a strong, short-range, attractive and a weak, long-range, repulsive potential. The long-range repulsive potential then acts as a barrier to confine the metastable state. We have chosen the potential to be of the form

$$V = -g_1\, e^{-r}/r + g_2\, e^{-r/a}/r , \tag{46}$$

where g_1 , g_2 and a are all positive. Figures 18 through 21 show the trajectory for such a potential. The values of s , in units of the range of the attractive potential are given as a running parameter. One immediate conclusion is that, to produce trajectories that move significantly towards the right starting from their threshold, one needs to make the ratio of the two ranges considerably different from one. Because of the large strength of the short-range potential and of the long-range of the repulsive potential, numerical integration of the Schrödinger equation is rather tedious, and we have not attempted to follow the entire trajectory.

V. MODIFICATION OF THE KHURI SERIES

As already mentioned, Regge[2,3,4] has shown that, for the superposition of Yukawa potentials (1), the partial-wave amplitude is meromorphic in the right-half λ plane and has the asymptotic form

$$A(\lambda,s) \sim \frac{C(s)e^{-\lambda\xi_1}}{\sqrt{\lambda}}, \qquad \mathrm{Re}\,\lambda > 0, \qquad |\lambda| \to \infty, \tag{47}$$

where $\lambda = \ell + \frac{1}{2}$ and $\xi_1 = \cosh^{-1}(1 + \frac{m_1^2}{2s})$, m_1 being the lower limit of the integral in Eq. (1). From this, using the Sommerfeld-Watson transformation, Regge obtained for the scattering amplitude the representation

$$f(s,z) = -i \int_{-i\infty}^{i\infty} \lambda\, d\lambda\, P_{\lambda-\frac{1}{2}}(-z)\, \frac{A(\lambda,s)}{\cos \pi\lambda} + 2\pi \sum_{n=1}^{N} \lambda_n \beta'_n \frac{P_{\lambda_n-\frac{1}{2}}(-z)}{\cos \pi\lambda_n}, \tag{48}$$

where $\beta'_n(s)$ are the residues of the poles of $A(\lambda,s)$ at $\lambda = \lambda_n(s) = \alpha_n(s) + \frac{1}{2}$, $\mathrm{Re}\,\lambda_n > 0$. Using Eqs. (47) and (48), considering the subclass of potentials (1) for which $A(\lambda,s)$ is also meromorphic in the left-half λ plane, and with the additional assumption

$$A(\lambda,s) \sim \frac{C(s)e^{-\lambda\xi_1}}{\sqrt{\lambda}}, \qquad \mathrm{Re}\,\lambda < 0, \qquad |\lambda| \to \infty, \tag{49}$$

Khuri[22] has found for the partial-wave amplitude the expansion

$$A(\ell,s) = \sum_{\text{all poles}} \beta'_n(s)\, \frac{\exp[-(\ell - \alpha_n)\xi_1]}{\ell - \alpha_n}, \tag{50}$$

with ℓ an integer.

In this section we first examine certain aspects of Eq. (50). We then modify this formula, starting from weaker asymptotic conditions on $A(\lambda,s)$. Finally, we examine the rate of convergence of Eq. (50) as well as the modified series for the case of a single Yukawa potential.

Now for the sake of simplicity let us consider Eq. (50) for a single Yukawa potential,

$$V(r) = -g \frac{e^{-m_1 r}}{r} . \tag{51}$$

The ideas can be easily generalized if the potential is of the form of Eq. (1) and behaves as $1/r$ near the origin. As s approaches ∞ from the Coulomb limits we have

$$\alpha_n(s) \to -n , \qquad n = 1,2, \cdots , \tag{52}$$

and, since we are considering the residues of the amplitudes rather than the S matrix,

$$\beta'_n(s) \to \frac{g}{2s} . \tag{53}$$

By assuming that for $s \to \infty$ the series (50) reduces to the Born term

$$A(\ell,s) = \frac{g}{2s} Q_\ell\left(1 + \frac{m_1^2}{2s}\right) , \tag{54}$$

Khuri[22] was able to find the correct asymptotic behavior of the residues, Eq. (53). Thus the series (50) does indeed converge to the Born term at high energies. For practical purposes, however, series (50) is not suitable at high energies because in that case it reduces to

$$A(\ell,s) \xrightarrow[s \to \infty]{} \frac{g}{2s} \sum_{n=1}^{\infty} \frac{\exp[-(\ell + n)m_1/\sqrt{s}\,]}{\ell + n} , \qquad (55)$$

and the convergence is very slow. Khuri[22] has suggested that in contrast to the high-energy behavior (53), at intermediate energies the residues $\beta'_n(s)$ may decrease for poles further to the left in the λ plane, improving the rate of convergence. Our numerical solution of the residues given at the end of this paper shows that this is not the case, and at any given energy the different residues are generally of the same order of magnitude. Aside from this difficulty, it seems plausible that for large $|\lambda|$, $A(\lambda,s)$ should approach the Born approximation, which for negative Re λ is dominated by the largest masses in the exponential. So, for a superposition of Yukawa potentials the asymptotic condition (49), which emphasizes the longest rather than the shortest-range component, seems to be too strong an assumption. These arguments suggest the need for a modification of the Khuri series in such a way as to single out the Born term and also deemphasize the contribution of the pole terms further out in the left-half λ plane.

Let us first rewrite the Regge formula, Eq. (48), in such a way as to accommodate the Born term. This, incidentally, would make closer the analogy with the relativistic case in which the Regge poles in the crossed channel are also important.) Our starting point is the mathematical identity

$$-i\,\frac{g}{2s}\int_{-i\infty}^{i\infty}\lambda\,d\lambda\,Q_{\lambda-\frac{1}{2}}\left(1+\frac{m^2}{2s}\right)\frac{P_{\lambda-\frac{1}{2}}(-z)}{\cos\pi\lambda}$$

$$=\frac{g}{2s}\sum_{\ell=0}^{\infty}(2\ell+1)P_\ell(z)\,Q_\ell\left(1+\frac{m^2}{2s}\right) \tag{56}$$

$$=\frac{g}{m^2-t}\,,$$

where $t=-2s(1-z)$. This equation is obtained simply by applying the Cauchy theorem to the integral on the left-hand side of Eq. (56) and closing the contour to the right. Now for the sake of convenience let us assume that the potential is of the form

$$V(r)=-\sum_{i=1}^{k}g_i\,\frac{e^{-m_i r}}{r}\,,\qquad m_{i+1}>m_i\,; \tag{57}$$

therefore the Born term would be

$$\sum_{i=1}^{k}\frac{g_i}{m_i^2-t}=\frac{1}{2s}\sum_{\ell=0}^{\infty}(2\ell+1)P_\ell(z)\sum_{i=1}^{k}g_i\,Q_\ell\left(1+\frac{m_i^2}{2s}\right). \tag{58}$$

Now adding and subtracting the quantity

$$i\lambda\sum_{i=1}^{k}\frac{g_i}{2s}\,Q_{\lambda-\frac{1}{2}}\left(1+\frac{m_i^2}{2s}\right)\frac{P_{\lambda-\frac{1}{2}}(-z)}{\cos\pi\lambda} \tag{59}$$

from the integrand in Regge's formula, Eq. (48), and using Eq. (56) we obtain

$$f(s,z) = -i\int_{-i\infty}^{i\infty} \lambda\, d\lambda\, \frac{P_{\lambda-\frac{1}{2}}(-z)}{\cos \pi\lambda}\left[A(\lambda,s) - \sum_{i=1}^{k} \frac{g_i}{2s}\, Q_{\lambda-\frac{1}{2}}\left(1 + \frac{m_i^2}{2s}\right)\right]$$

$$+\sum_{i=1}^{k} \frac{g_i}{m_i^2 - t} + 2\pi \sum_{n=1}^{N} \lambda_n \beta_n' \frac{P_{\lambda_n-\frac{1}{2}}(-z)}{\cos \pi\lambda_n}\,. \qquad (60)$$

Therefore, in modifying the background integral of the Regge's formula, Eq. (48), we have been able to incorporate the Born term.

One advantage of Eq. (60) over Regge's formula is that by including the Born term we have made the background integral less important. In particular, at high energies where the Regge poles in Eq. (60) are all absent (since all the trajectories have moved to the left-half λ plane), and on the other hand the background integral does not contribute [since $A(\lambda,s)$ approaches the Born term and the integrand vanishes], we simply obtain the Born term, as we should. Another advantage of Eq. (60) is that by incorporating the Born term we have made more meaningful the analogy with the relativistic case, where the Regge poles in the crossed channel are important. The Born term in the nonrelativistic case is the analogue of the contribution from crossed-channel Regge poles in the relativistic scattering. To say that at high energies the potential scattering amplitude is well approximated by the Born term is analogous to the relativistic statement that at high energies the amplitude is well approximated by only the contribution of the crossed-channel Regge poles.

Now starting with Eq. (60) we follow the same procedure as Khuri. Using the relation[22]

$$\frac{\pi \lambda P_{\lambda-\frac{1}{2}}(-z)}{\cos \pi \lambda} = \frac{1}{(2)^{3/2}} \int_{-\infty}^{\infty} \frac{e^{\lambda x} \sinh x \, dx}{(\cosh x - z)^{3/2}} , \tag{61}$$

we can write Eq. (60) as

$$f(s,z) = \frac{-i}{\pi(2)^{3/2}} \int_{-i\infty}^{i\infty} d\lambda \left[A(\lambda,s) - \sum_{i=1}^{k} \frac{g_i}{2s} Q_{\lambda-\frac{1}{2}}\left(1 + \frac{m_i^2}{2s}\right) \right]$$

$$\times \int_{-\infty}^{\infty} \frac{e^{\lambda x} \sinh x \, dx}{(\cosh x - z)^{3/2}} + \sum_{i=1}^{k} \frac{g_i}{m_i^2 - t}$$

$$+ 2\pi \sum_{n=1}^{N} \frac{\lambda_n \beta_n' P_{\lambda_n-\frac{1}{2}}(-z)}{\cos \pi \lambda_n} . \tag{62}$$

Instead of Eqs. (47) and (49) we assume the asymptotic condition

$$A(\lambda,s) - \sum_{i=1}^{k} \frac{g_i}{2s} Q_{\lambda-\frac{1}{2}}\left(1 + \frac{m_i^2}{2s}\right) \xrightarrow[|\lambda| \to \infty]{} C(s) \frac{e^{-\lambda\xi}}{\lambda} , \tag{63}$$

where $\xi = \cosh^{-1}(1 + m^2/2s)$. The choice of m is discussed below. Let us rewrite the integral in Eq. (62) as

$$f_1(s,z) = \frac{-i}{\pi(2)^{3/2}} \int_{-i\infty}^{i\infty} d\lambda \left[A(\lambda,s) - \sum_{i=1}^{k} \frac{g_i}{2s} Q_{\lambda-\frac{1}{2}}\left(1 + \frac{m_i^2}{2s}\right) \right]$$

$$\times \int_{\xi}^{\infty} \frac{e^{\lambda x} \sinh x \, dx}{(\cosh x - z)^{3/2}} - \frac{i}{\pi(2)^{3/2}} \int_{-i\infty}^{i\infty} d\lambda \left[A(\lambda,s) - \sum_{i=1}^{k} \frac{g_i}{2s} Q_{\lambda-\frac{1}{2}}\left(1 + \frac{m_i^2}{2s}\right) \right]$$

$$\times \int_{-\infty}^{\xi} \frac{e^{\lambda x} \sinh x \, dx}{(\cosh x - z)^{3/2}}$$

$$= f_2(s,z) + f_3(s,z) , \tag{64}$$

where

$$f_2(s,z) = \frac{-i}{\pi(2)^{3/2}} \int_{-i\infty}^{i\infty} d\lambda \left[A(\lambda,s) - \sum_{i=1}^{k} \frac{g_i}{2s} Q_{\lambda-\frac{1}{2}}\left(1 + \frac{m_i^2}{2s}\right) \right]$$

$$\times \int_{\xi}^{\infty} \frac{e^{\lambda x} \sinh x \, dx}{(\cosh x - z)^{3/2}} \tag{65}$$

and

$$f_3(s,z) = \frac{-i}{\pi(2)^{3/2}} \int_{-i\infty}^{i\infty} d\lambda \left[A(\lambda,s) - \sum_{i=1}^{k} \frac{g_i}{2s} Q_{\lambda-\frac{1}{2}}\left(1 + \frac{m_i^2}{2s}\right) \right]$$

$$\times \int_{-\infty}^{\xi} \frac{e^{\lambda x} \sinh x \, dx}{(\cosh x - z)^{3/2}} \, . \tag{66}$$

In Eq. (66), using condition (63), we can close the contour of integration to the right in the λ plane and obtain only the poles of $A(\lambda,s)$ in the right-hand λ plane

$$f_3(s,z) = \frac{-1}{\sqrt{2}} \sum_{n=1}^{N} \beta_n' \int_{-\infty}^{\xi} \frac{e^{\lambda_n x} \sinh x \, dx}{(\cosh x - z)^{3/2}} \, . \tag{67}$$

In Eq. (65), by closing the contour to the left in the λ plane, in addition to the poles of $A(\lambda,s)$, we pick up the poles of the Q functions. The result is

$$f_2(s,z) = \frac{1}{\sqrt{2}} \sum_{\text{left poles}} \beta_n' \int_{\xi}^{\infty} \frac{e^{\lambda_n x} \sinh x \, dx}{(\cosh x - z)^{3/2}}$$

$$- \frac{1}{\sqrt{2}} \sum_{i=1}^{k} \frac{g_i}{2s} \sum_{n=1}^{\infty} P_{n-1}\left(1 + \frac{m_i^2}{2s}\right) \int_{\xi}^{\infty} \frac{\exp[-(n - \tfrac{1}{2})x] \sinh x \, dx}{(\cosh x - z)^{3/2}} . \tag{68}$$

Using these results in Eq. (62) we obtain

$$f(s,z) = \frac{1}{\sqrt{2}} \sum_{\text{left poles}} \beta_n' \int_{\xi}^{\infty} \frac{e^{\lambda_n x} \sinh x \, dx}{(\cosh x - z)^{3/2}}$$

$$- \frac{1}{\sqrt{2}} \sum_{i=1}^{k} \frac{g_i}{2s} \sum_{n=1}^{\infty} P_{n-1}\left(1 + \frac{m_i^2}{2s}\right) \int_{\xi}^{\infty} \frac{\exp[-(n - \tfrac{1}{2})x] \sinh x \, dx}{(\cosh x - z)^{3/2}}$$

$$+ \sum_{i=1}^{k} \frac{g_i}{m_i^2 - t} + \sum_{\substack{\text{right} \\ \text{poles}}} \beta_n' \left[\frac{-1}{\sqrt{2}} \int_{-\infty}^{\xi} \frac{e^{\lambda_n x} \sinh x \, dx}{(\cosh x - z)^{3/2}} \right.$$

$$\left. + \frac{2\pi \lambda_n P_{\lambda_n - \frac{1}{2}}(-z)}{\cos \pi \lambda_n} \right] . \tag{69}$$

On the right-hand side of Eq. (69) the first term is the contribution of the poles in the left-half plane, the second and third terms are due to introducing the Born term, and, finally, the term in the brackets is the contribution of the poles in the right-half λ plane. Khuri[22] has shown that the combination of the two

terms in the last bracket for each pole has no branch cut in the region $1 \leqslant z \leqslant \cosh \xi$, and therefore it has only a branch cut in z for $z > \cosh \xi$. It is evident that each term in the first summation on the right-hand side of Eq. (69) has only this same cut in z. Also, by inspection it can be seen that, provided $\lambda_n(s)$ and $\beta_n'(s)$ are free from left-hand cuts in s, each Regge-pole term in the first and last summations on the right-hand side of Eq. (69) satisfies the Mandelstam representation with the cut in t from m^2 to infinity, and in s the cut from the two-particle threshold to infinity plus a spurious left-hand cut due to ξ, from $s = -m^2/4$ to $s = -\infty$. (Note that here we have been using $s = k^2$. If we had defined s as $4(k^2 + M^2)$, the right-hand cut in s would start at $s = 4M^2$.)

For integer ℓ the partial-wave amplitude is given by

$$A(\ell,s) = \tfrac{1}{2} \int_{-1}^{1} f(s,z)\, P_\ell(z)\, dz \,. \tag{70}$$

Using Eqs. (70), (69), and (56) together with[22] the inverse of (61),

$$\frac{\sinh x}{(\cosh x - z)^{3/2}} = -i\sqrt{2} \int_{-i\infty}^{i\infty} \lambda'\, d\lambda'\, P_{\lambda'-\frac{1}{2}}(-z)\, \frac{e^{-\lambda' x}}{\cos \pi\lambda'} \,, \tag{71}$$

we obtain

$$A(\ell,s) = \sum_{\text{all poles}} \beta_n' \frac{\exp[-(\ell - \alpha_n)\xi]}{\ell - \alpha_n} + \sum_{i=1}^{k} \frac{g_i}{2s}\, Q_\ell\!\left(1 + \frac{m_i^2}{2s}\right)$$

$$- \sum_{i=1}^{k} \frac{g_i}{2s} \sum_{n=1}^{\infty} P_{n-1}\left(1 + \frac{m_i^2}{2s}\right) \frac{\exp[-(\ell + n)\xi]}{\ell + n} \,. \tag{72}$$

Now let us consider Eq. (72) for the case of a single Yukawa potential,

$$V(r) = -g e^{-m_1 r}/r ,$$

$$A(\ell,s) = \sum_{\text{all poles}} \beta_n \frac{\exp[-(\ell - \alpha_n)\xi]}{\ell - \alpha_n}$$

$$- \frac{g}{2s} \sum_{n=1}^{\infty} P_{n-1}(1 + \frac{m_1^2}{2s}) \frac{\exp[-(\ell + n)\xi]}{\ell + n} + \frac{g}{2s} Q_\ell(1 + \frac{m_1^2}{2s}) . \tag{73}$$

For $\xi = \xi_1 = \cosh^{-1}(1 + \frac{m_1^2}{2s})$ the last two terms exactly cancel and, mathematically, series (73) is identical with the Khuri series, Eq. (50). In deriving Eq. (73), however, we have used a weaker assumption than the one used in Khuri's paper. Two immediate advantages of Eq. (73) over the Khuri series are immediately apparent. At high energies the first two terms on the right-hand side cancel, and we simply obtain the Born term in closed form. Also, at large values of ℓ, the two summations are small, and, for $\xi > \xi_1$, the Born term stands out as it should.

There is a one-to-one correspondence between the terms in the two summations, and in practice the first N terms of each summation are used. By considering the first N terms, we obtain the approximate expression

$$A(\ell,s) \simeq \sum_{n=1}^{N} \beta_n \frac{\exp[-(\ell - \alpha_n)\xi]}{\ell - \alpha_n}$$

$$- \frac{g}{2s} \sum_{n=1}^{N} P_{n-1}(1 + \frac{m_1^2}{2s}) \frac{\exp[-(\ell + n)\xi]}{\ell + n} + \frac{g}{2s} Q_\ell(1 + \frac{m_1^2}{2s}) . \tag{74}$$

Now we conjecture that[24] in Eq. (63), $m = 2m_1$. For $\mathrm{Re}\,\lambda > 0$, this seems to be correct, because once the Born term is taken out of $f(s,z)$, the dispersion integral[25] in t starts at $t = 4m_1^2$. The asymptotic behavior of $A(\lambda,s)$ for $|\lambda| \to \infty$, $\mathrm{Re}\,\lambda < 0$ is not known, and Eq. (63) with $m = 2m_1$ is the weakest asymptotic behavior we can afford and still be correct in the right half λ plane.

That the asymptotic condition (63) with $m = 2m_1$ is correct for $\mathrm{Re}\,\lambda > 0$ can be seen from the dispersion relation of $f(s,t)$ for fixed s.[25]

$$f(s,t) - \sum_{i=1}^{k} \frac{g_i}{m_i^2 - t} = \frac{1}{\pi} \int_{4m_1^2}^{\infty} \frac{D_t(s,t')dt'}{t' - t} . \tag{75}$$

Now projecting the ℓth partial wave from Eq. (75), we obtain

$$A(\ell,s) - \sum_{i=1}^{k} \frac{g_i}{2s} Q_\ell(1 + \frac{m_i^2}{2s}) = C_1(s) \int_{4m_1^2}^{\infty} Q_\ell(1 + \frac{t'}{2s}) D_t(s,t')dt' . \tag{76}$$

For large $|\ell|$ the right-hand side of Eq. (76) is

$$C_1(s)\int_{4m_1^2}^{\infty} Q_\ell(1+\frac{t'}{2s})D_t(s,t')dt' \underset{\substack{|\ell|\to\infty \\ \mathrm{Re}\,\ell>0}}{\sim} \frac{C_2(s)}{\sqrt{\ell}}\int_{4m_1^2}^{\infty}\exp[-\ell\xi(t')]D_t(s,t')dt'$$

$$\sim \frac{C(s)}{\sqrt{\ell}}\exp[-\ell\xi_2]\ , \tag{77}$$

where $\xi(t') = \cosh^{-1}[1+(t'/2s)]$ and $\xi_2 = \cosh^{-1}[1+(4m_1^2/2s)]$.

Also for $m = 2m_1$, Eq. (72) correctly implies that the left-hand cut of $A(\ell,s)$ in s , for s in the region $-m_1^2 \leqslant s \leqslant -m_1^2/4$, is entirely due to the Born term. Furthermore, as we have already mentioned, each Regge pole term in Eq. (69) has a cut in t from $t = m^2$ to $t = \infty$. Therefore, from Eq. (75), for $m^2 = 4m_1^2$, each Regge-pole term has the same cut in t as the scattering amplitude. We should also like to mention that there is no essential difficulty in generalizing our results to the case of potentials (1). In that case, Eq. (72), for example, would be

$$A(\ell,s) = \sum_{\text{all poles}} \beta_n' \frac{\exp[-(\ell-\alpha_n)\xi]}{\ell-\alpha_n} - \frac{1}{2s}\int_{m_1}^{\infty}\sigma(\mu)d\mu\ Q_\ell(1+\frac{\mu^2}{2s})$$

$$+\frac{1}{2s}\int_{m_1}^{\infty}\sigma(\mu)d\mu\sum_{n=1}^{\infty}P_{n-1}(1+\frac{\mu^2}{2s})\frac{\exp[-(\ell+n)\xi]}{\ell+n}\ . \tag{78}$$

where $\xi = \cosh^{-1}[1+(4m_1^2/2s)]$.

We shall now present the results of our numerical calculations applied to series (50) as well as the modified series (73). For our purposes it is more convenient to work with the S matrix rather than with the amplitude. If we take the first N terms, series (50) for the S matrix is

$$S(\ell,s) = 1 + \sum_{n=1}^{N} \beta_n \frac{\exp[-(\ell - \alpha_n)\xi_1]}{\ell - \alpha_n} . \qquad (79)$$

Then instead of Eq. (73) we have

$$S(\ell,s) = 1 + \sum_{n=1}^{N} \beta_n \frac{\exp[-(\ell - \alpha_n)\xi]}{\ell - \alpha_n} - \frac{ig}{\sqrt{s}} \sum_{n=1}^{N} P_{n-1}\left(1 + \frac{m_1^2}{2s}\right) \frac{\exp[-(\ell + n)\xi]}{\ell + n}$$

$$+ \frac{i g}{\sqrt{s}} Q_\ell\left(1 + \frac{m_1^2}{2s}\right) , \qquad (80)$$

since $S(\ell,s) = 1 + 2i\sqrt{s}\ A(\ell,s)$.

In Eqs. (79) and (80), $\beta_n(s) = 2i\sqrt{s}\ \beta_n'(s)$ are now the residues of the partial-wave S matrix rather than the partial-wave amplitude.

Figures 22 through 57 are plots of the real and imaginary parts of the S matrix vs the number of terms in the original and the modified Khuri series, for both $m = m_1$ and $m = 2m_1$. The horizontal lines correspond to the actual values of the S matrix. The Regge parameters as well as the actual S-matrix values have been calculated by numerical integration of the Schrödinger equation.

From Fig. 22 through 57 the modified series with $m = 2m_1$ is considerably favored. In particular, for $g = 1.8$ the agreement with

the actual S-matrix values is remarkable. The fact that the agreement is not as good for $g = 5$ as for $g = 1.8$ may in part be due to the error in the residues. For stronger potentials our numerical calculation of the residues is less accurate, because in the integration of the Schrödinger equation for stronger potentials, we have to start the integration closer to the origin and integrate the wave function to a larger distance from the origin to get to the asymptotic region. Because of the large interval of the integration, the truncation error increases. For $g = 5$ in some cases it turns out that only a few percent error in the residues introduces a considerable error in the values of the real or imaginary parts of the S matrix calculated from the series. As we shall see in the next section, aside from the error of the residues, the magnitude of the residues grows with the strength of the potential, and for stronger potentials a larger number of terms in the series should be considered.

VI. REGGE PARAMETERS AND THE PARTIAL-WAVE S MATRIX FOR A SINGLE YUKAWA POTENTIAL

Several examples of $\alpha_i(s)$ for a single Yukawa potential already exist in the literature.[20,21] The residues, however, have not been given in these references. In this section, we shall give the detailed energy variation of the Regge parameters for the first three trajectories of a single Yukawa potential $V = -1.8\, e^{-r}/r$ and $-5e^{-r}/r$. We shall also give the energy variation of the S matrix for the first three physical partial waves, hoping that the S-matrix values together with the details of the corresponding Regge parameters will be of future use, in connection with questions similar to the convergence of the Khuri series that we discussed in the previous section.

Figures 58 through 97 show the magnitude of the real and imaginary parts of the Regge parameters α_i , β_i , B_i, and b_i vs s for the first three trajectories of a single Yukawa potential $V = -1.8\, e^{-r}/r$ and $V = -5\, e^{-r}/r$. In order to cover a wide range of values, these figures are given in logarithmic form. The + or - signs next to the curves indicate the sign of these quantities. The threshold and the asymptotic behavior can be seen roughly in most cases. Note, however, that in some cases the energies considered are not large enough to show the asymptotic behavior. (For example, the residues of the second and third trajectories of $V = -5\, e^{-r}/r$ have not been followed to their asymptotic region.)

Figures 98 through 103 give the values of the real and imaginary parts of the partial-wave S matrix for the above potentials. Again, the + or - sign shows the sign of these quantities.

Finally, to show how residues grow with the strength of the potential, the residues of the first trajectory are given for a range of values of the potential strength. Figures 104 through 108 show plots of $\mathrm{Im}\ \beta_1(s)$ vs $\mathrm{Re}\ \beta_1(s)$ for a single Yukawa potential $V = -g\, e^{-r}/r$ with g ranging from 0.05 to 5. The energy is given as a running parameter.

ACKNOWLEDGMENTS

I would like to take this opportunity to express my deepest gratitude to Professor Geoffrey F. Chew for suggesting these investigations. His numerous suggestions and criticisms were very helpful throughout the course of this work. I am also grateful to Professor C. Zemach and Dr. E. Leader and the other members of the Physics Department of the Lawrence Radiation Laboratory for numerous helpful discussions. Thanks are also due to the staff of the Computing Center at the Laboratory for the use of their facilities.

This work was done under the auspices of the U. S. Atomic Energy Commission.

REFERENCES

1. A. Sommerfeld, Partielle Differential--Gleichungen der Physik (Leipzig, 1947), p. 285.
2. T. Regge, Nuovo Cimento 14, 951 (1959).
3. T. Regge, Nuovo Cimento 18, 947 (1960).
4. A. Bottino, A. M. Longoni, and T. Regge, Nuovo Cimento 23, 954 (1962).
5. S. Mandelstam, Revs. Modern Phys. 33, 470 (1961).
6. M. Froissart, Report to La Jolla Conference on Weak and Strong Interactions, (1961), (unpublished).
7. V. N. Gribov, Soviet Physics JETP 14, 1395 (1962).
8. G. F. Chew and S. Frautschi, Phys. Rev. Letters 7, 934 (1961).
9. G. F. Chew and S. Frautschi, Phys. Rev. Letters 8, 41 (1962).
10. V. N. Gribov, Soviet Physics JETP 14, 478 (1962).
11. W. Selove, V. Hagopian, H. Brody, A. Baker, and E. Leboy, Phys. Rev. Letters 9, 272 (1962). See also J. J. Vellet, J. Hennessy, H. Bingham, M. Bloch, D. Drijard, A. Lagarrigue, P. Mittner, A. Rousset, G. Bellini, M. di Corato, E. Fiorini, and P. Negri, Phys. Rev. Letters 10, 29 (1963).
12. V. Singh, Phys. Rev. 127, 632 (1962).
13. A. Barut and F. Calogero, Phys. Rev. 128, 1383 (1962).
14. P. Burke and C. Tate, University of California, Lawrence Radiation Laboratory Report UCRL-10384, July 1962.
15. S. Mandelstam, Ann. Phys. (N. Y.) 19, 254 (1962).
16. M. Froissart, J. Math. Phys. 3, 922 (1962).
17. C. Zemach, Department of Physics, University of California, private communication.

18. J. R. Taylor, Phys. Rev. 127, 2257 (1962).

19. A. O. Barut and D. Zwanziger, Phys. Rev. 127, 974 (1962).

20. C. Lovelace and D. Masson, Nuovo Cimento 26, 472 (1962).

21. A. Ahmadzadeh, P. Burke, and C. Tate, Phys. Rev. 131, 1315 (1963).

22. N. Khuri, Phys. Rev. 130, 429 (1963).

23. P. Burke and C. Tate, private communication.

24. G. F. Chew, private communication.

25. R. Blankenbecler, M. L. Goldberger, N. N. Khuri, and S. B. Treiman, Ann. Phys. (N. Y.) 10, 62 (1960).

FIGURE LEGENDS

Fig. 1. Graph of α_1 vs $-s$ for $g = 1.8$ and $g = 5$. The marks on the curves are the results of the dispersion relation.

Fig. 2. Graph of Re α_1 vs s for $g = 1.8$ and $g = 5$. The marks on the curves are the results of the dispersion relation.

Fig. 3. Graph of Im α_1 vs s for $g = 1.8$ and $g = 5$.

Fig. 4. Graph of Re B_1 vs s for $g = 5$.

Fig. 5. Graph of Im B_1 vs s for $g = 5$.

Fig. 6. Graph of Re B_1 vs s for $g = 1.8$.

Fig. 7. Graph of Im B_1 vs s for $g = 1.8$.

Fig. 8. Graph of Re b_1 vs s for $g = 5$.

Fig. 9. Graph of b_1 vs $-s$ for $g = 5$ (from the dispersion relation).

Fig. 10. Graph of Im b_1 vs s for $g = 5$.

Fig. 11. Graph of Re b_1 vs s for $g = 1.8$.

Fig. 12. Graph of b_1 vs $-s$ for $g = 1.8$ (from the dispersion relation).

Fig. 13. Graph of Im b_1 vs for $g = 1.8$.

Fig. 14. Graph of Im α_1 vs Re α_1 for $g = -1.8$ with s given as a running parameter

Fig. 15. Graph of $\alpha_1(s)$ vs s for $g = -1.8$ in the neighborhood of $s \simeq -3.1$ where the branch point occurs.

Fig. 16. Graph of Im $\alpha_1(s)$ vs s for $g = -1.8$.

Fig. 17. Graph of the two possible contours (if there were no complex branch points) of the Cauchy integral in the dispersion relation for $\alpha_1(s)$ with $g = -1.8$.

Fig. 18. Graph of $\mathrm{Im}\,\alpha_1$ vs $\mathrm{Re}\,\alpha_1$ for potential $V = -50\, e^{-r}/r + (30\, e^{-r/10})/r$ with the energy s as a running parameter. For comparison, the same curve for $V = -5\, e^{-r}/r$ is also given.

Fig. 19. A portion of the first and second trajectories of $V = -25\, e^{-r}/r + 5\, e^{-r/10}/r$.

Fig. 20. A portion of the first trajectory of $V = -30\, e^{-r}/r + 10\, e^{-r/10}/r$.

Fig. 21. A portion of the first trajectory for $V = -18\, e^{-r}/r + 5\, e^{-r/10}/r$ and for

$$V = -18\, e^{-r}/r + 3\, e^{-r/10}/r \ .$$

Figs. 22 through 57. Real and imaginary parts of S vs the number of terms in the expansion.

Δ Ex. (79)

$\bigcirc$ Eq. (80) with $m = m_1$

$\circledcirc$ Eq. (80) with $m = 2m_1$.

Figs. 58 through 97. Magnitudes of the real and imaginary parts of the Regge parameters vs s for the first three trajectories for $g = 1.8$ and $g = 5$. The sign of these quantities is indicated along the curves in each case.

Fig. 98 through 103. Real and imaginary parts of the S matrix vs s for the first three partial waves, $\ell = 0$, 1, and 2 .

Fig. 104 through 108. Imaginary β_1 vs real β_1 for $g = 0.05$, 1.8, 3, 4, and 5. The energy is given as a running parameter.

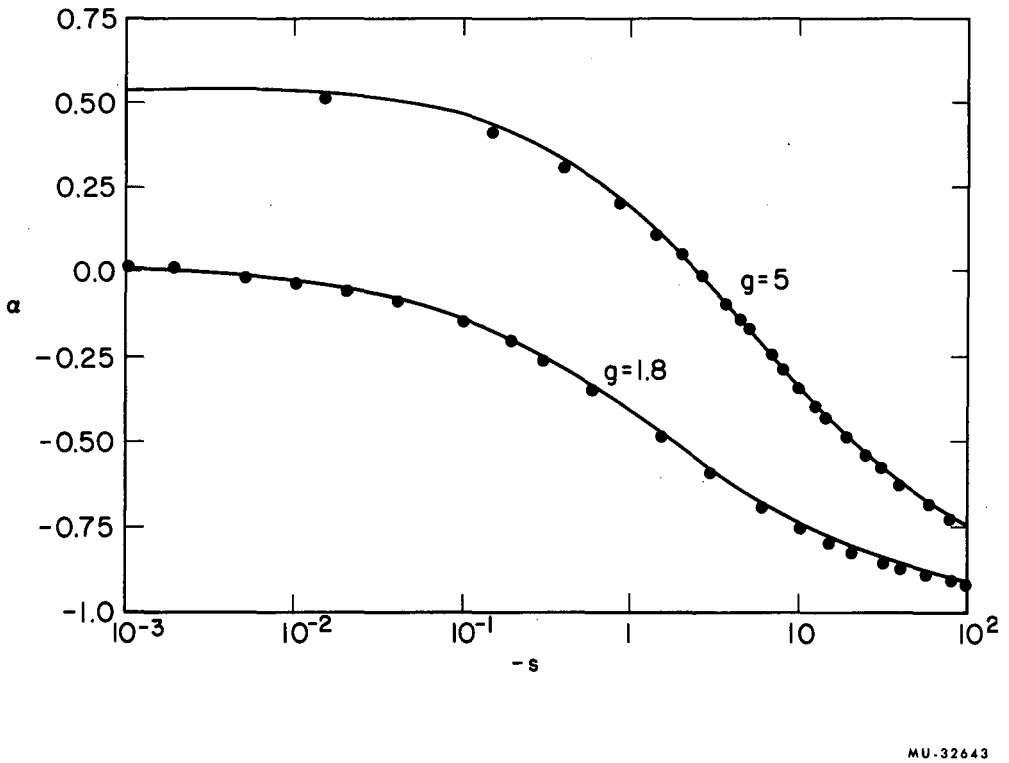
0.75
0.50
0.25
0.0
-0.25
-0.50
-0.75
-1.0
α
g=5
g=1.8
10⁻³
10⁻²
10⁻¹
1
10
10²
-s
MU-32643

Fig. 1

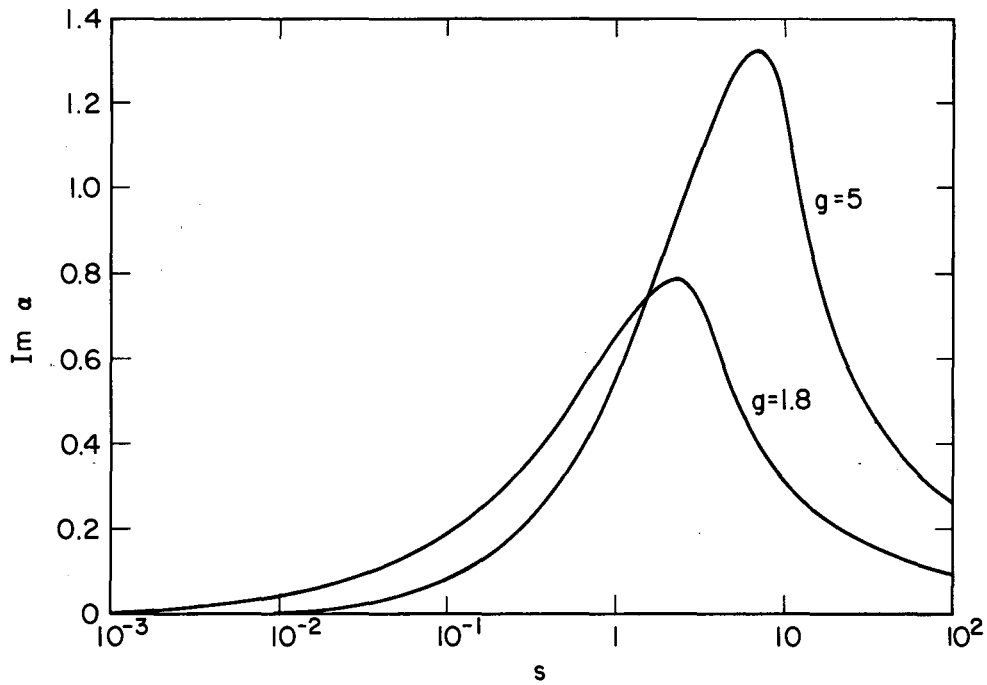

Fig. 2

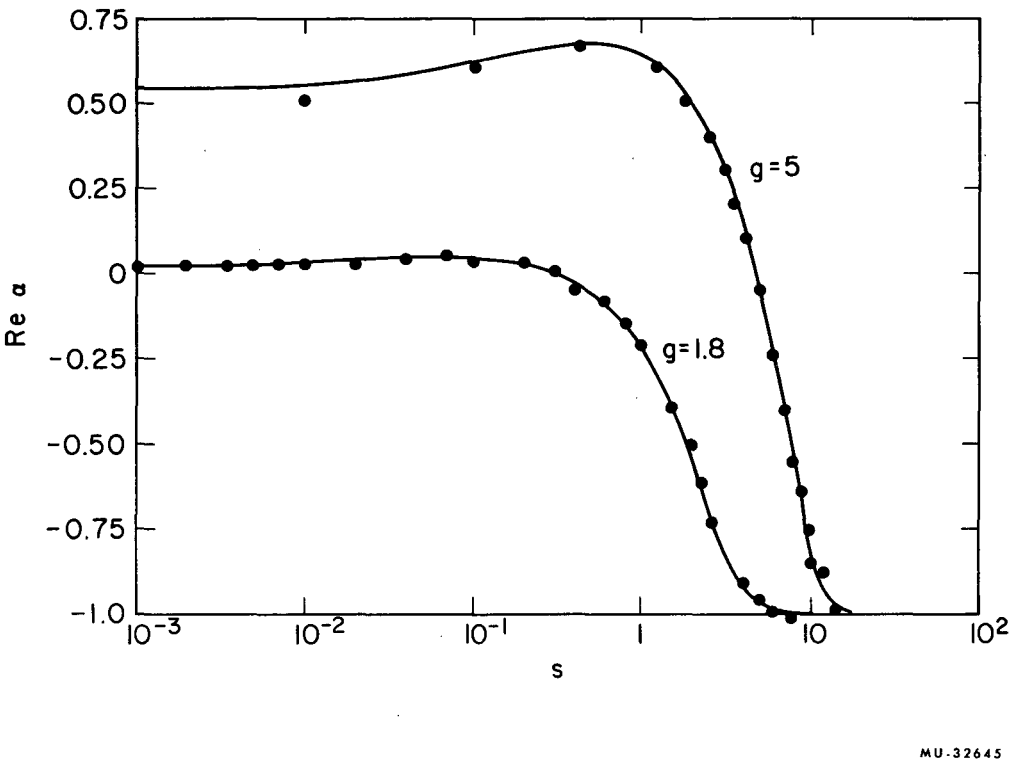
0.75
0.50
0.25
0
-0.25
-0.50
-0.75
-1.0
Re α
g=5
g=1.8
10^-3
10^-2
10^-1
1
10
10^2
s
MU-32645

Fig. 3

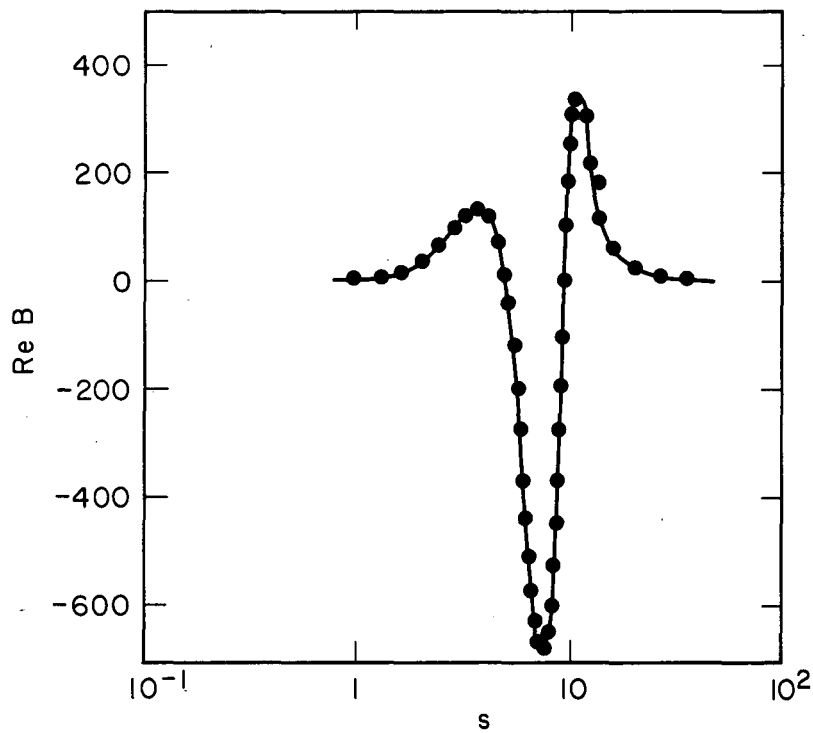

Fig. 4

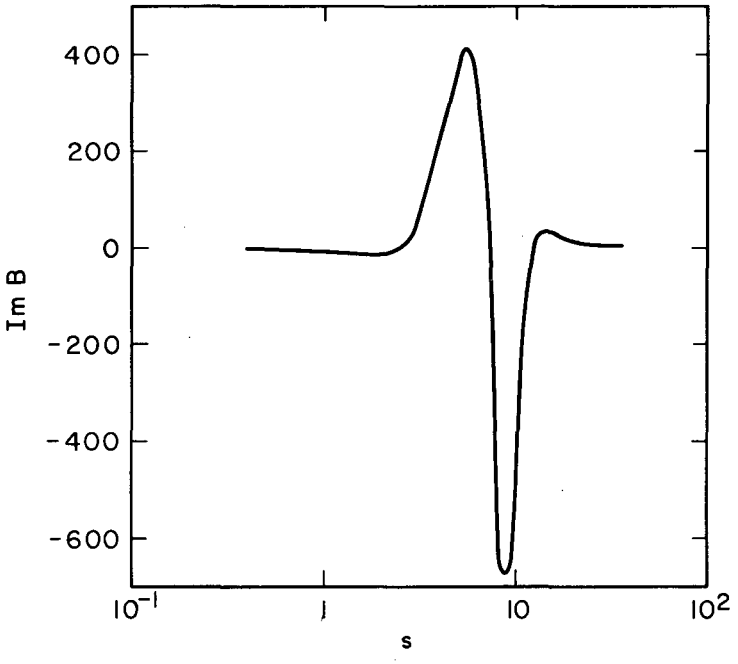

Fig. 5

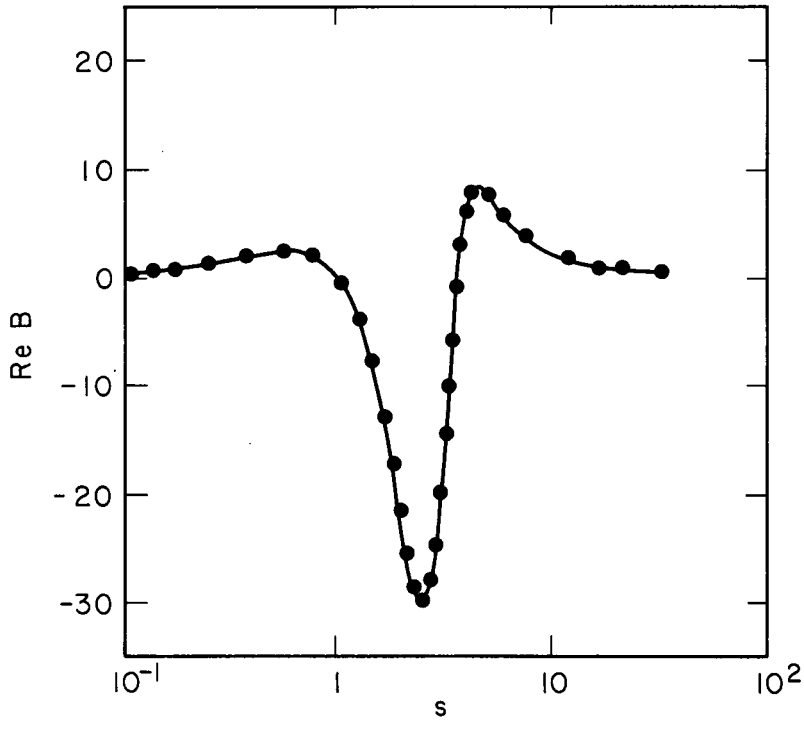

Fig. 6

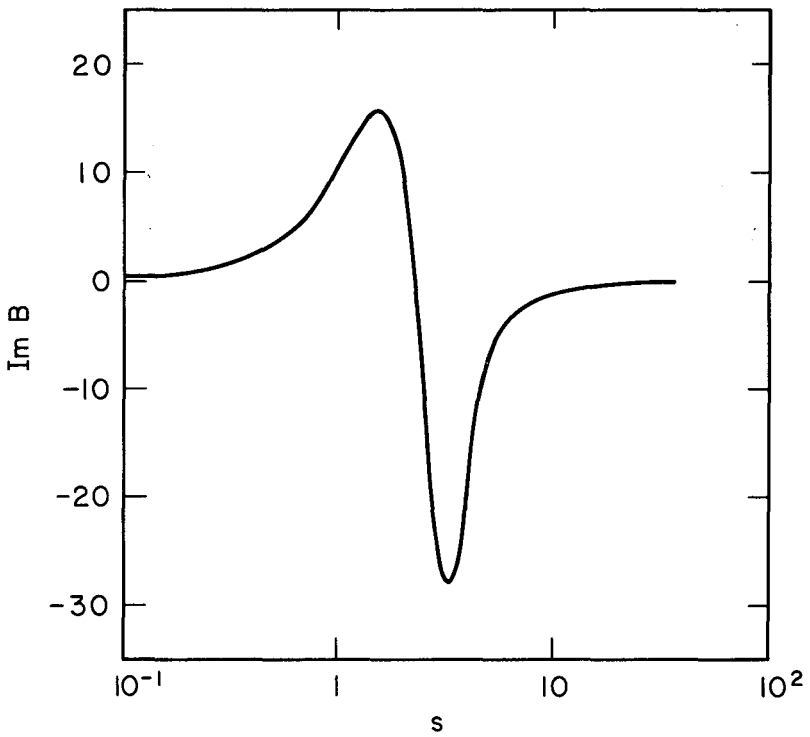

Fig. 7

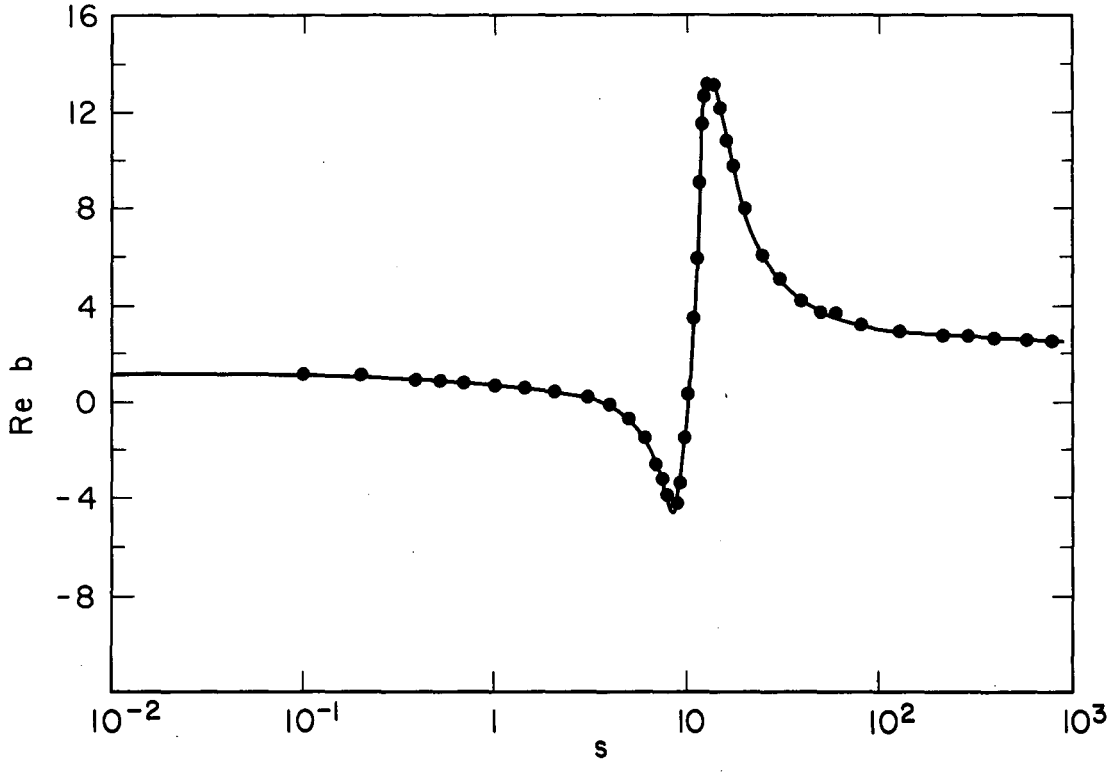

Fig. 8

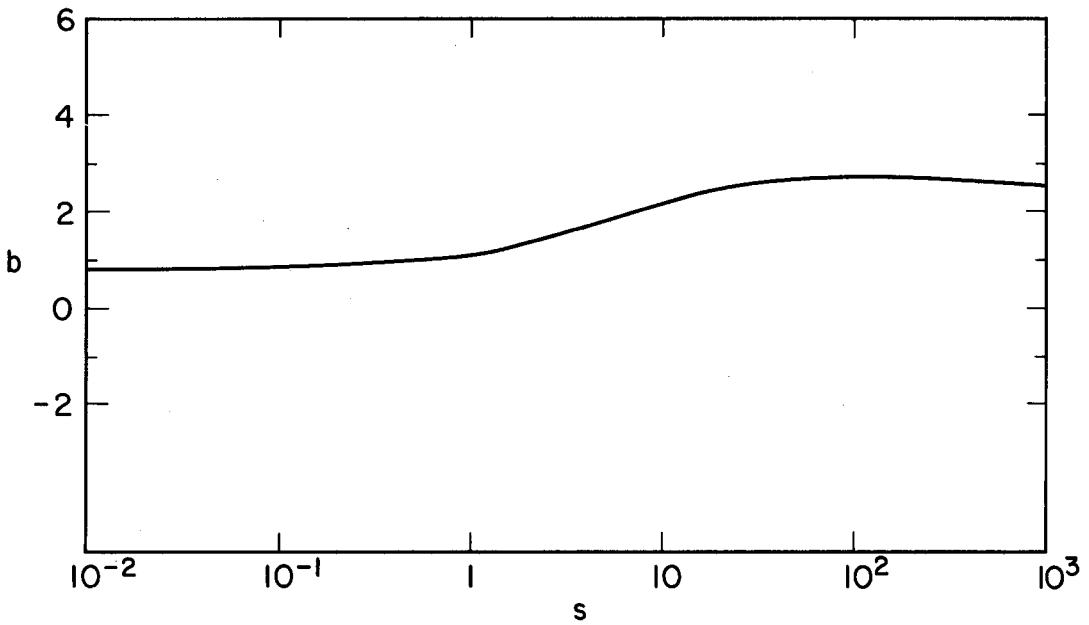

Fig. 9

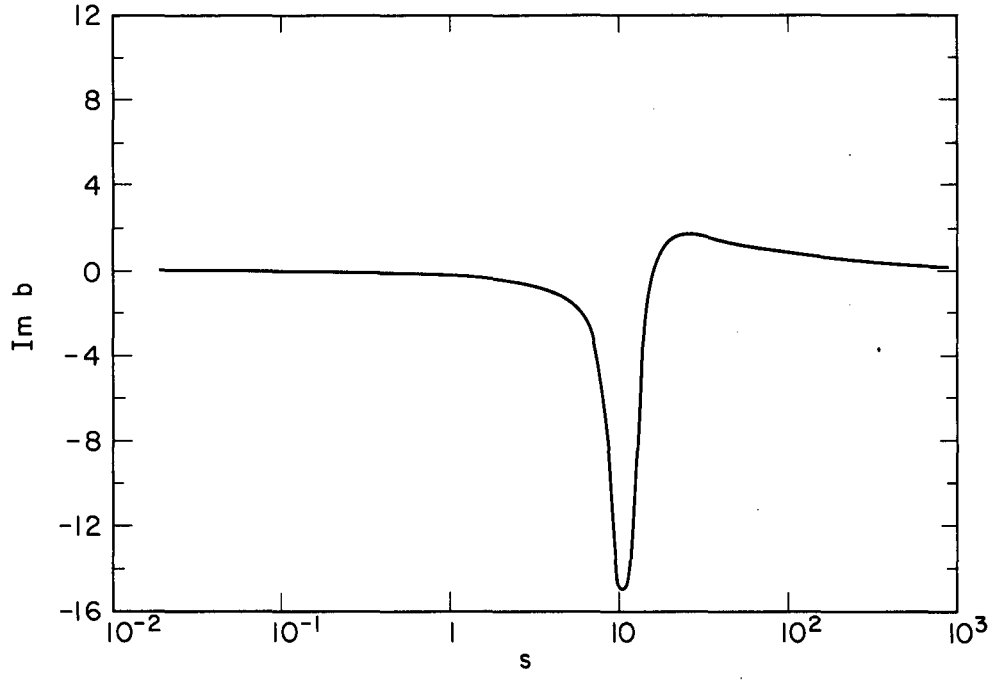

Fig. 10

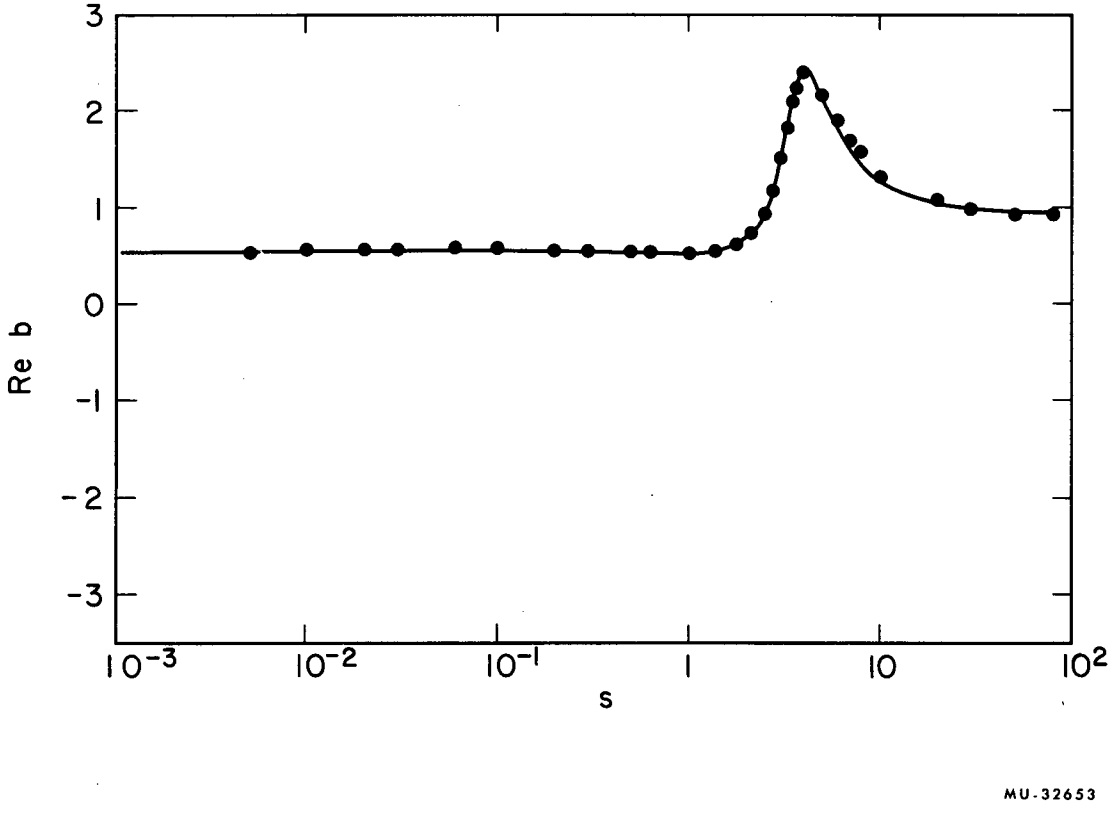

Fig. 11

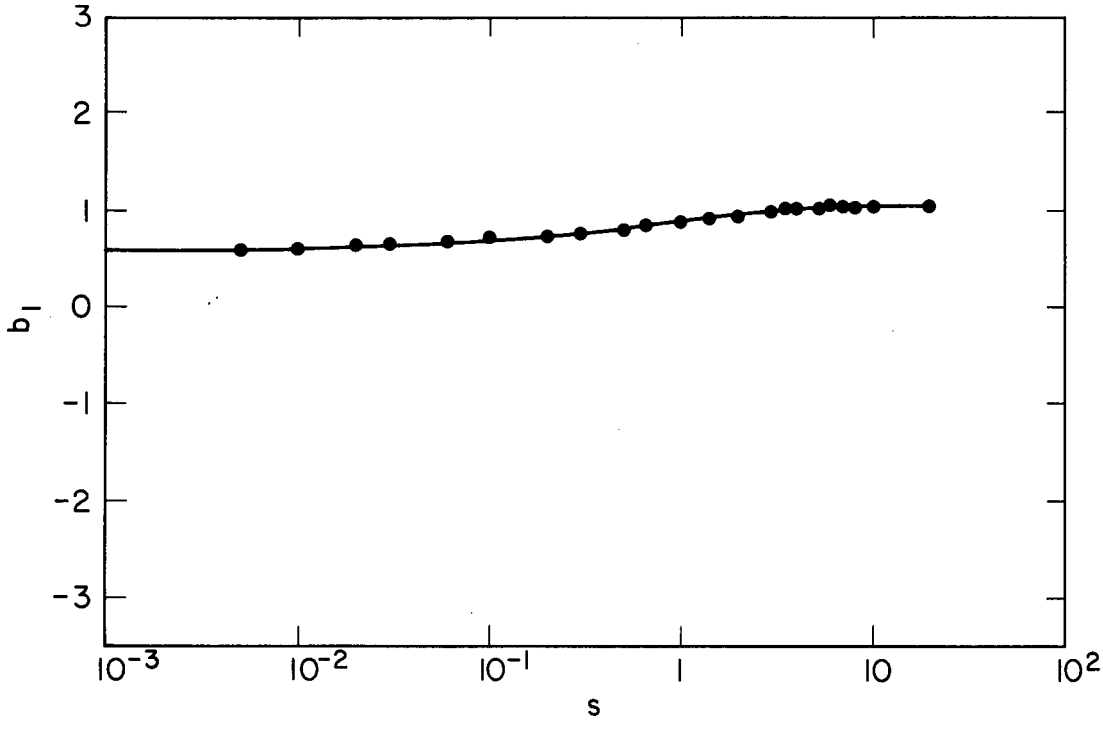

Fig. 12

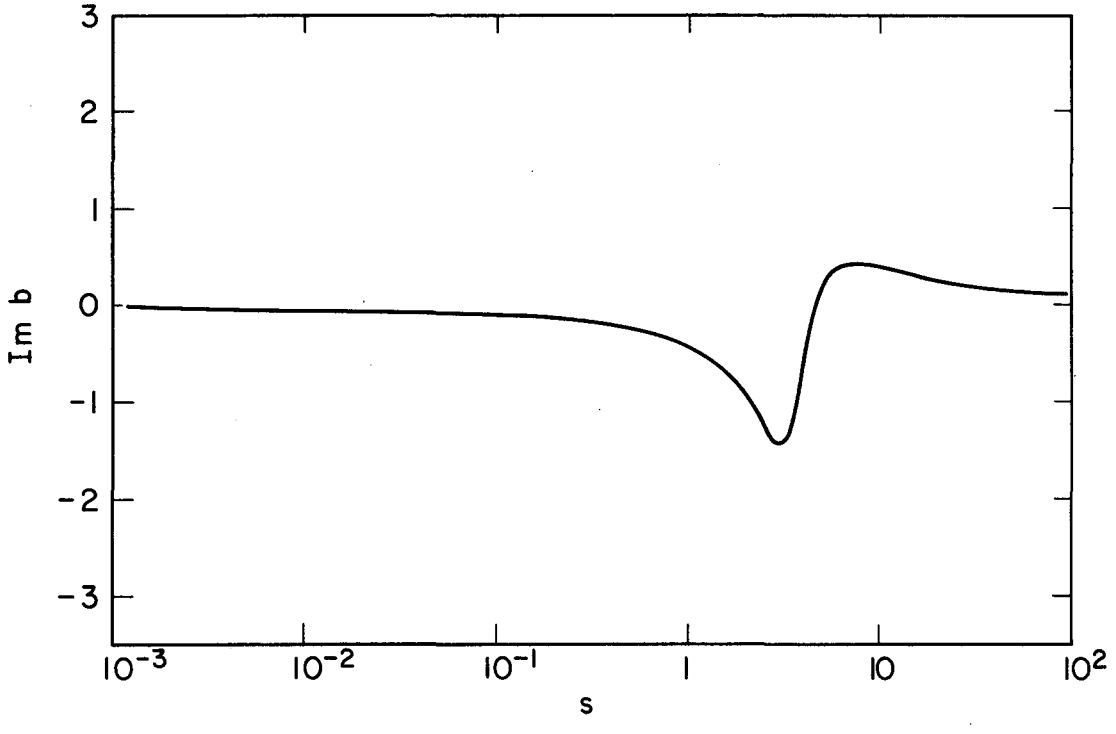

Fig. 13

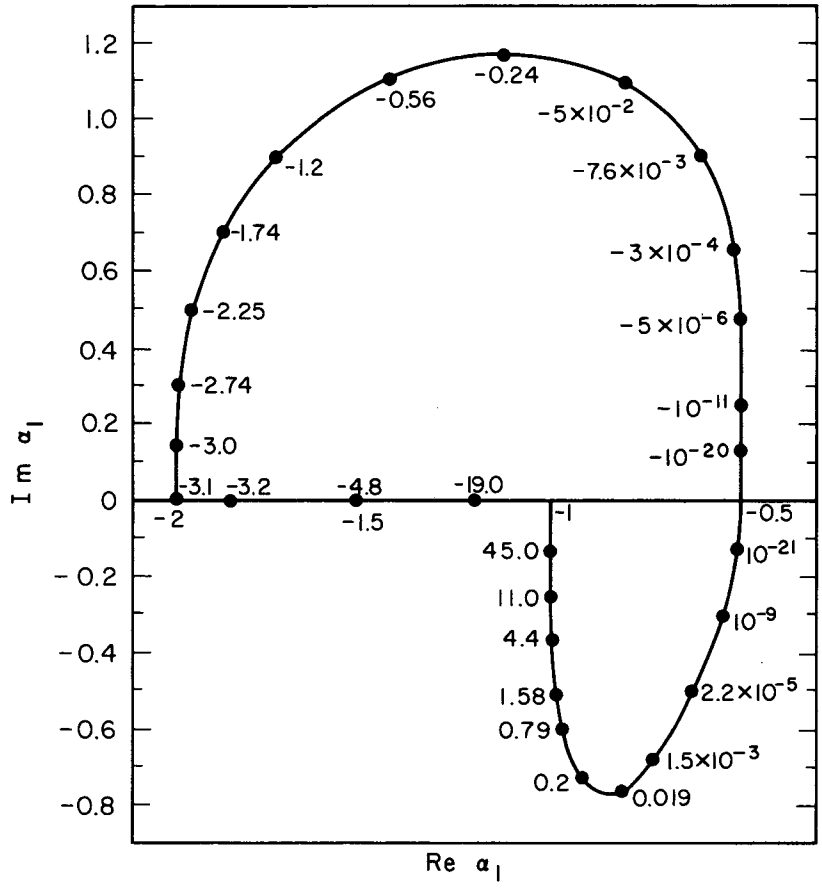

MU-32656

Fig. 14

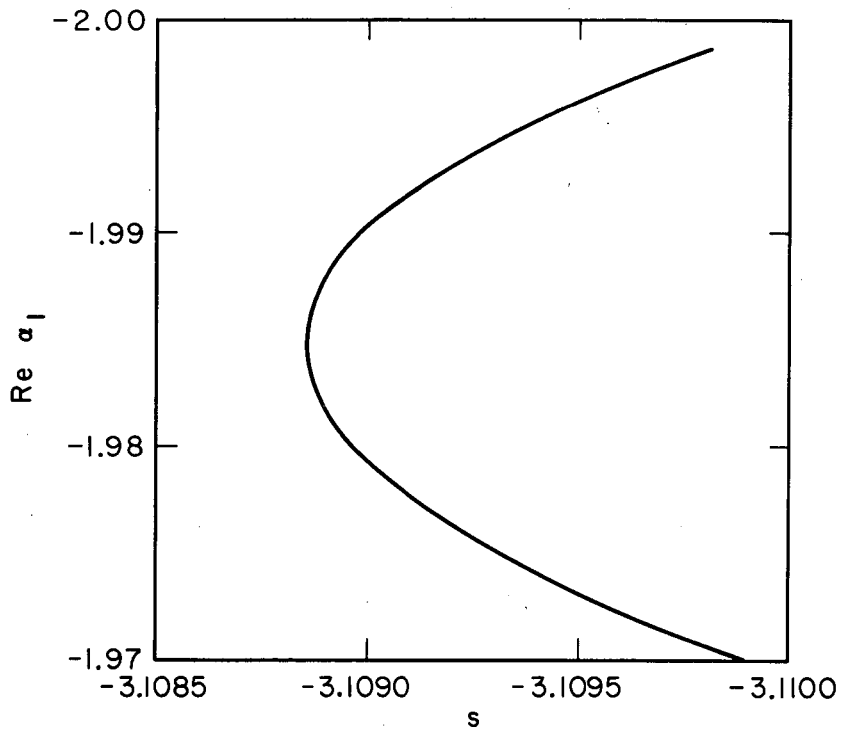

Fig. 15

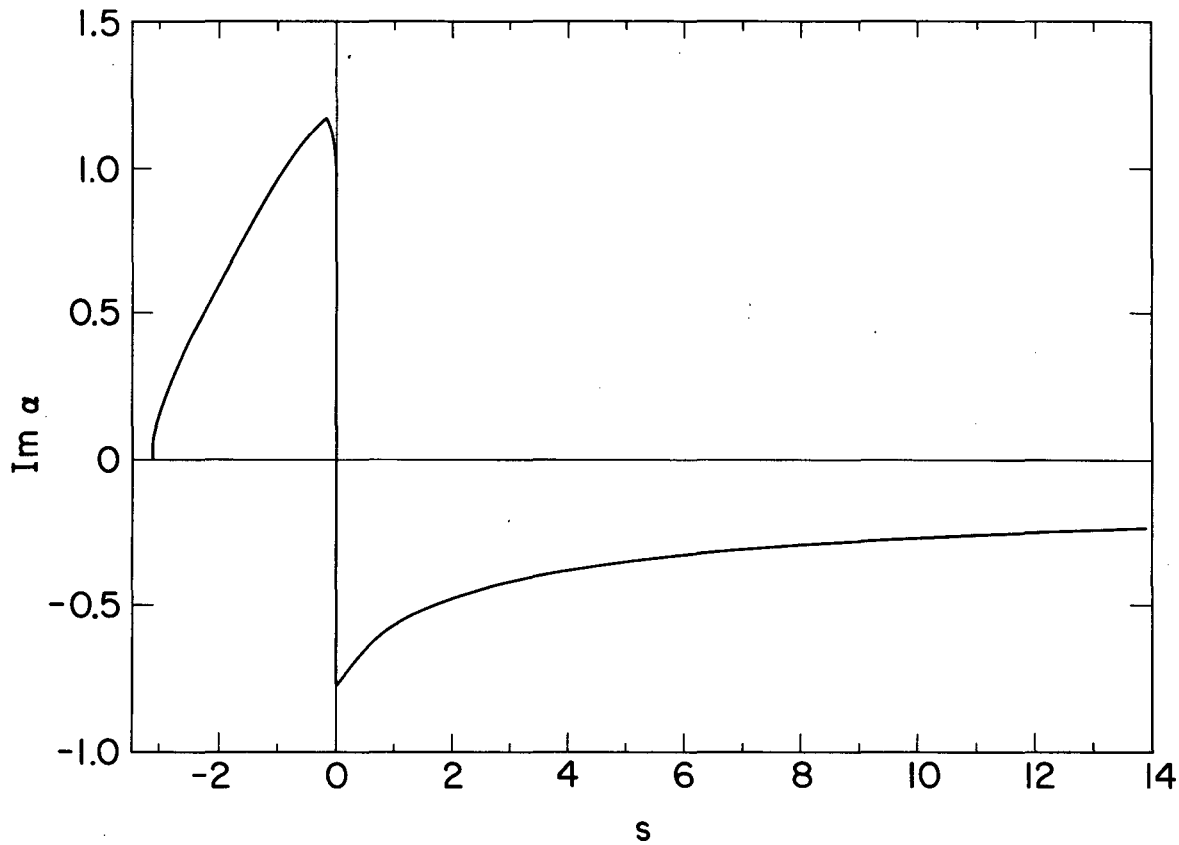

Fig. 16

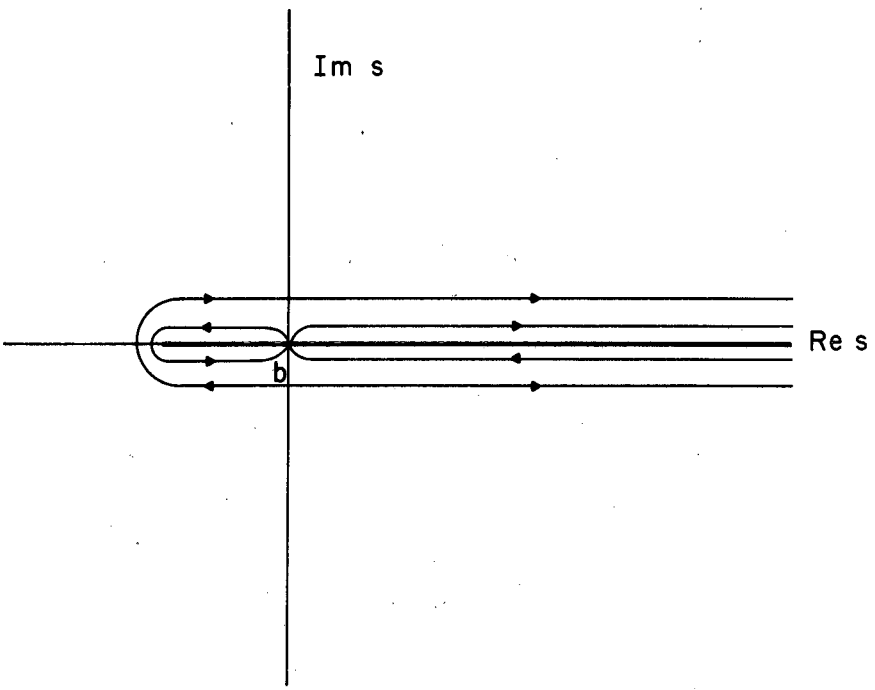

MU-32658

Fig. 17

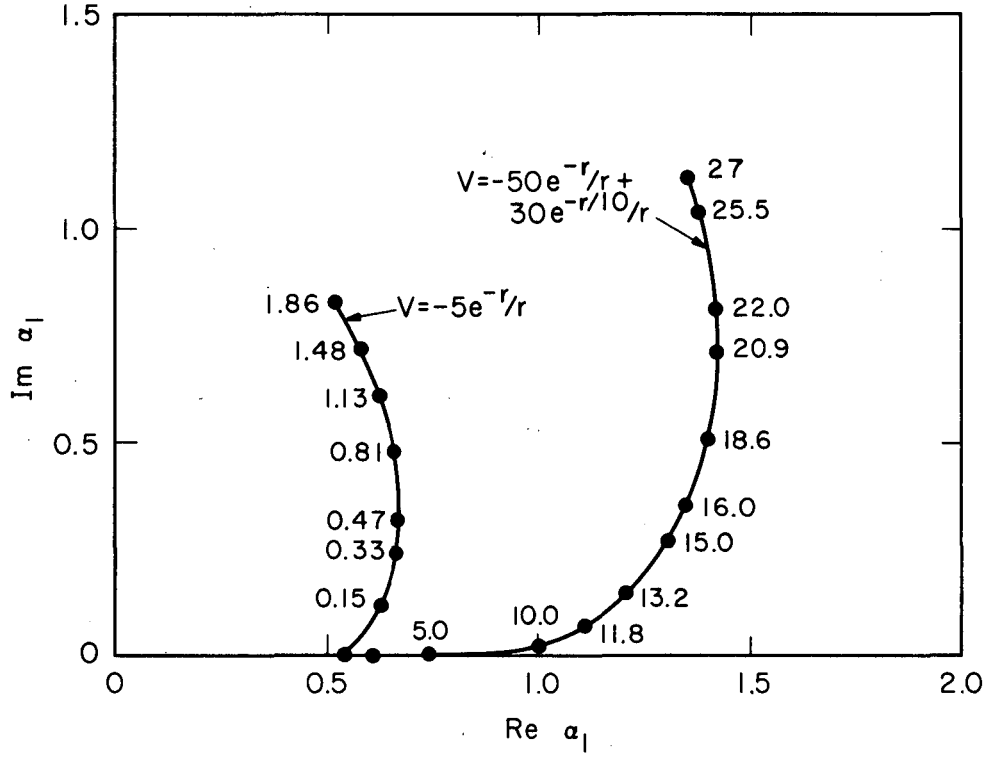
1.5
1.0
0.5
0
0
0.5
1.0
1.5
2.0
Im α_l
Re α_l
$V=-50e^{-r}/r+30e^{-r/10}/r$
$V=-5e^{-r}/r$
27
25.5
22.0
20.9
18.6
16.0
15.0
13.2
11.8
10.0
5.0
1.86
1.48
1.13
0.81
0.47
0.33
0.15
MU-32659

Fig. 18

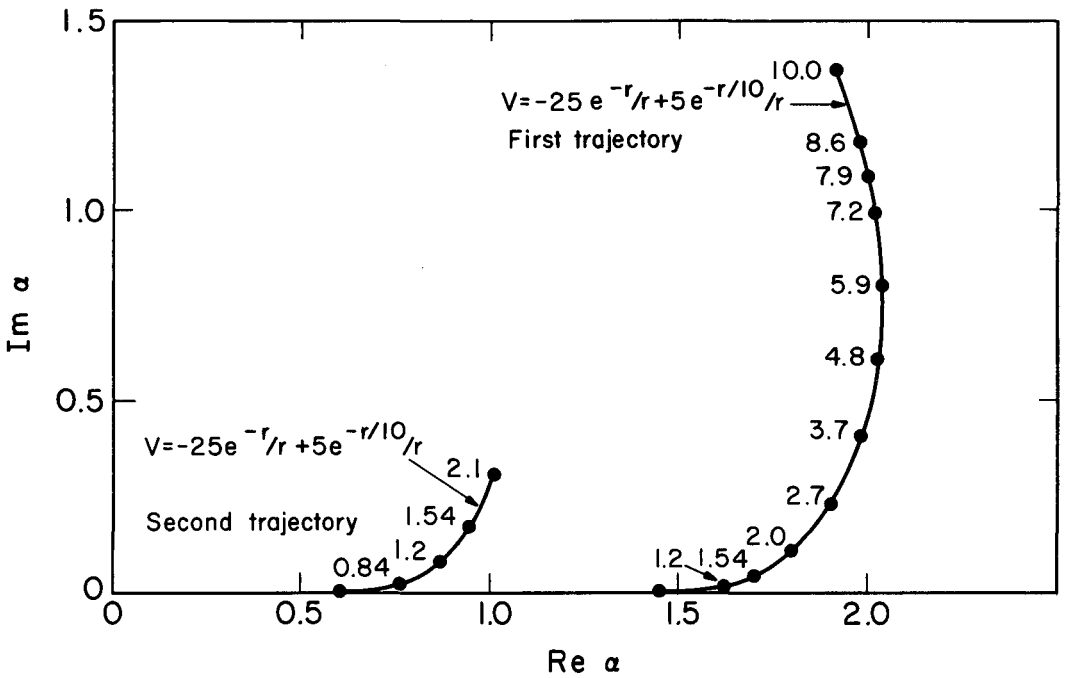
1.5
1.0
0.5
0
Im α
0
0.5
1.0
1.5
2.0
Re α
V=-25 e^-r/r+5e^-r/10/r
First trajectory
10.0
8.6
7.9
7.2
5.9
4.8
3.7
2.7
2.0
1.2
1.54
V=-25e^-r/r +5e^-r/10/r
Second trajectory
2.1
1.54
1.2
0.84
MU-32660

Fig. 19

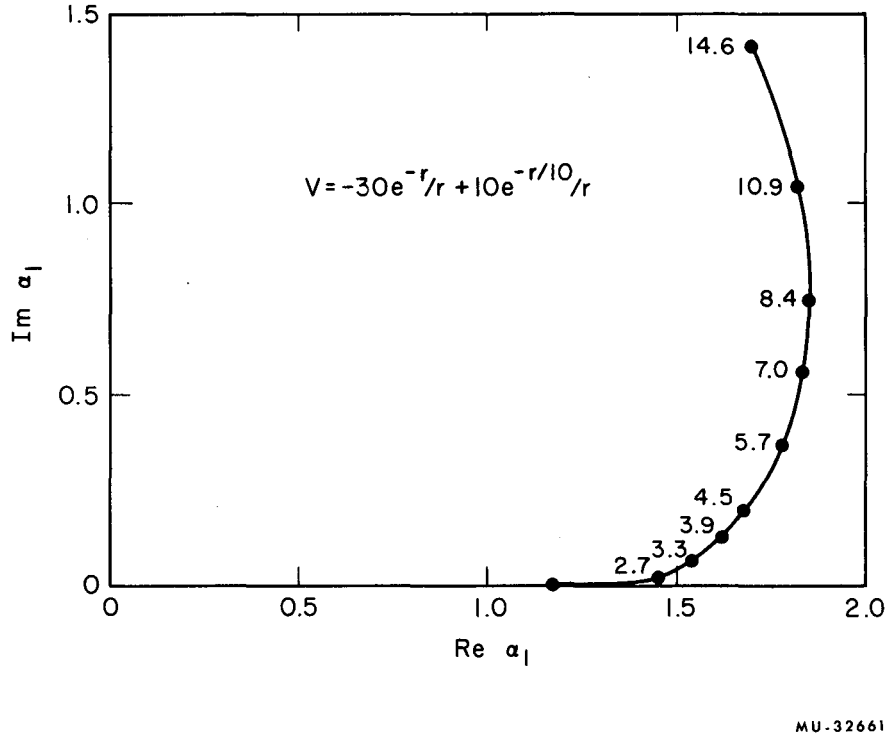
1.5
1.0
0.5
0
0
0.5
1.0
1.5
2.0
Im α_l
Re α_l
$V=-30e^{-r}/r+10e^{-r/10}/r$
14.6
10.9
8.4
7.0
5.7
4.5
3.9
3.3
2.7
MU-32661

Fig. 20

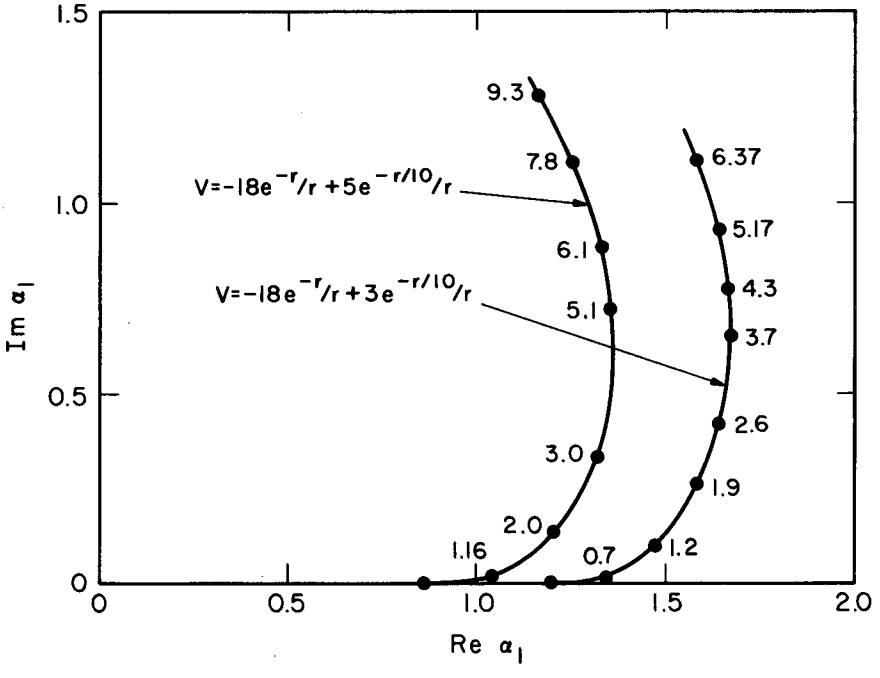
1.5
1.0
0.5
0
0
0.5
1.0
1.5
2.0
Im α_l
Re α_l
$V=-18e^{-r}/r+5e^{-r/10}/r$
$V=-18e^{-r}/r+3e^{-r/10}/r$
9.3
7.8
6.1
5.1
3.0
2.0
1.16
6.37
5.17
4.3
3.7
2.6
1.9
1.2
0.7
MU-32662

Fig. 21

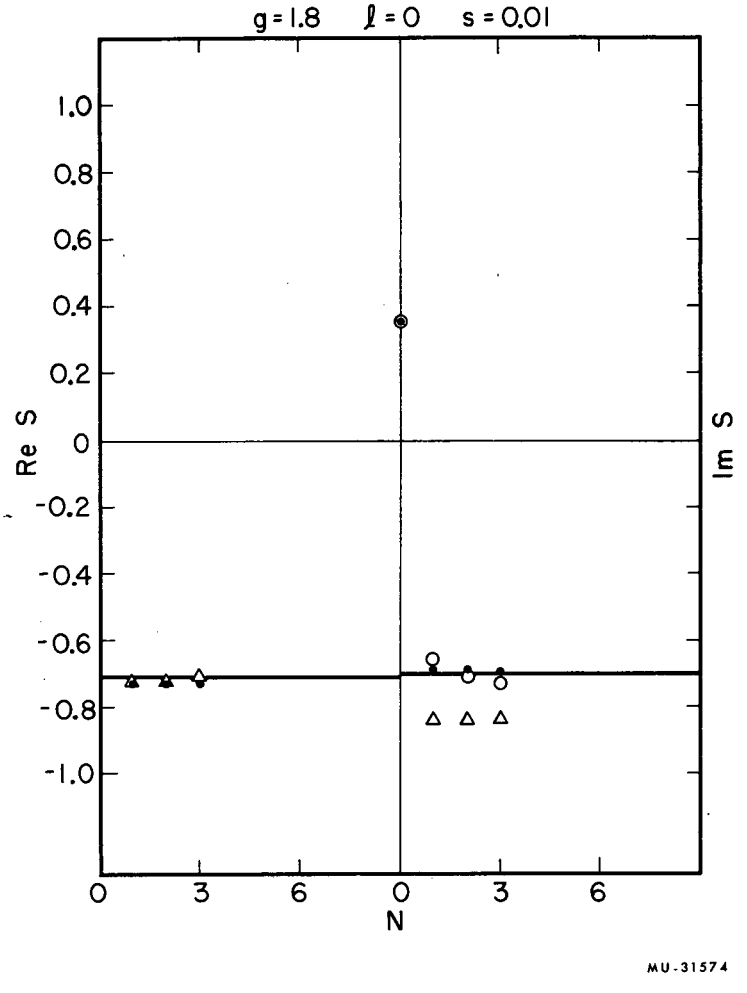
g = 1.8 ℓ = 0 s = 0.01
1.0
0.8
0.6
0.4
0.2
0
-0.2
-0.4
-0.6
-0.8
-1.0
Re S
Im S
0
3
6
0
3
6
N
MU-31574

Fig. 22

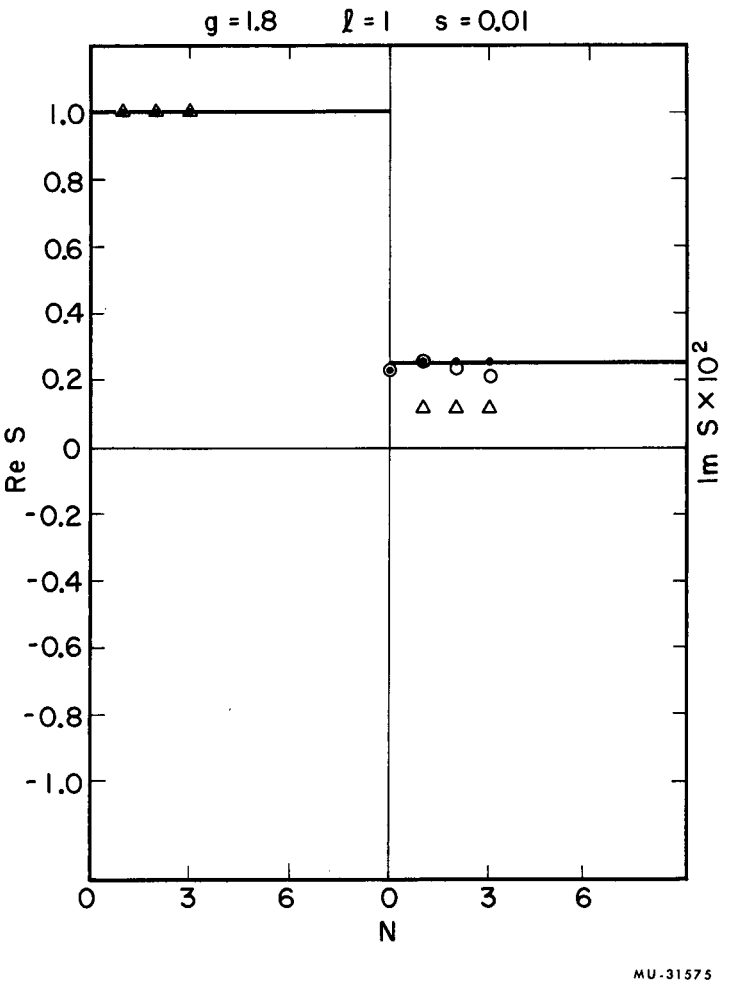
g = 1.8 ℓ = 1 s = 0.01
1.0
0.8
0.6
0.4
0.2
0
-0.2
-0.4
-0.6
-0.8
-1.0
Re S
Im S X 10²
0
3
6
0
3
6
N
MU-31575

Fig. 23

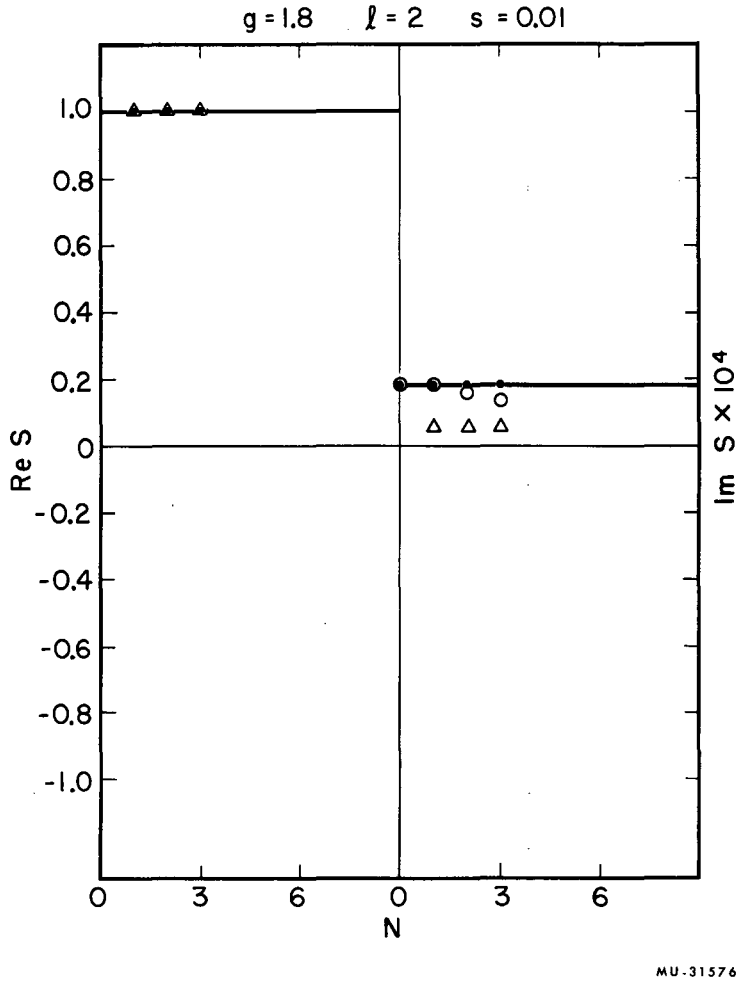
g = 1.8 ℓ = 2 s = 0.01
1.0
0.8
0.6
0.4
0.2
0
-0.2
-0.4
-0.6
-0.8
-1.0
Re S
Im S X 10⁴
0
3
6
0
3
6
N
MU-31576

Fig. 24

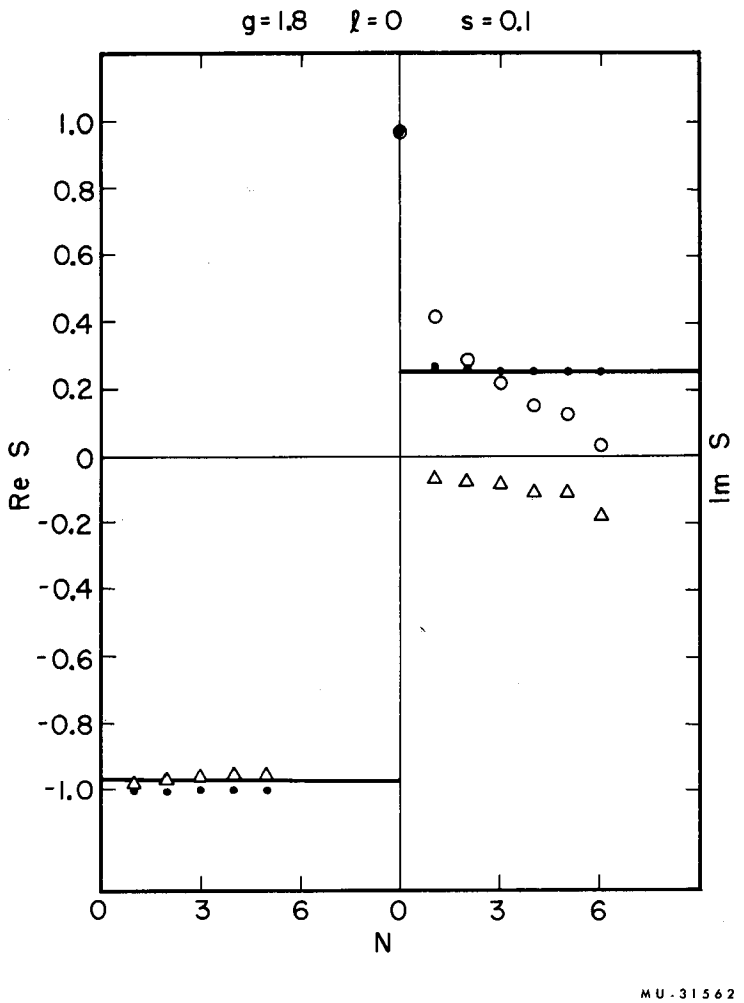

Fig. 25

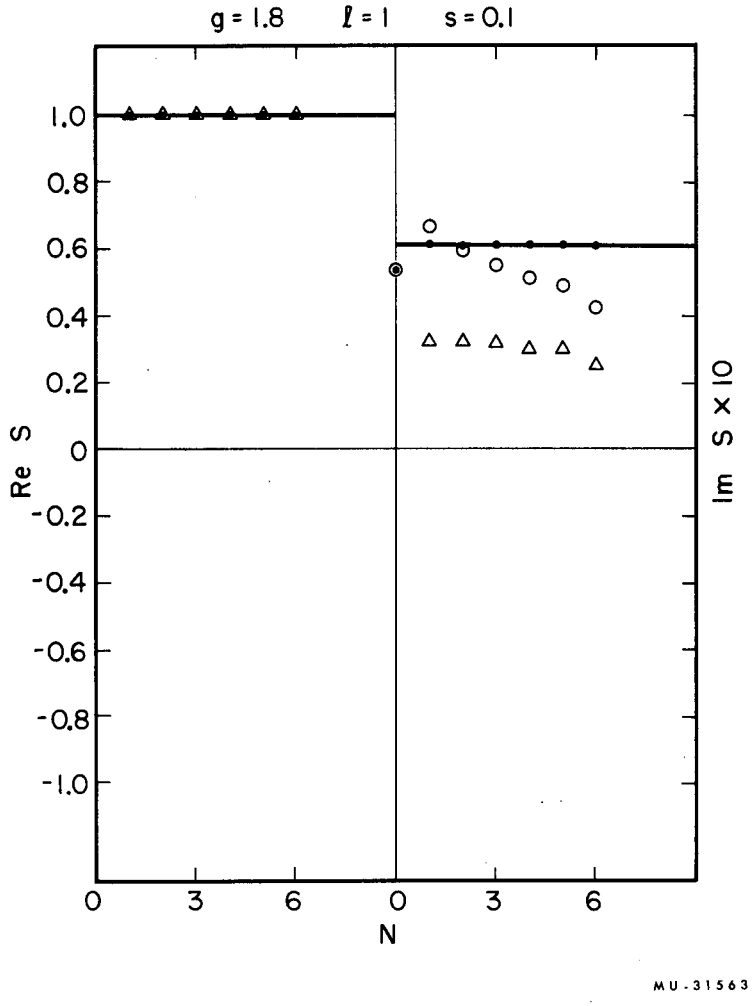
g = 1.8 l = 1 s = 0.1
1.0
0.8
0.6
0.4
0.2
0
-0.2
-0.4
-0.6
-0.8
-1.0
Re S
Im S X 10
0
3
6
0
3
6
N
MU-31563

Fig. 26

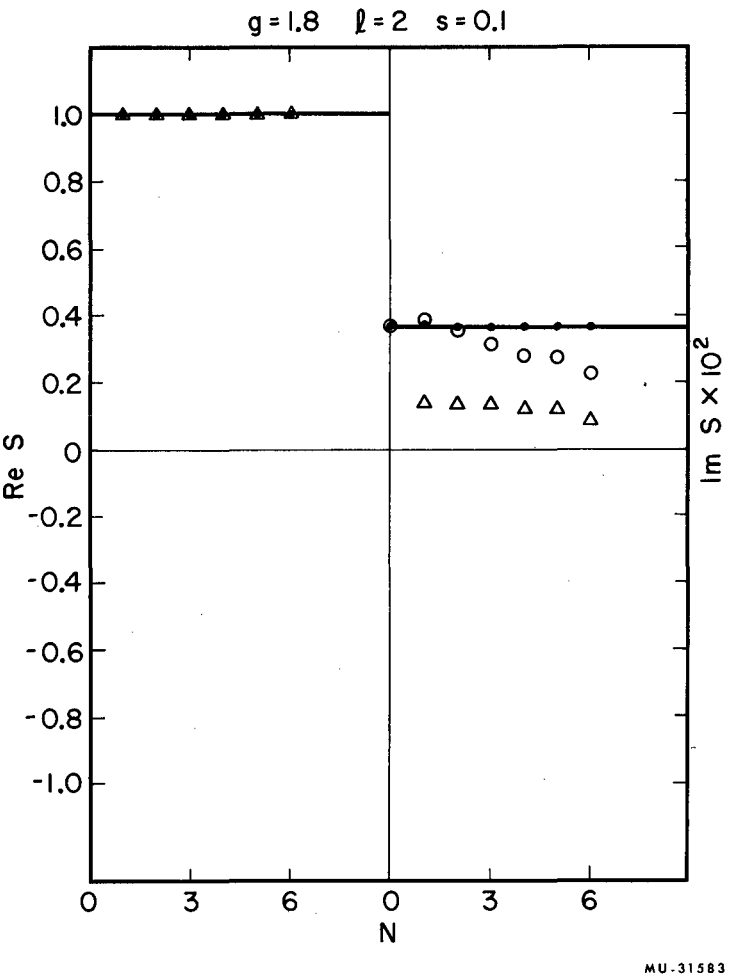
g = 1.8 ℓ = 2 s = 0.1
1.0
0.8
0.6
0.4
0.2
0
-0.2
-0.4
-0.6
-0.8
-1.0
Re S
Im S X 10²
0
3
6
0
3
6
N
MU-31583

Fig. 27

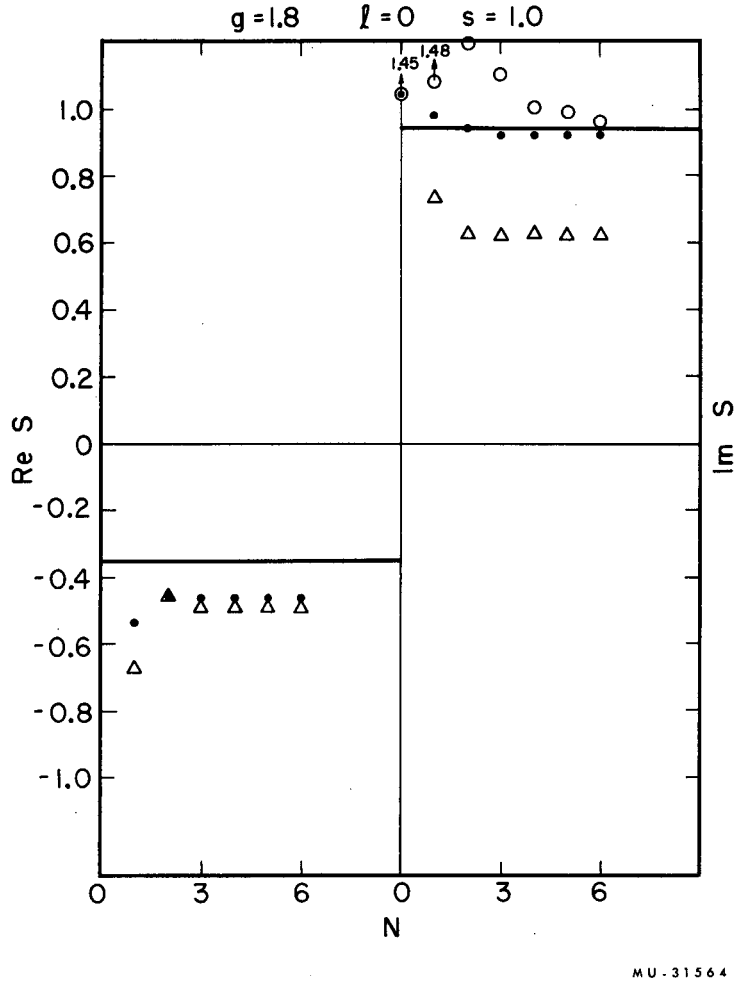
g = 1.8 ℓ = 0 s = 1.0
1.45
1.48
1.0
0.8
0.6
0.4
0.2
0
-0.2
-0.4
-0.6
-0.8
-1.0
Re S
Im S
0
3
6
0
3
6
N
MU-31564

Fig. 28

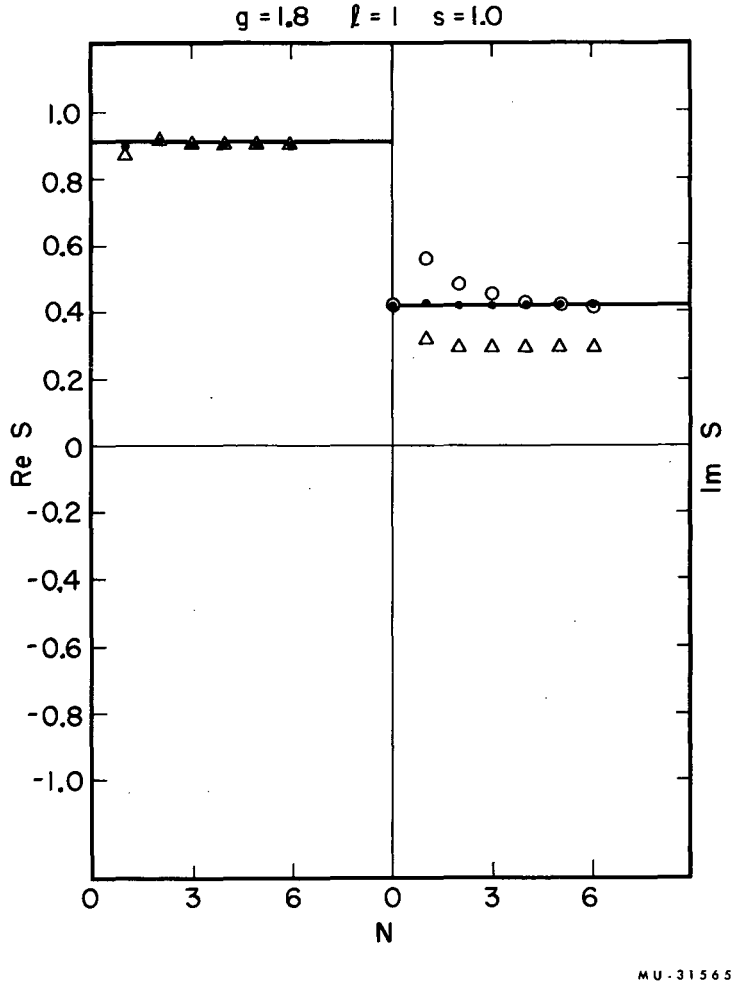

Fig. 29

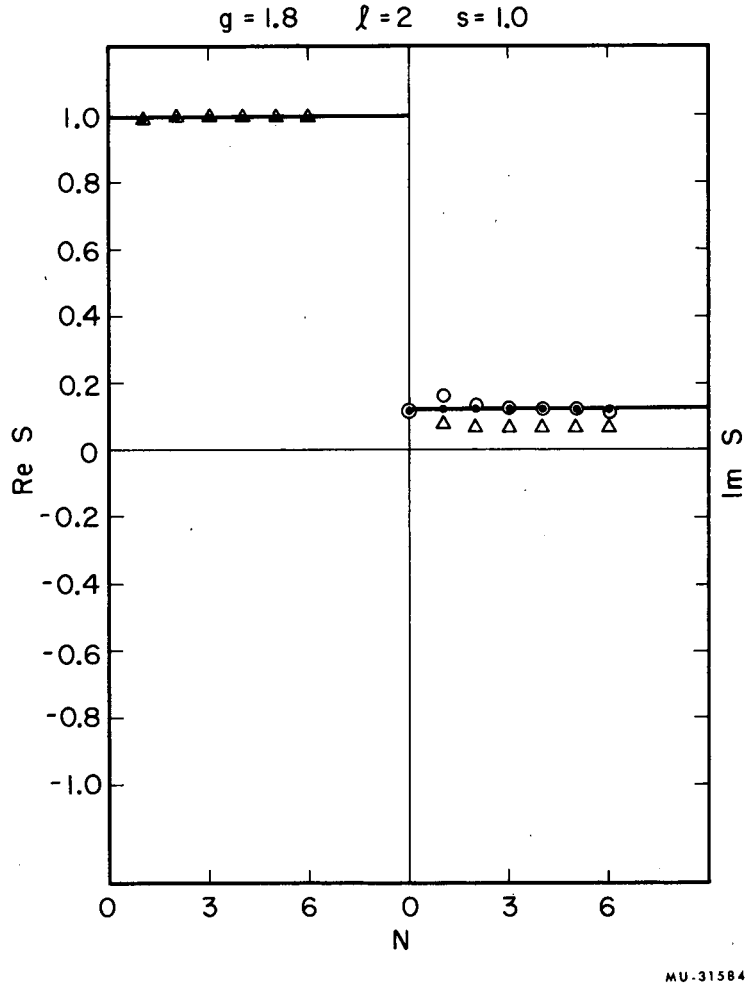

Fig. 30

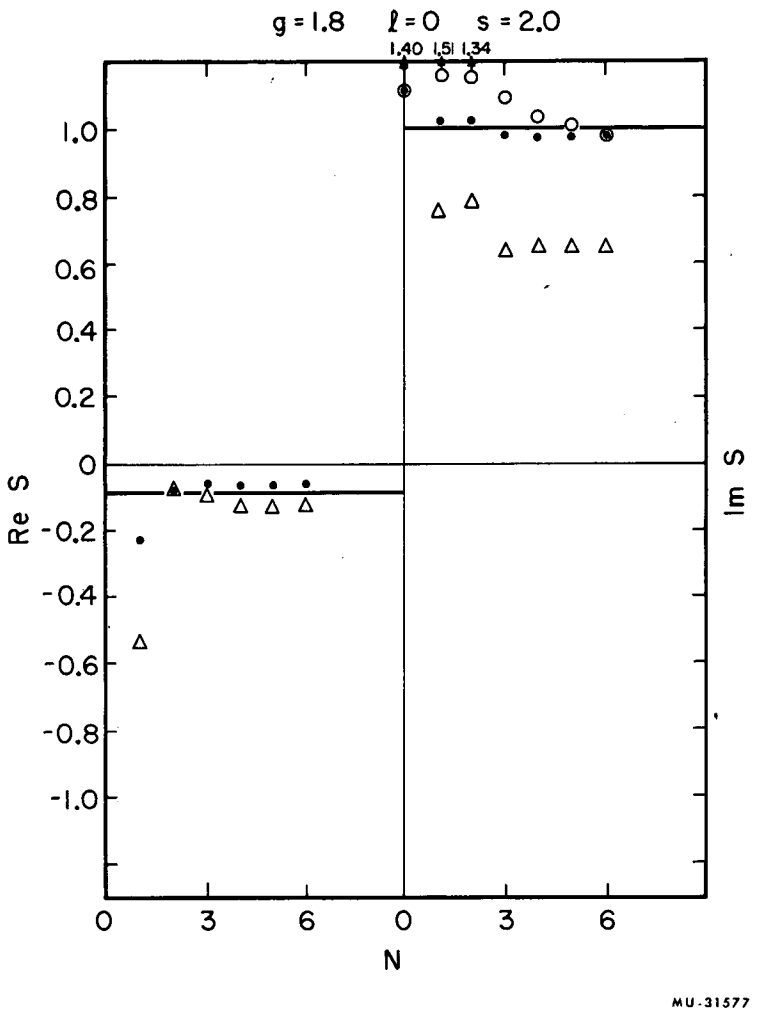
g = 1.8 ℓ = 0 s = 2.0
1.40 1.51 1.34
1.0
0.8
0.6
0.4
0.2
0
-0.2
-0.4
-0.6
-0.8
-1.0
Re S
Im S
0
3
6
0
3
6
N
MU-31577

Fig. 31

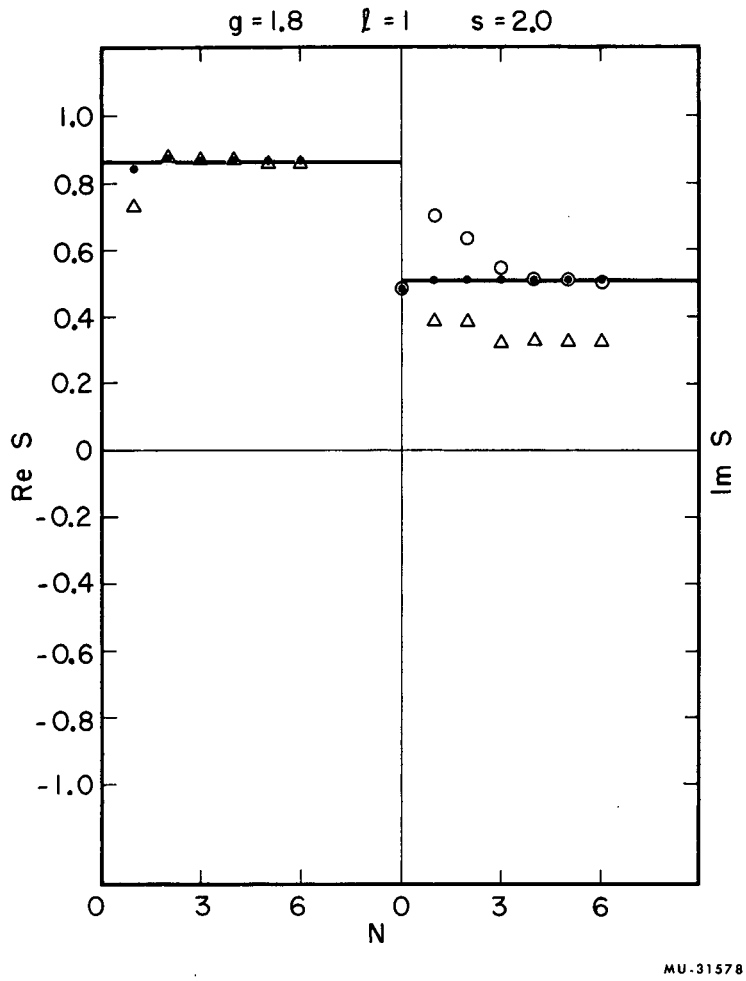

Fig. 32

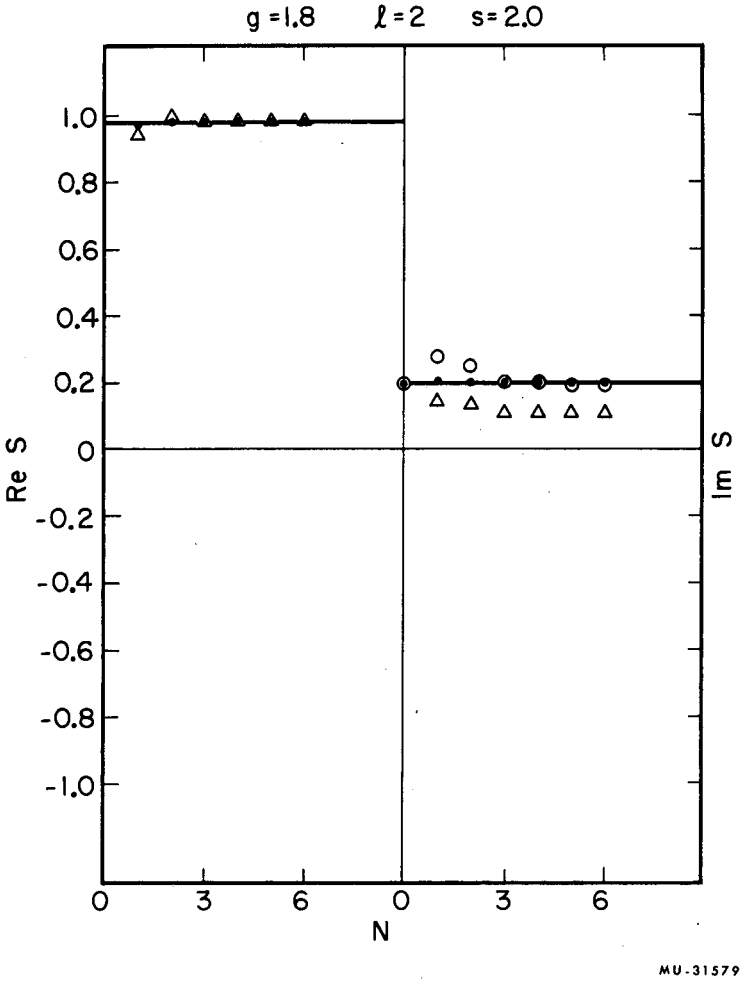

Fig. 33

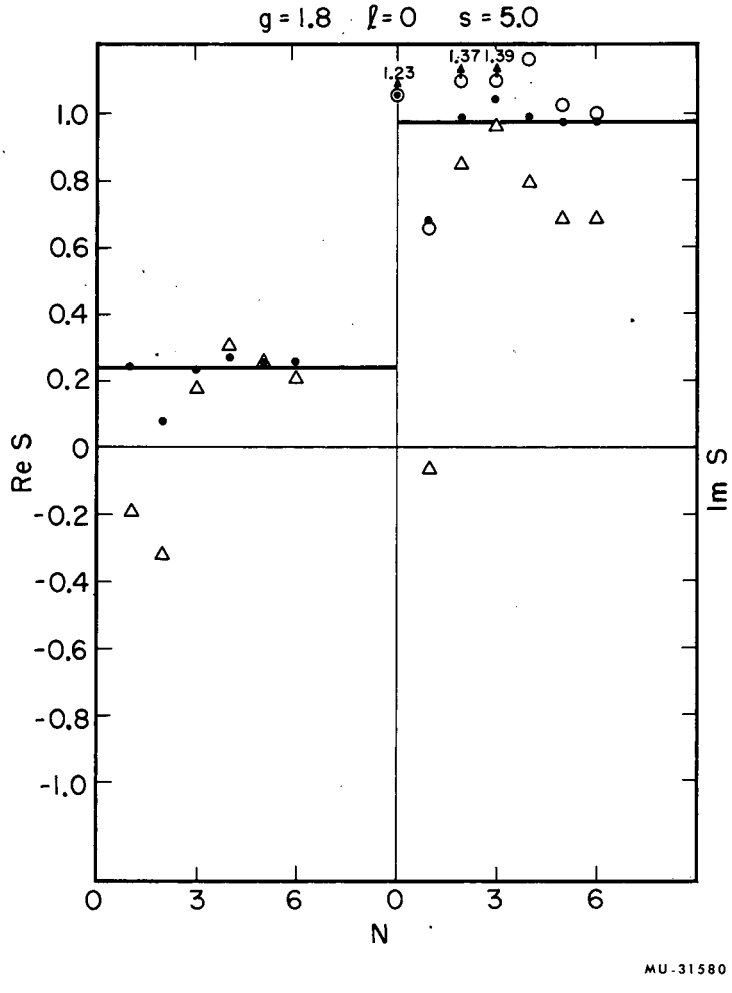
g = 1.8 ℓ = 0 s = 5.0
1.23
1.37 1.39
1.0
0.8
0.6
0.4
0.2
0
-0.2
-0.4
-0.6
-0.8
-1.0
Re S
Im S
0
3
6
0
3
6
N
MU-31580

Fig. 34

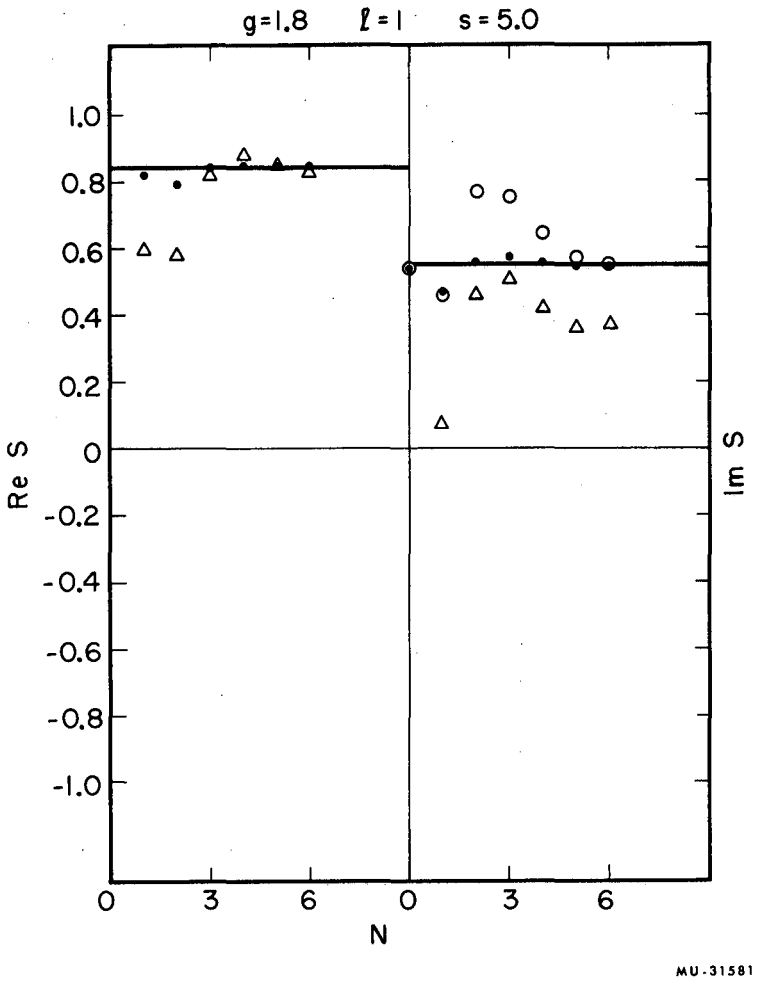

Fig. 35

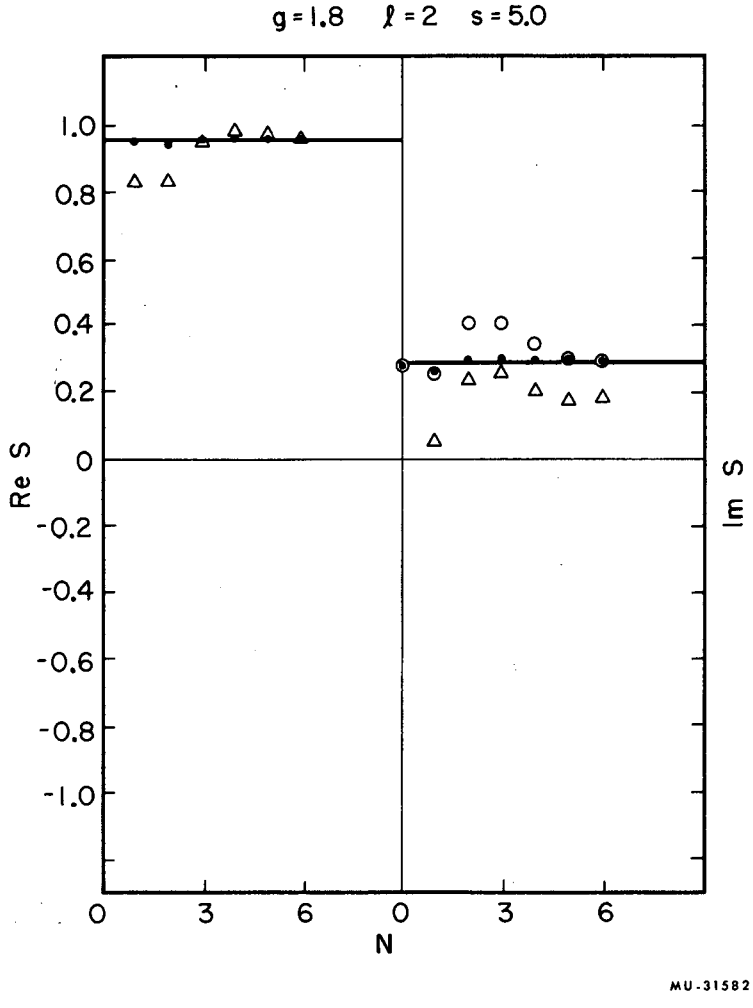

Fig. 36

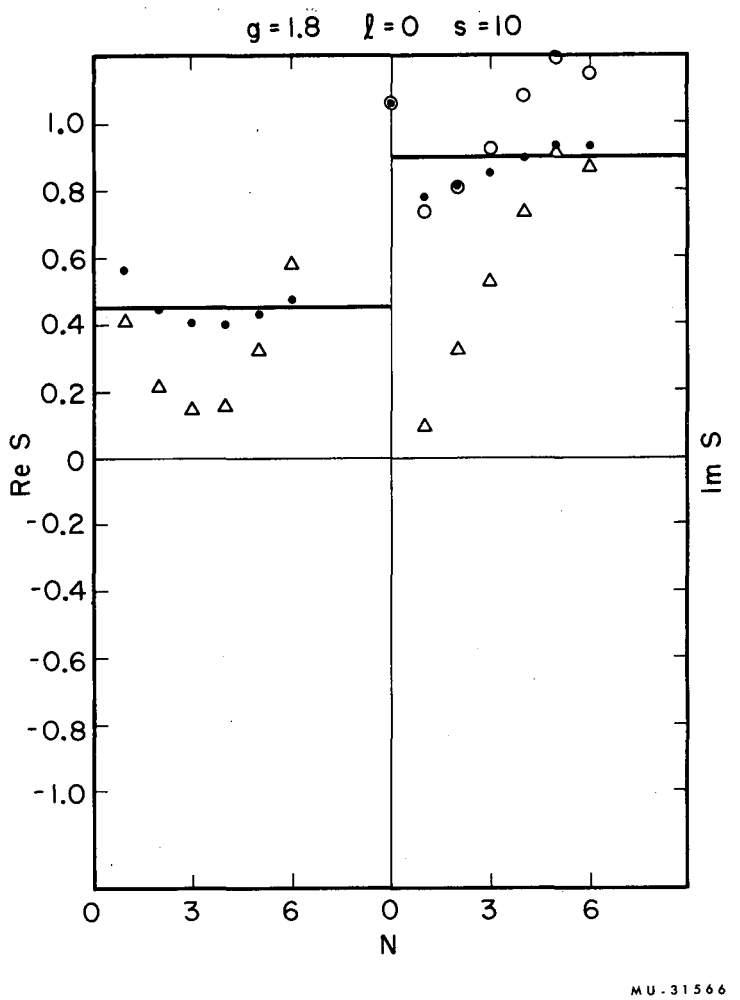

Fig. 37

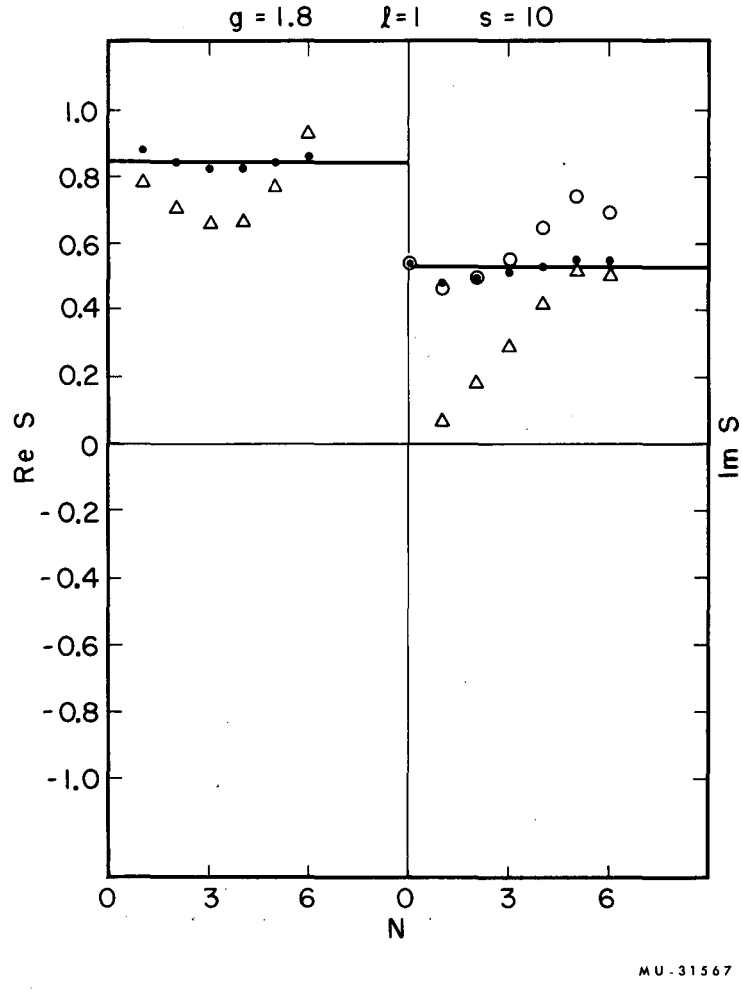

Fig. 38

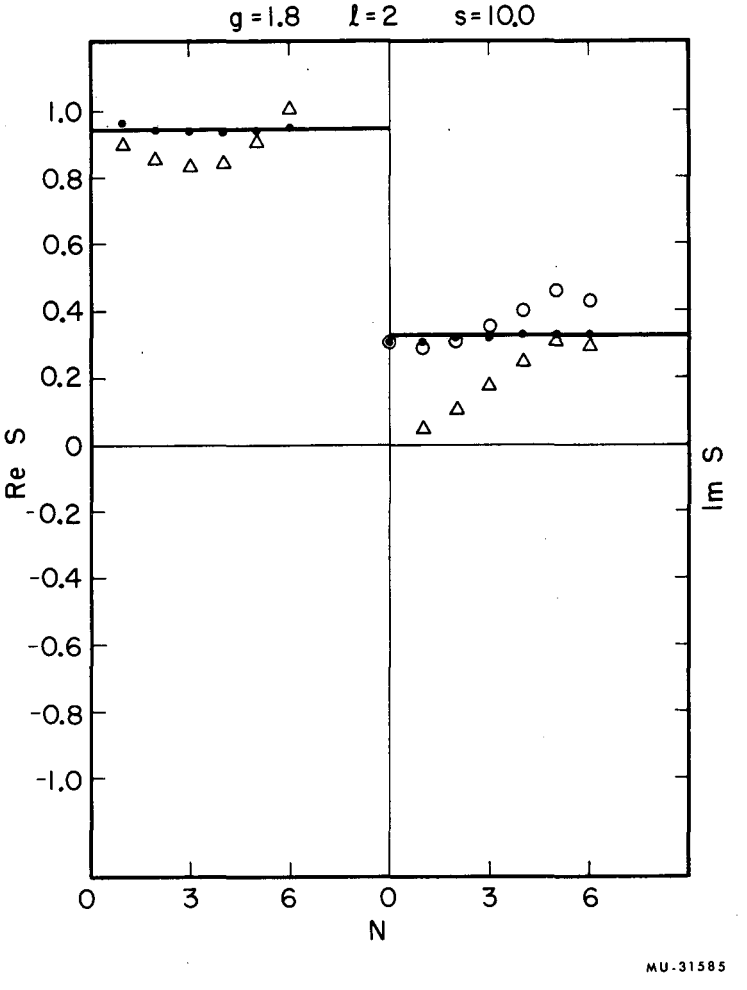
g = 1.8 ℓ = 2 s = 10.0
1.0
0.8
0.6
0.4
0.2
0
-0.2
-0.4
-0.6
-0.8
-1.0
Re S
Im S
0
3
6
0
3
6
N
MU-31585

Fig. 39

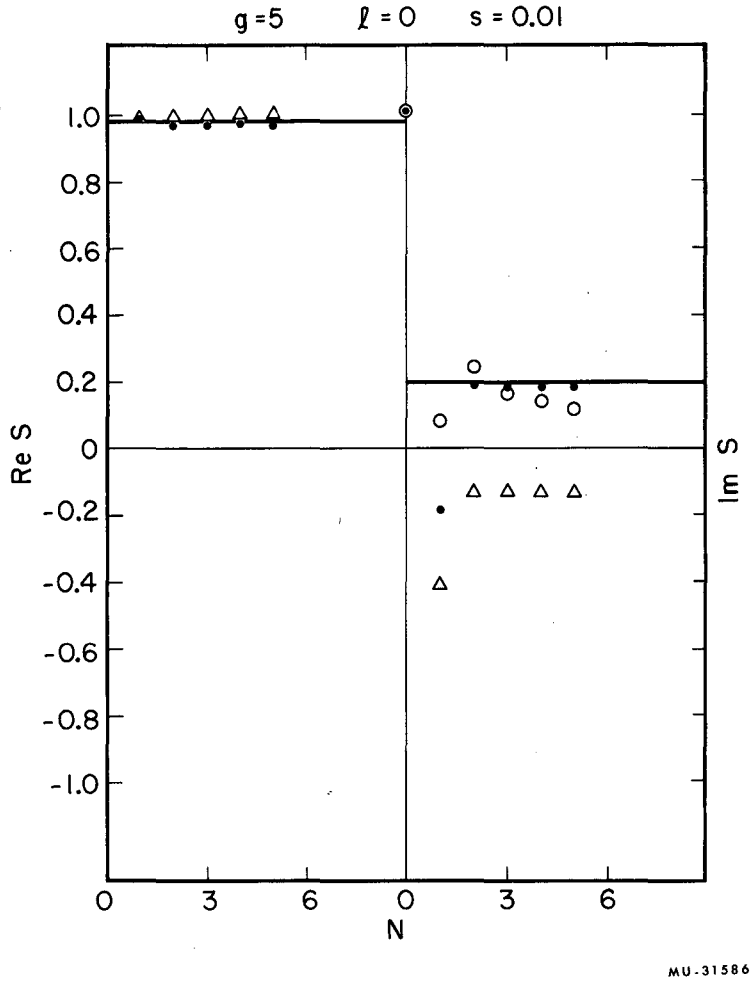

Fig. 40

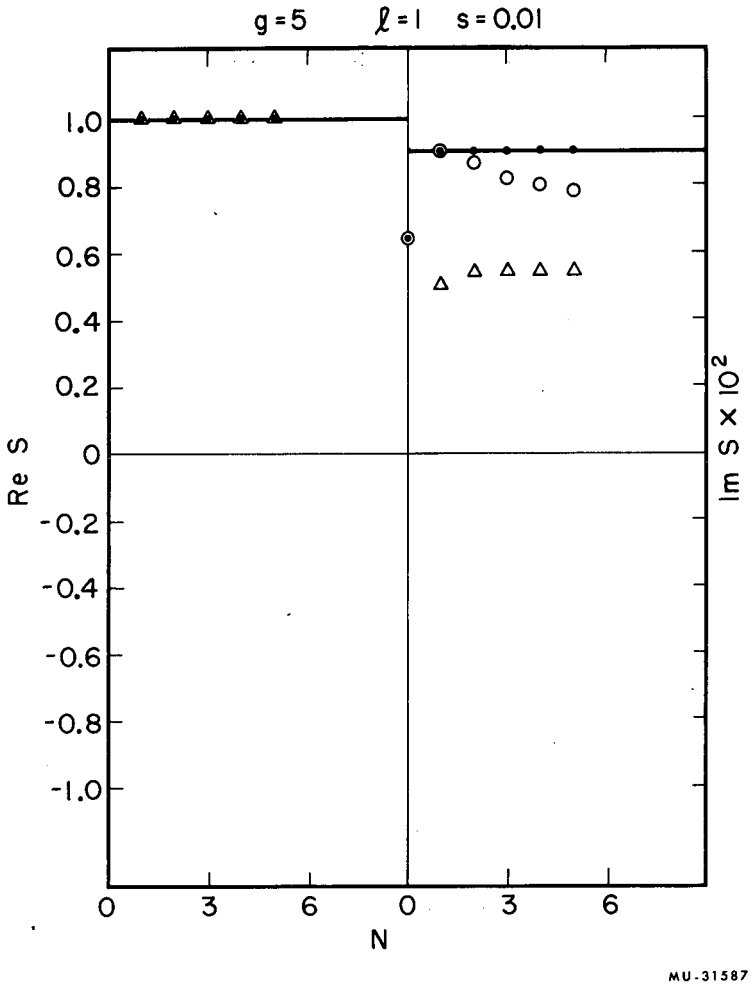
g=5 ℓ=1 s=0.01
1.0
0.8
0.6
0.4
0.2
0
-0.2
-0.4
-0.6
-0.8
-1.0
Re S
Im S x 10²
0
3
6
0
3
6
N
MU-31587

Fig. 41

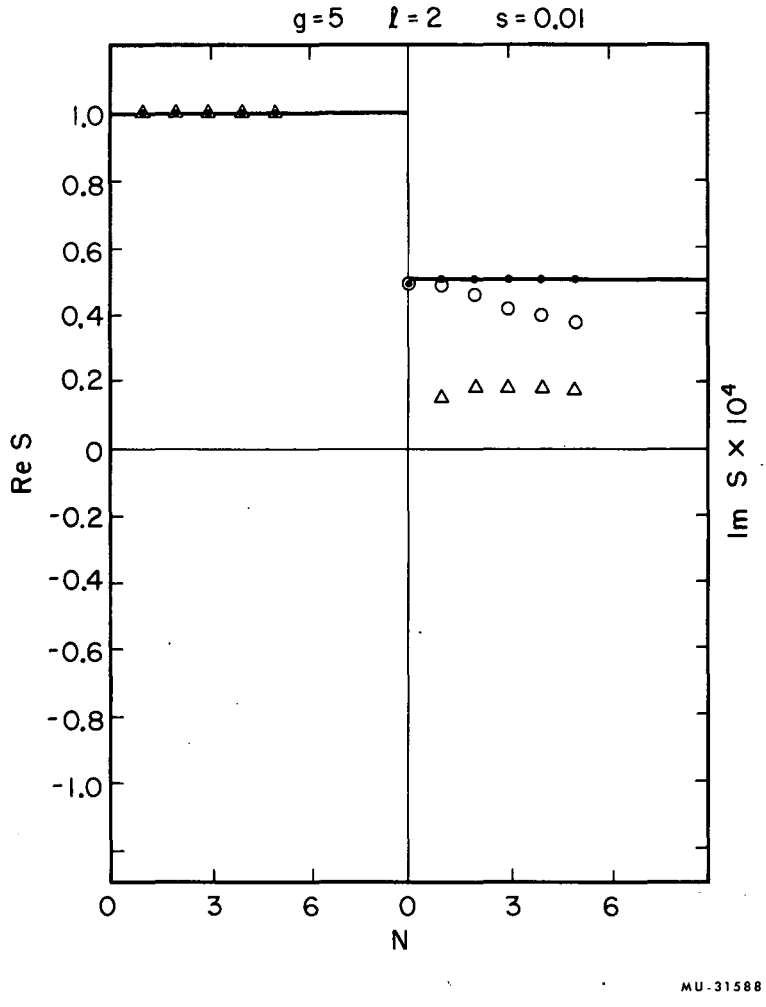
g=5 ℓ=2 s=0.01
1.0
0.8
0.6
0.4
0.2
0
-0.2
-0.4
-0.6
-0.8
-1.0
Re S
Im S x 10⁴
0
3
6
0
3
6
N
MU-31588

Fig. 42

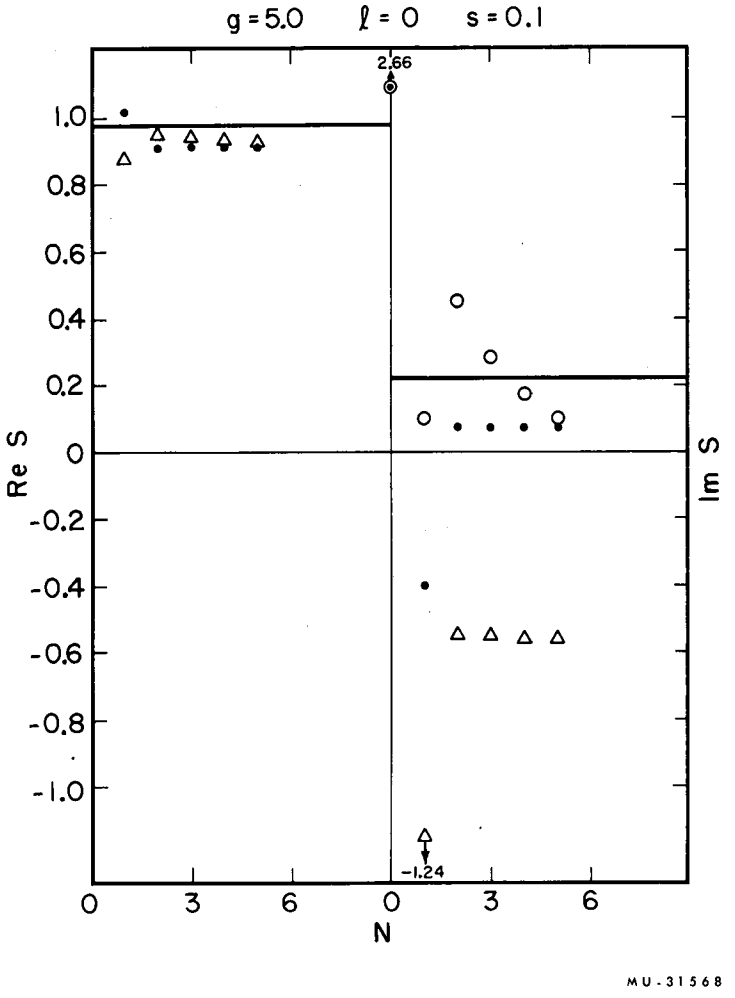
g = 5.0 ℓ = 0 s = 0.1
2.66
1.0
0.8
0.6
0.4
0.2
0
-0.2
-0.4
-0.6
-0.8
-1.0
Re S
Im S
-1.24
0
3
6
0
3
6
N
MU-31568

Fig. 43

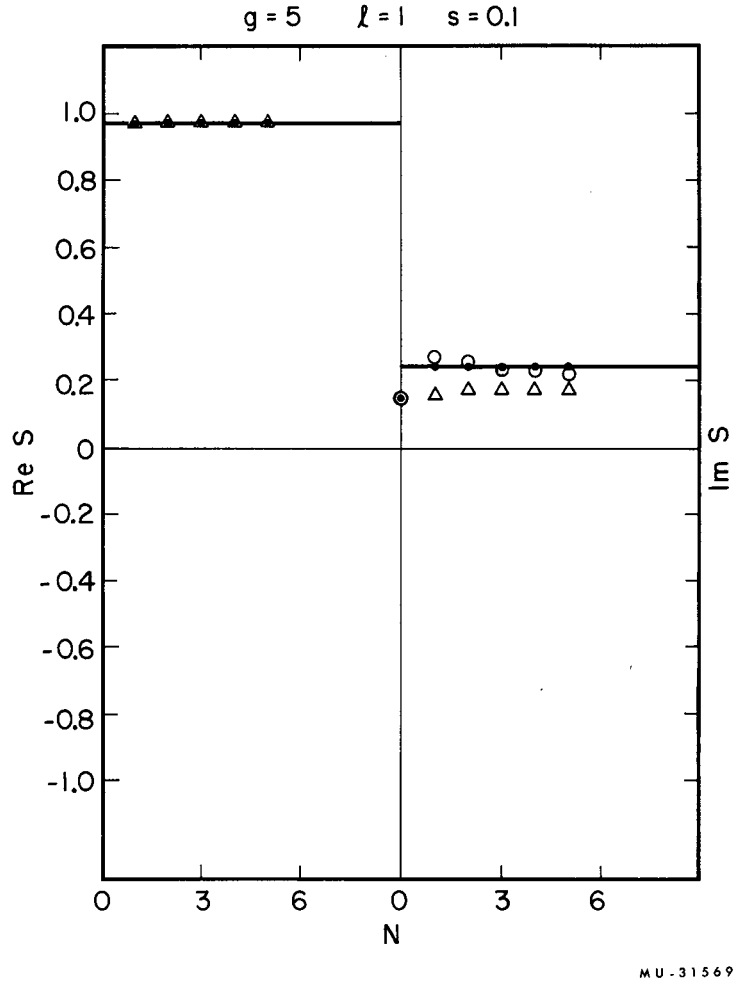

Fig. 44

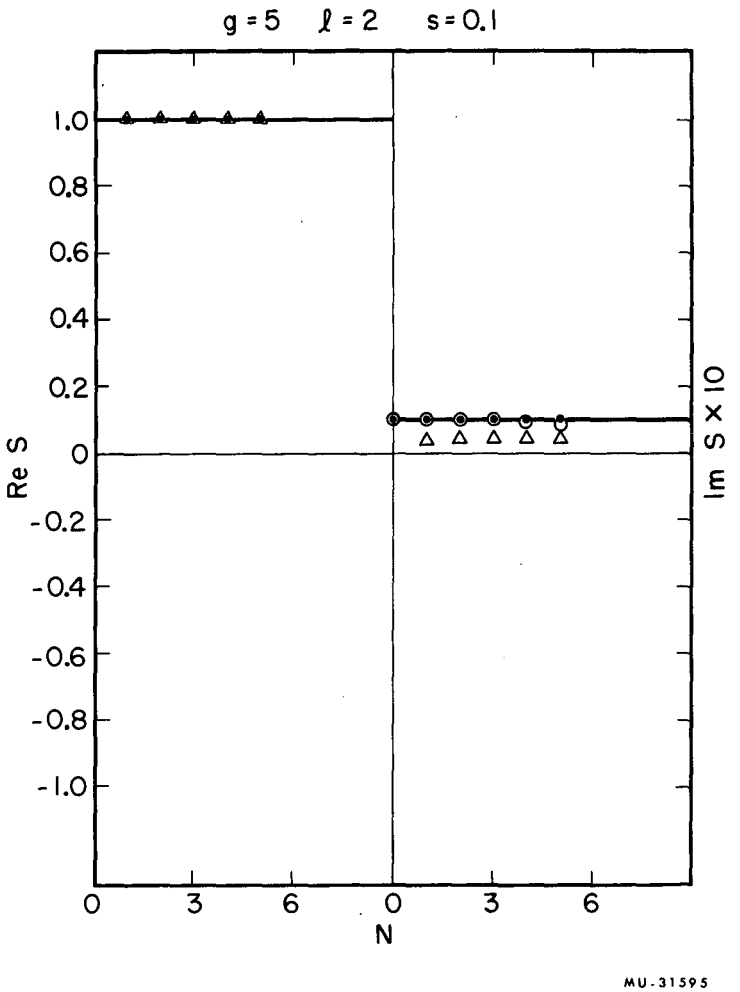
g = 5 ℓ = 2 s = 0.1
1.0
0.8
0.6
0.4
0.2
0
-0.2
-0.4
-0.6
-0.8
-1.0
Re S
Im S X 10
0
3
6
0
3
6
N
MU-31595

Fig. 45

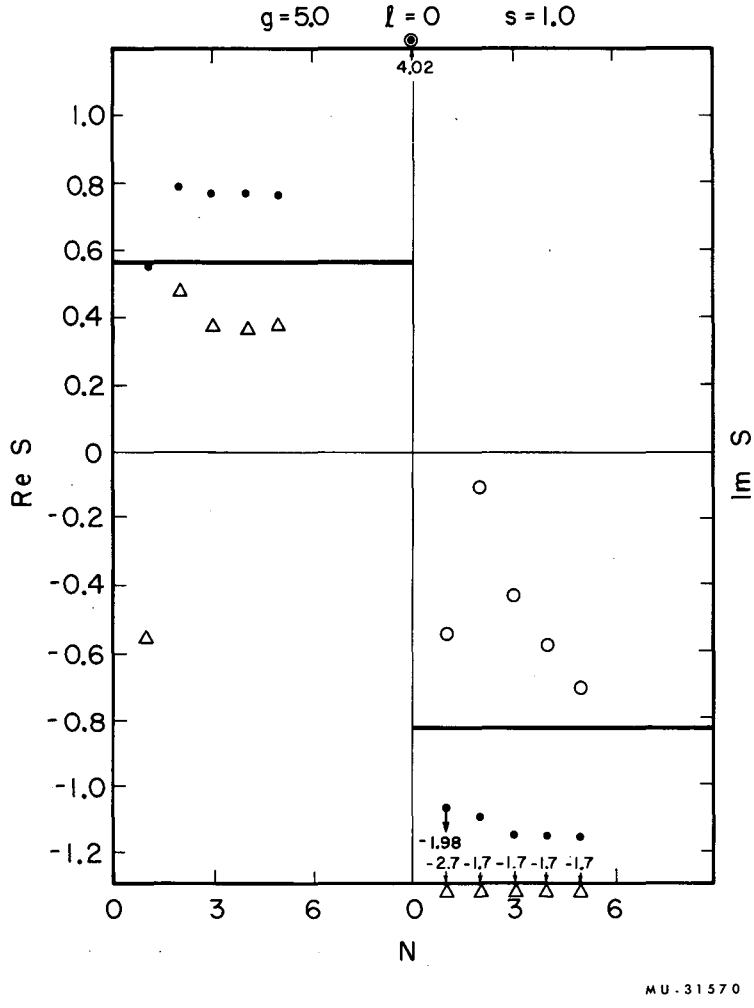
g=5.0
ℓ = 0
s = 1.0
4.02
1.0
0.8
0.6
0.4
0.2
0
-0.2
-0.4
-0.6
-0.8
-1.0
-1.2
Re S
Im S
-1.98
-2.7 -1.7 -1.7 -1.7 -1.7
0
3
6
0
3
6
N
MU-31570

Fig. 46

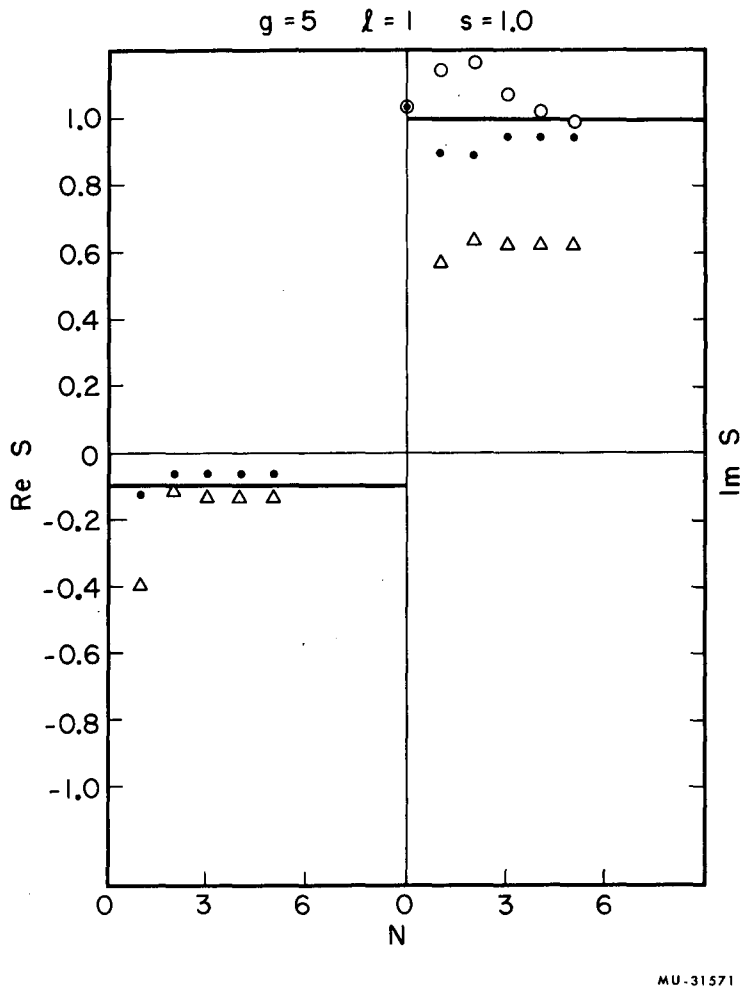

Fig. 47

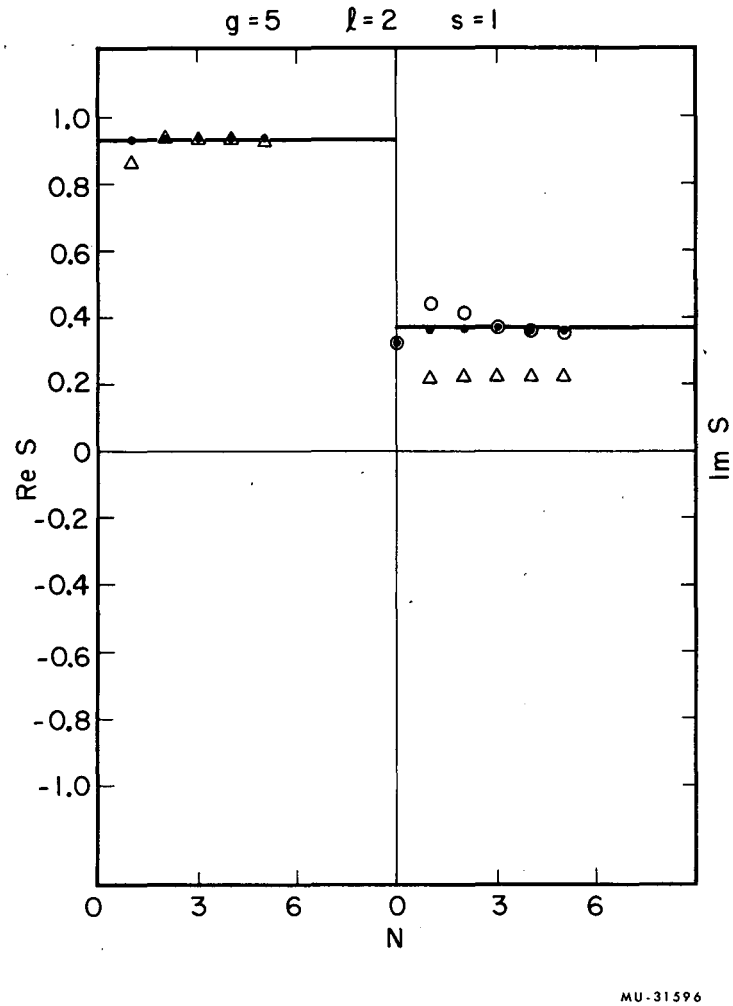

Fig. 48

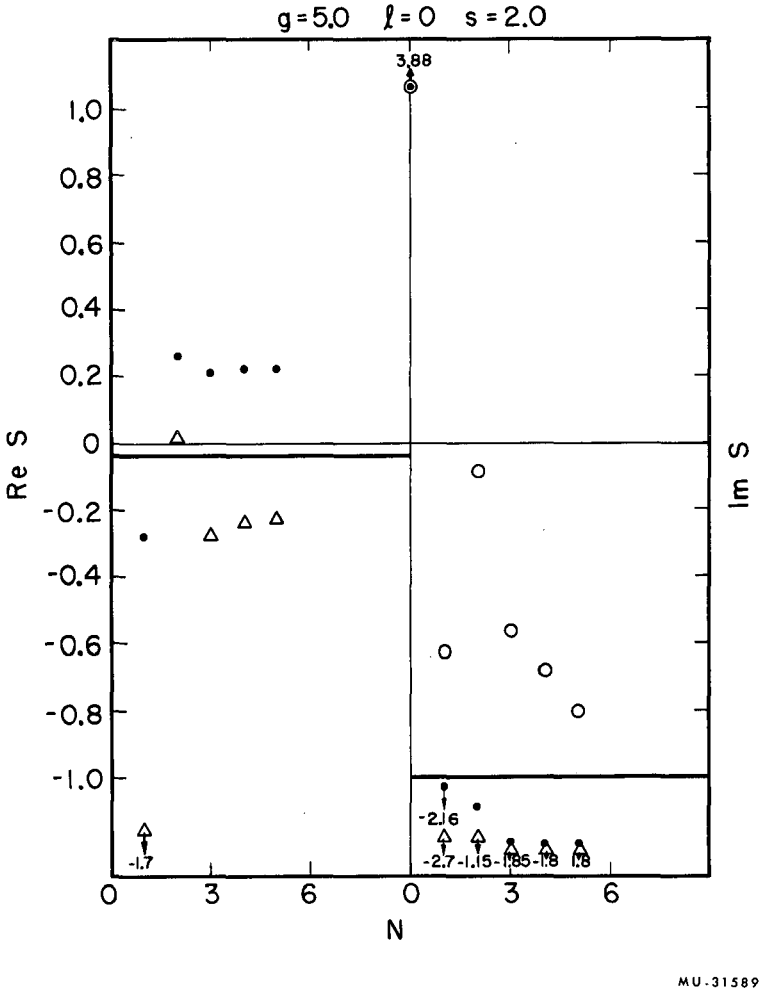
g=5.0 ℓ=0 s=2.0
3.88
1.0
0.8
0.6
0.4
0.2
0
-0.2
-0.4
-0.6
-0.8
-1.0
Re S
Im S
-1.7
-2.16
-2.7
-1.15
-1.85
-1.8
-1.8
0
3
6
0
3
6
N
MU-31589

Fig. 49

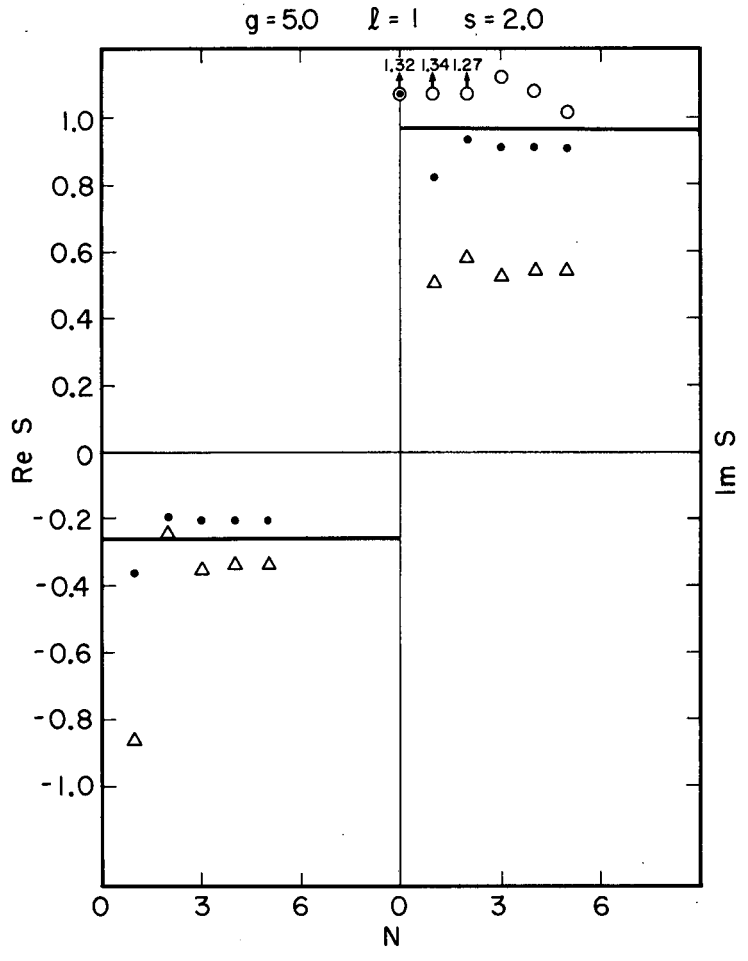
g = 5.0 ℓ = 1 s = 2.0
1.32 1.34 1.27
1.0
0.8
0.6
0.4
0.2
0
-0.2
-0.4
-0.6
-0.8
-1.0
Re S
Im S
0 3 6 0 3 6
N
MU-31590

Fig. 50

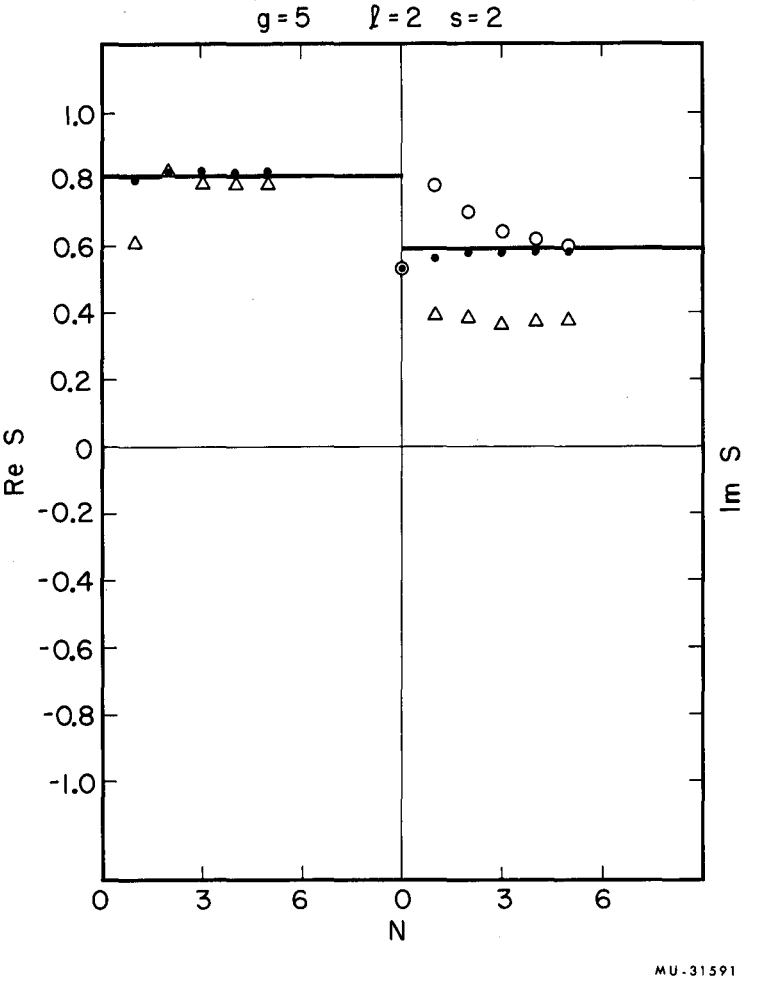

Fig. 51

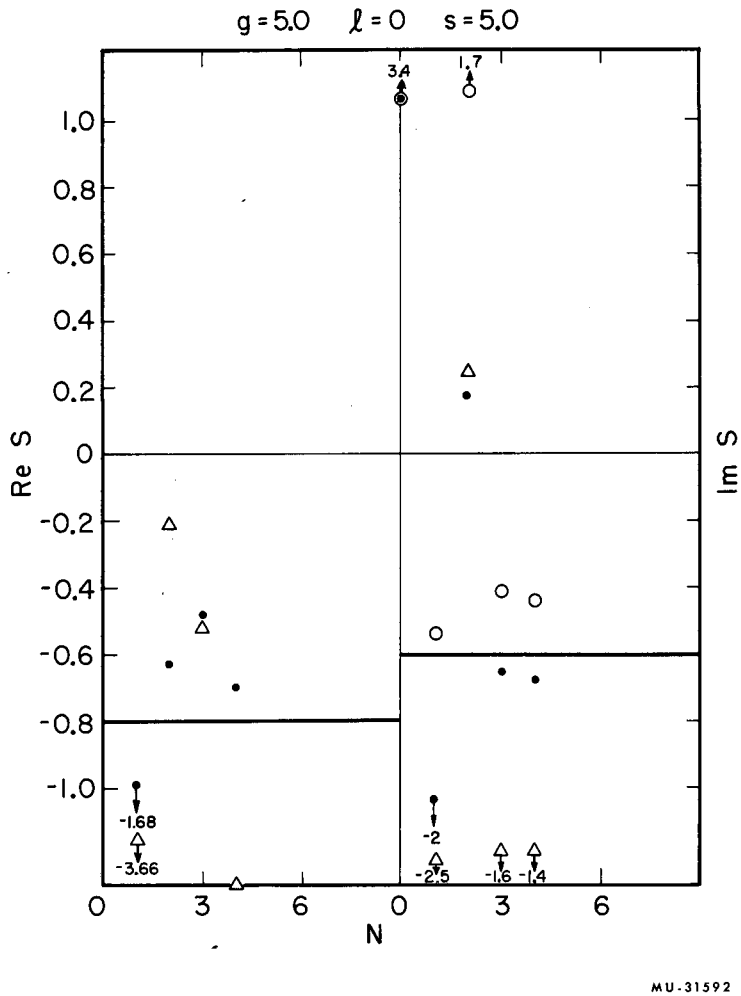

Fig. 52

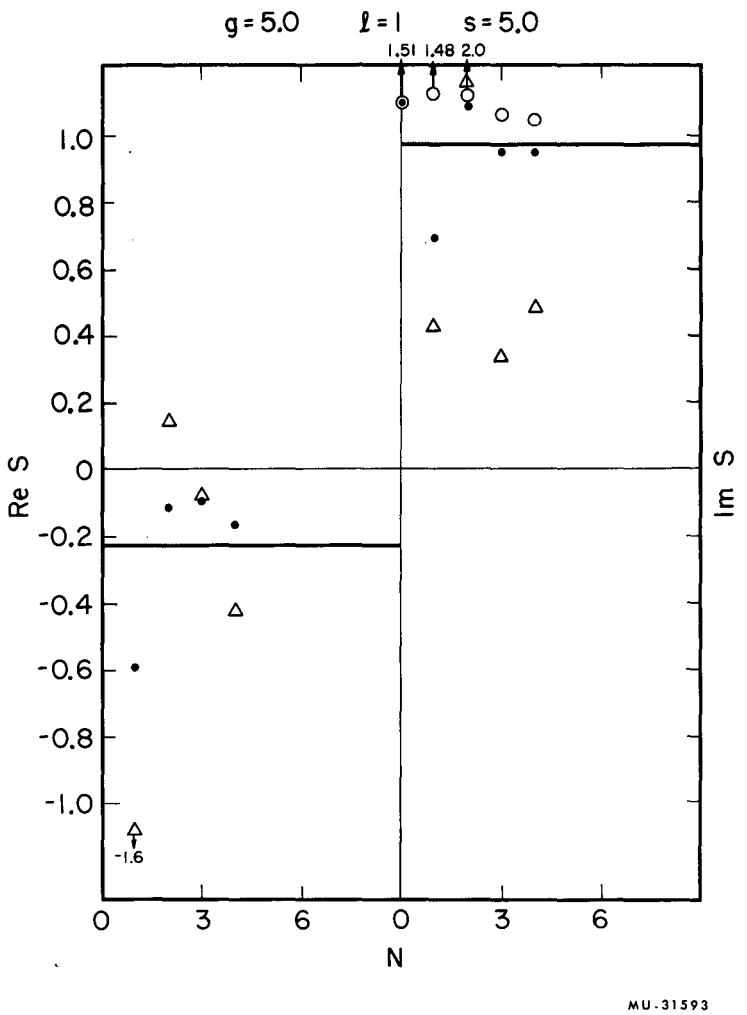
g = 5.0
ℓ = 1
s = 5.0
1.51 1.48 2.0
1.0
0.8
0.6
0.4
0.2
0
-0.2
-0.4
-0.6
-0.8
-1.0
Re S
Im S
-1.6
0
3
6
0
3
6
N
MU-31593

Fig. 53

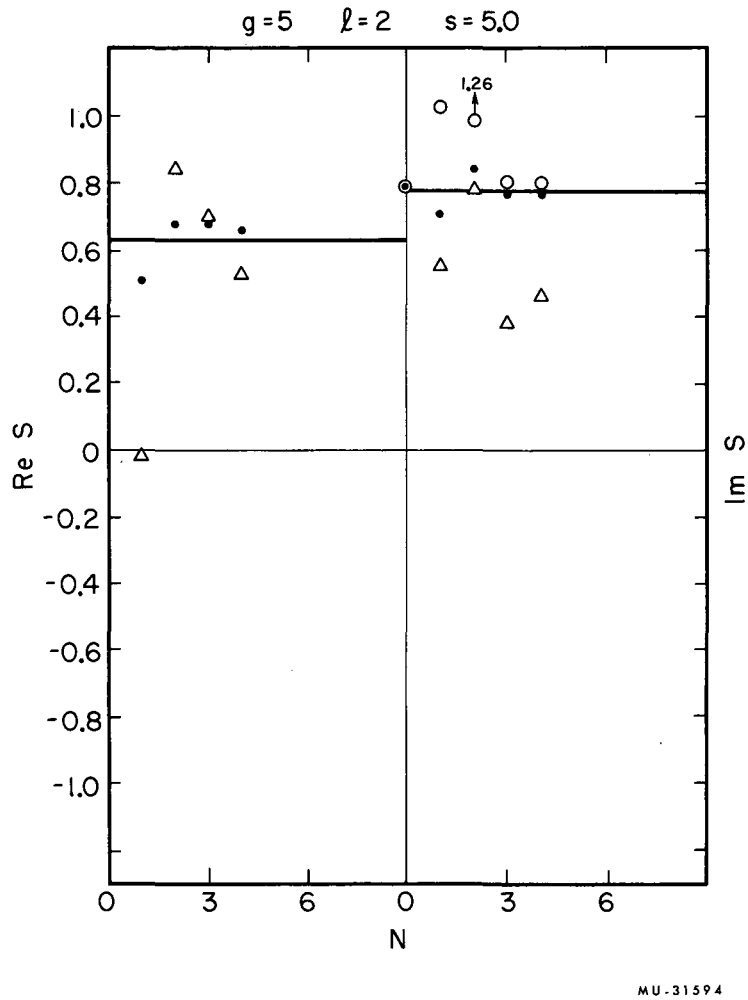
g=5 ℓ=2 s=5.0
1.26
1.0
0.8
0.6
0.4
0.2
0
-0.2
-0.4
-0.6
-0.8
-1.0
Re S
Im S
0
3
6
0
3
6
N
MU-31594

Fig. 54

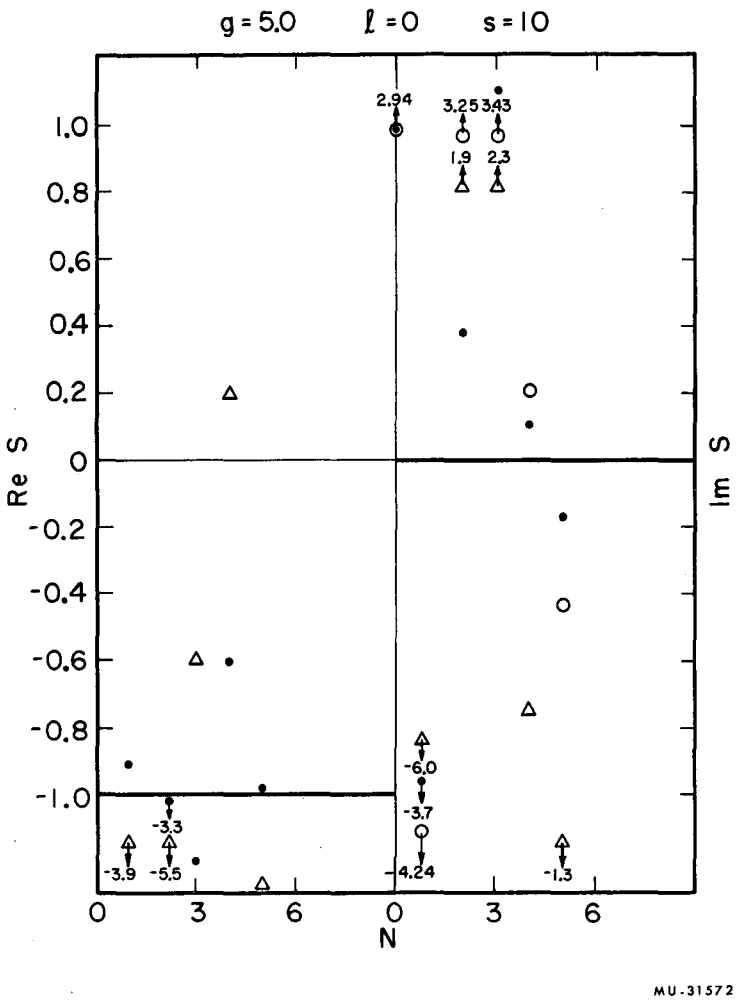
g = 5.0
ℓ = 0
s = 10
Re S
Im S
N
2.94
3.25
3.43
1.9
2.3
-6.0
-3.7
-4.24
-3.3
-3.9
-5.5
-1.3
MU-31572

Fig. 55

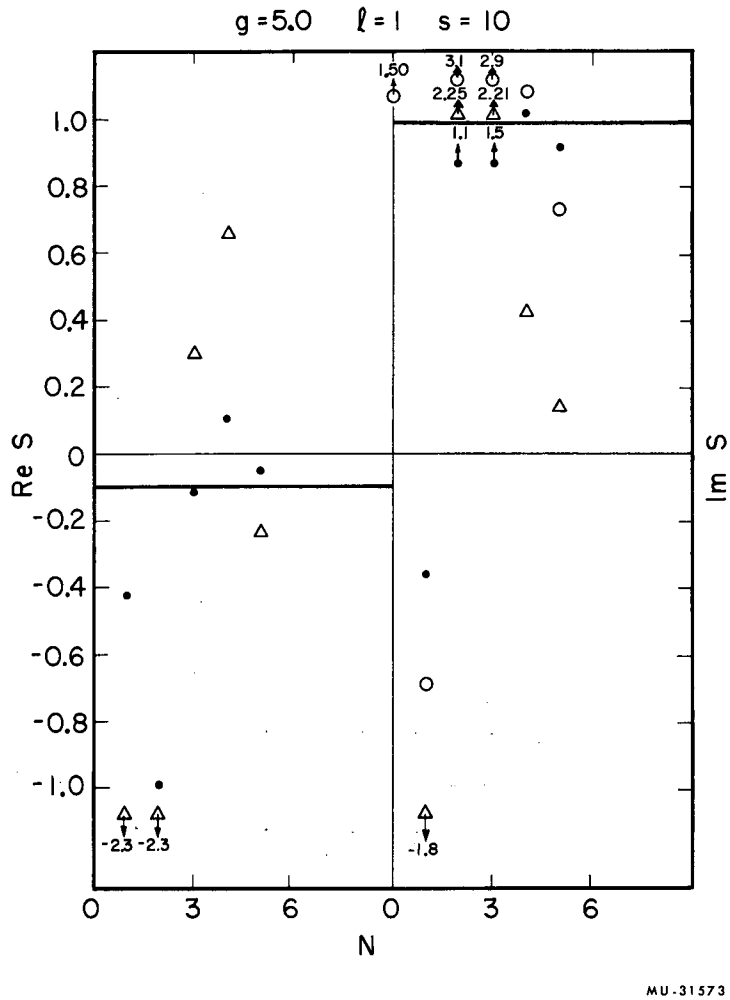
g = 5.0 ℓ = 1 s = 10
1.50
3.1
2.9
2.25
2.21
1.1
1.5
1.0
0.8
0.6
0.4
0.2
0
-0.2
-0.4
-0.6
-0.8
-1.0
Re S
Im S
-2.3
-2.3
-1.8
0
3
6
0
3
6
N
MU-31573

Fig. 56

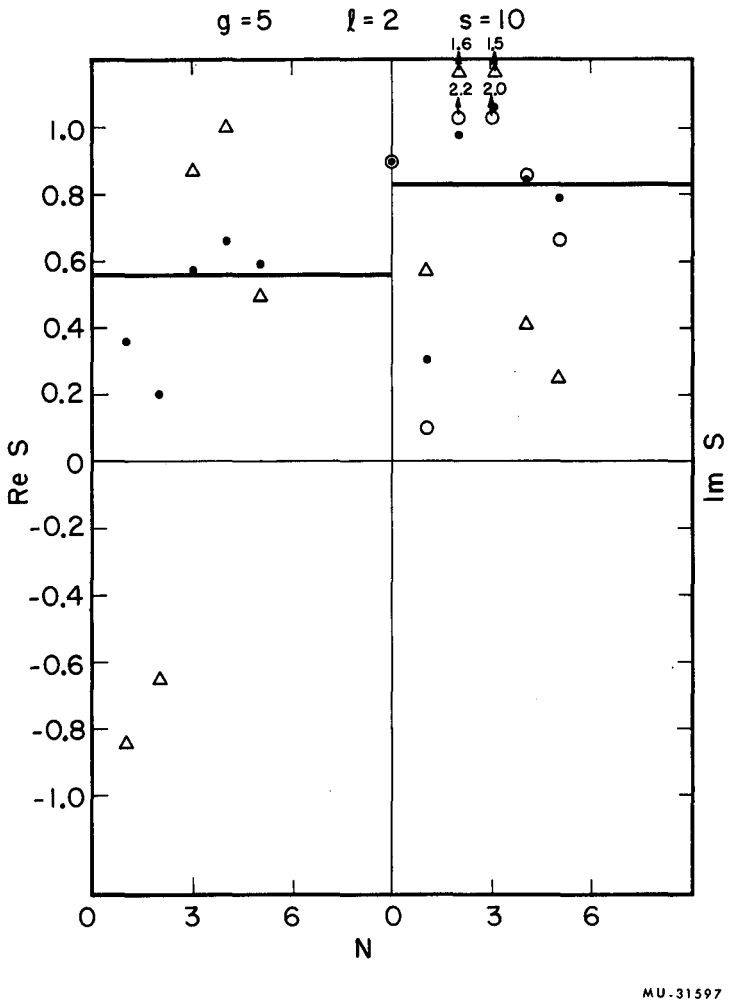
g = 5
l = 2
s = 10
1.6
1.5
2.2
2.0
1.0
0.8
0.6
0.4
0.2
0
-0.2
-0.4
-0.6
-0.8
-1.0
Re S
Im S
0
3
6
0
3
6
N
MU-31597

Fig. 57

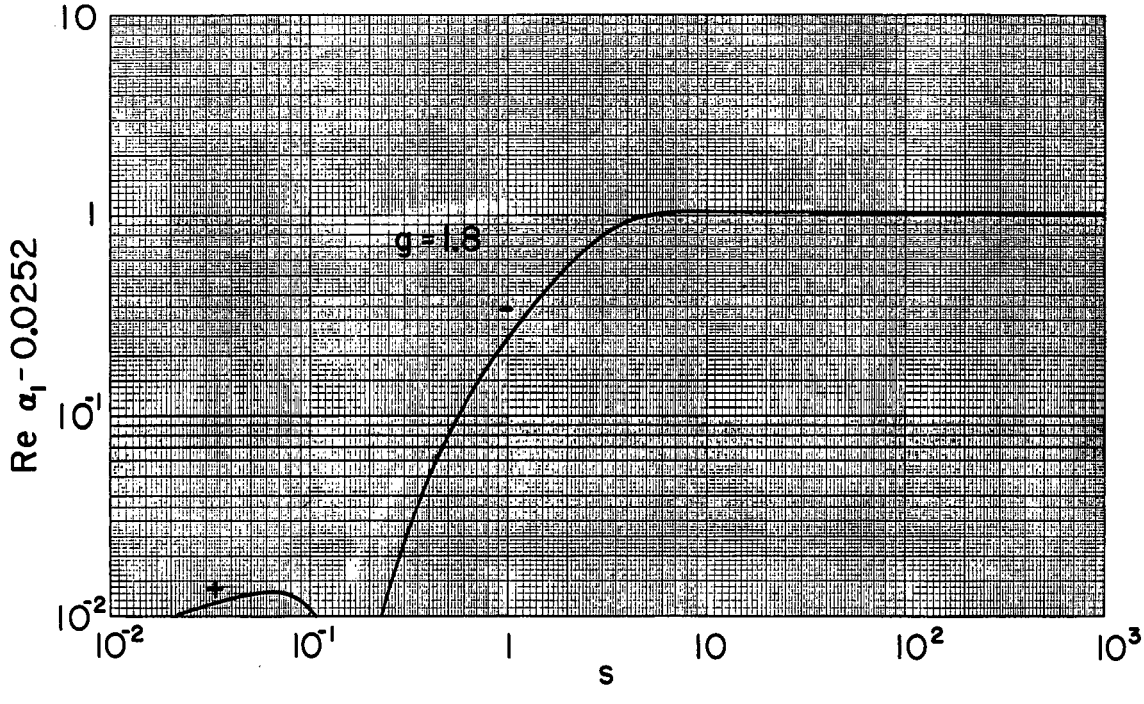

Fig. 58

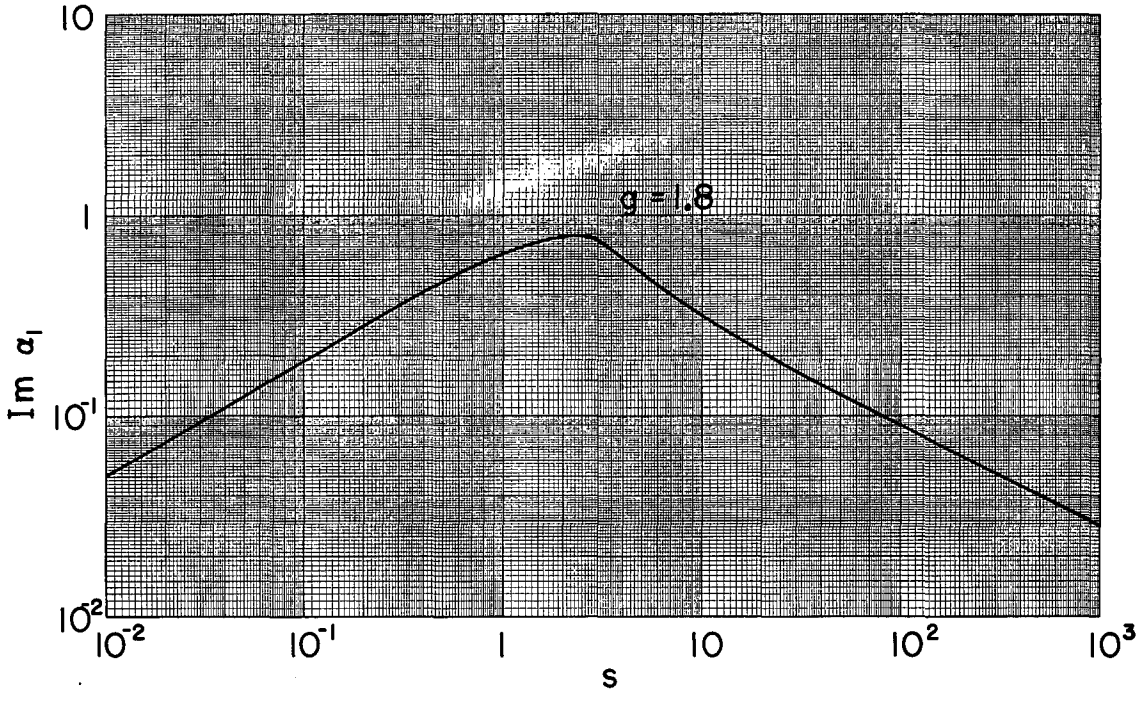

Fig. 59

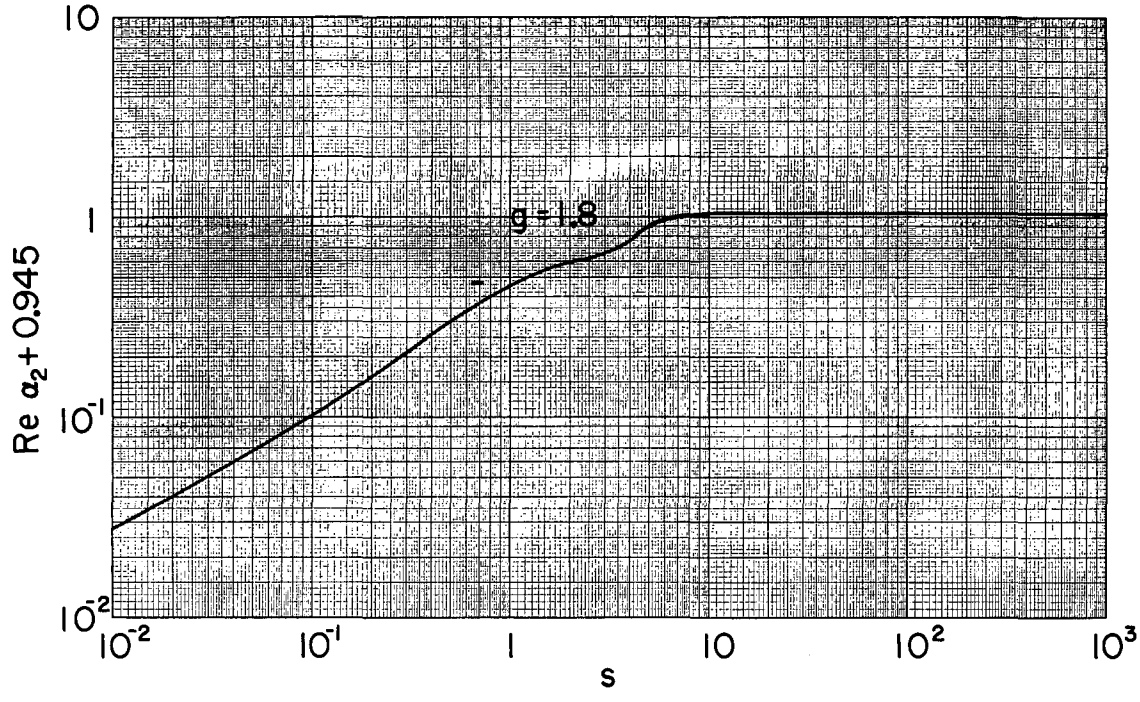

Fig. 60

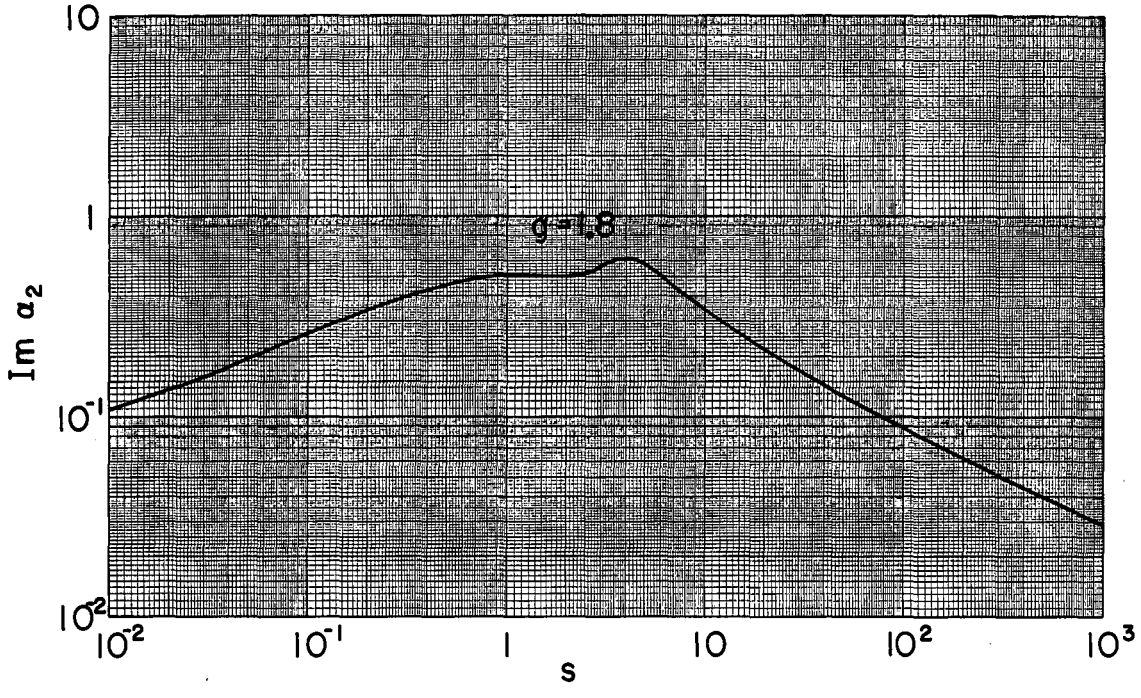

Fig. 61

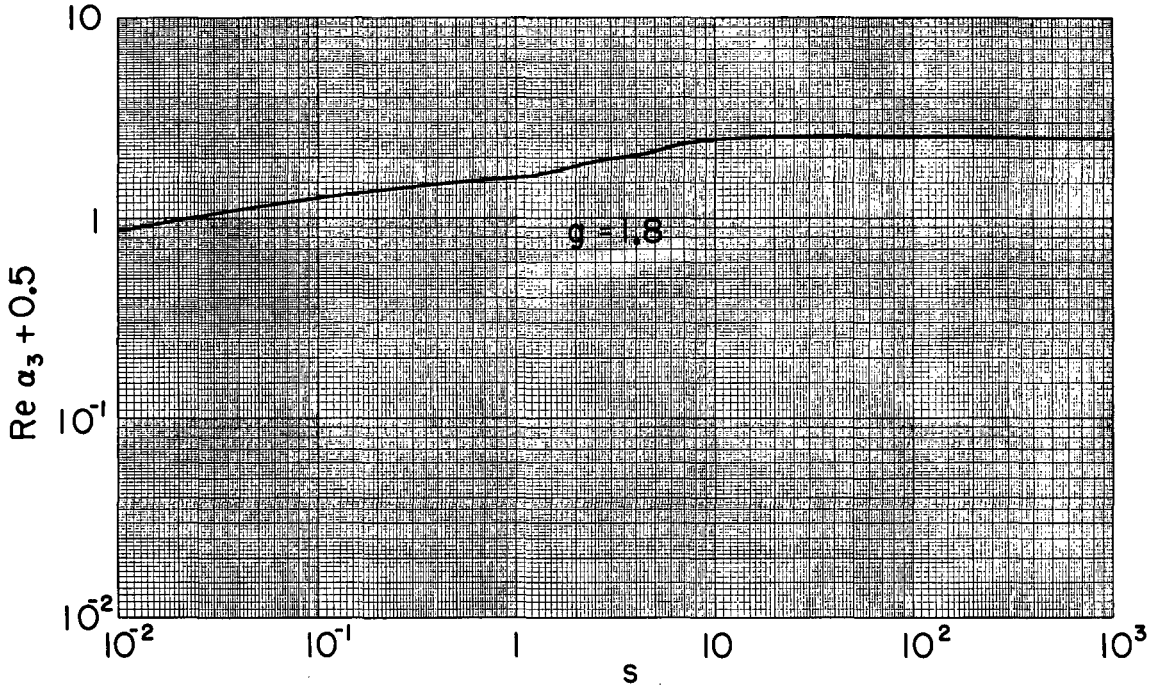

Fig. 62

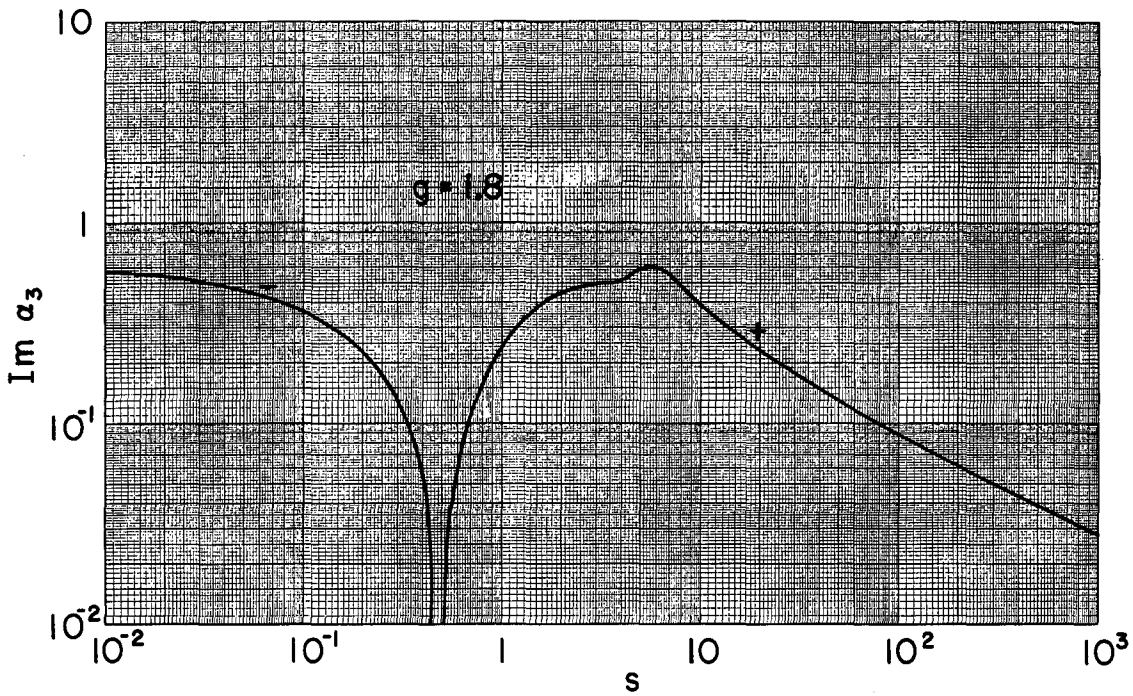

Fig. 63

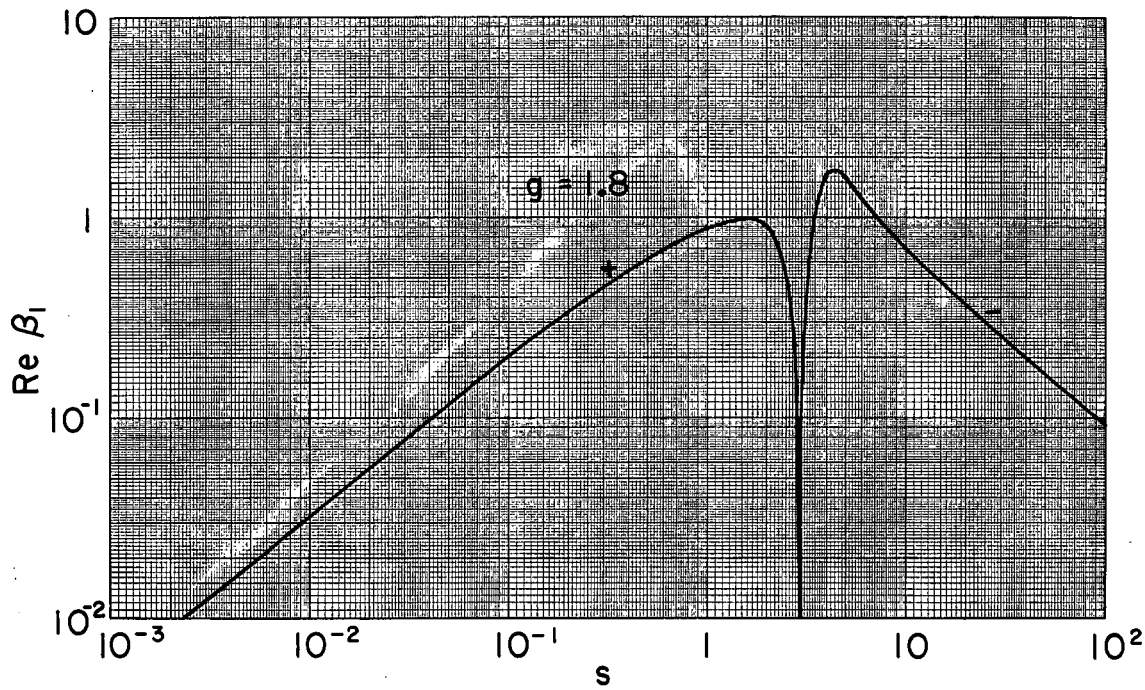

Fig. 64

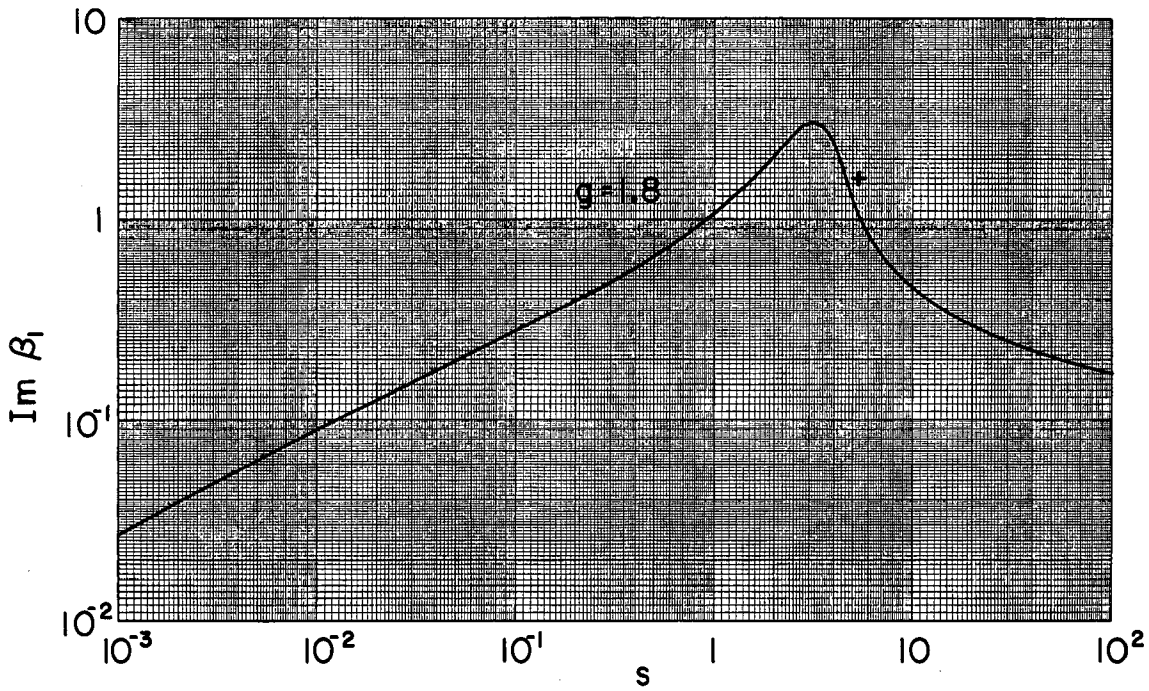

Fig. 65

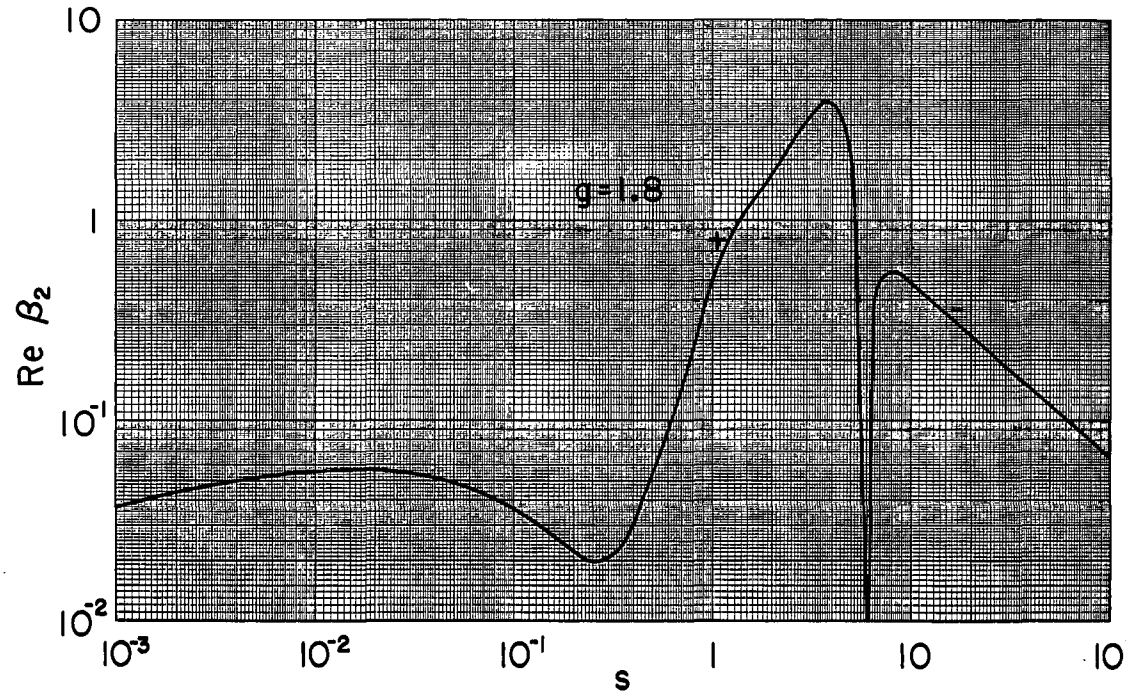

Fig. 66

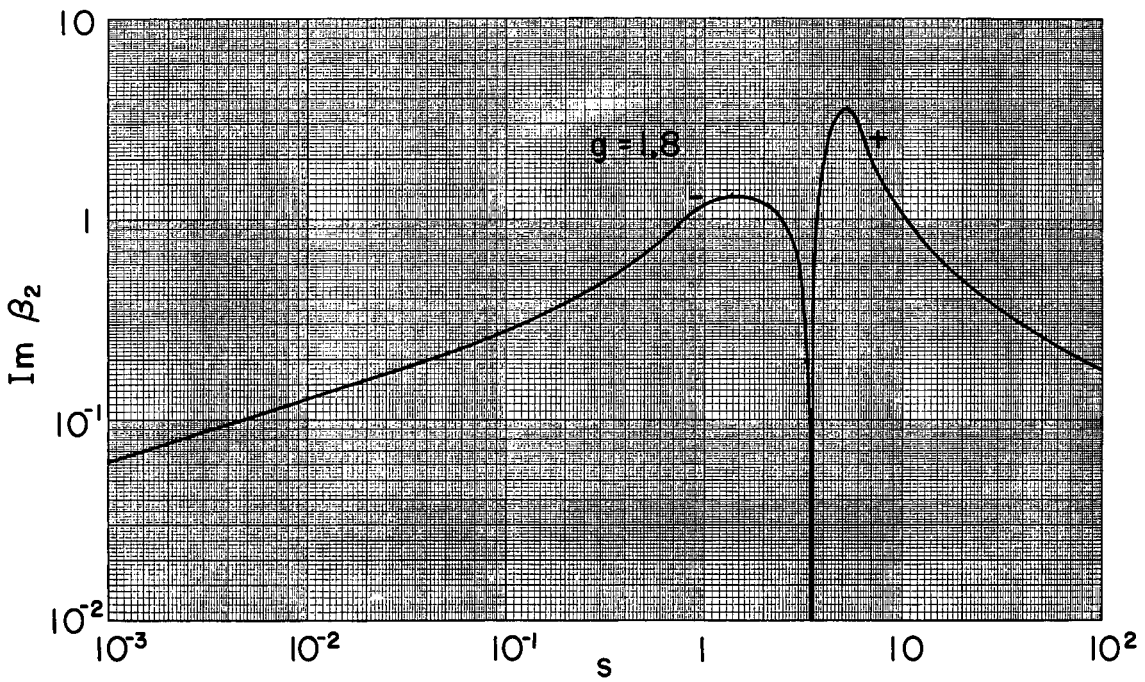

Fig. 67

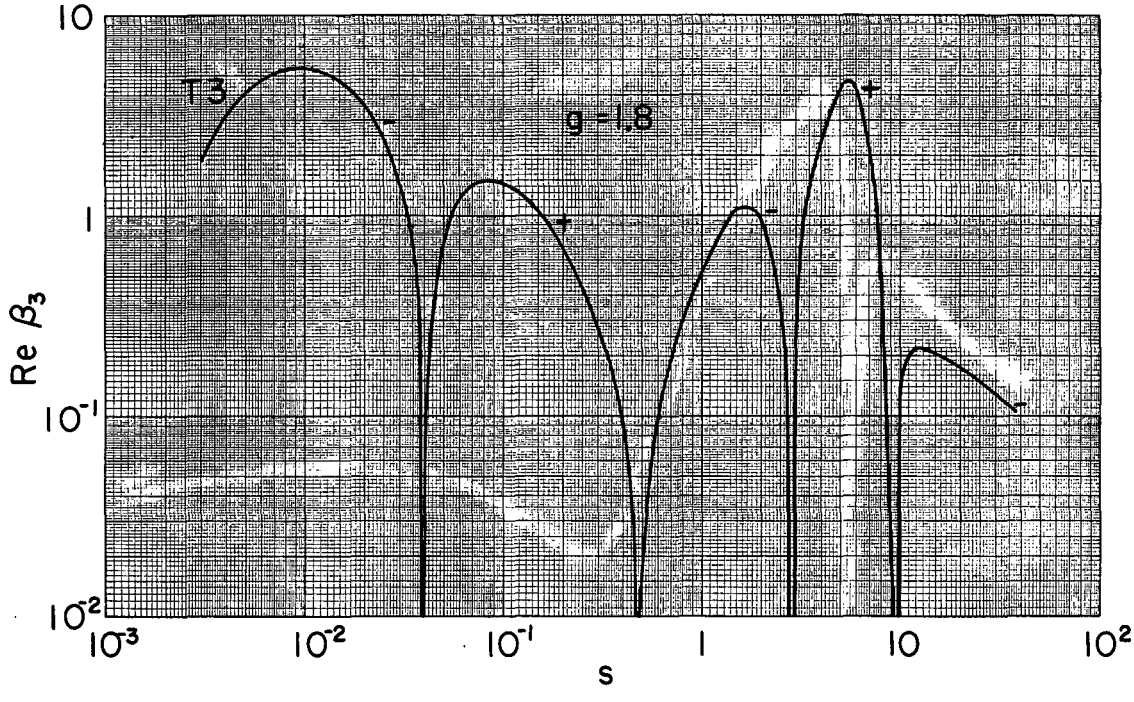

Fig. 68

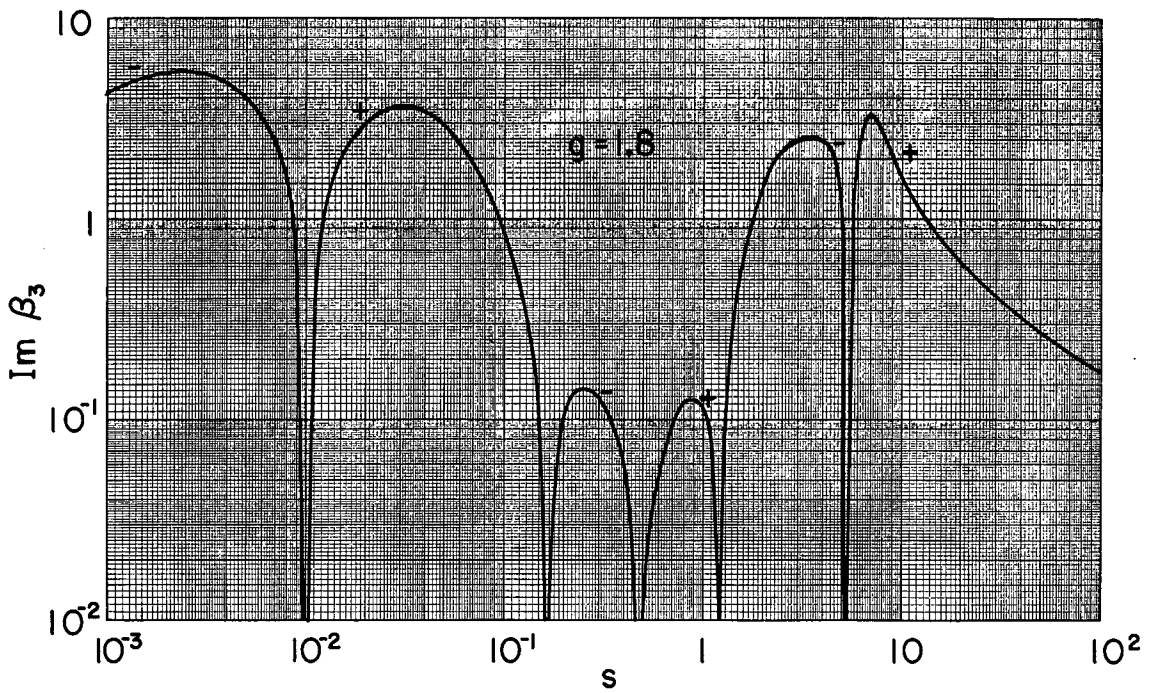

Fig. 69

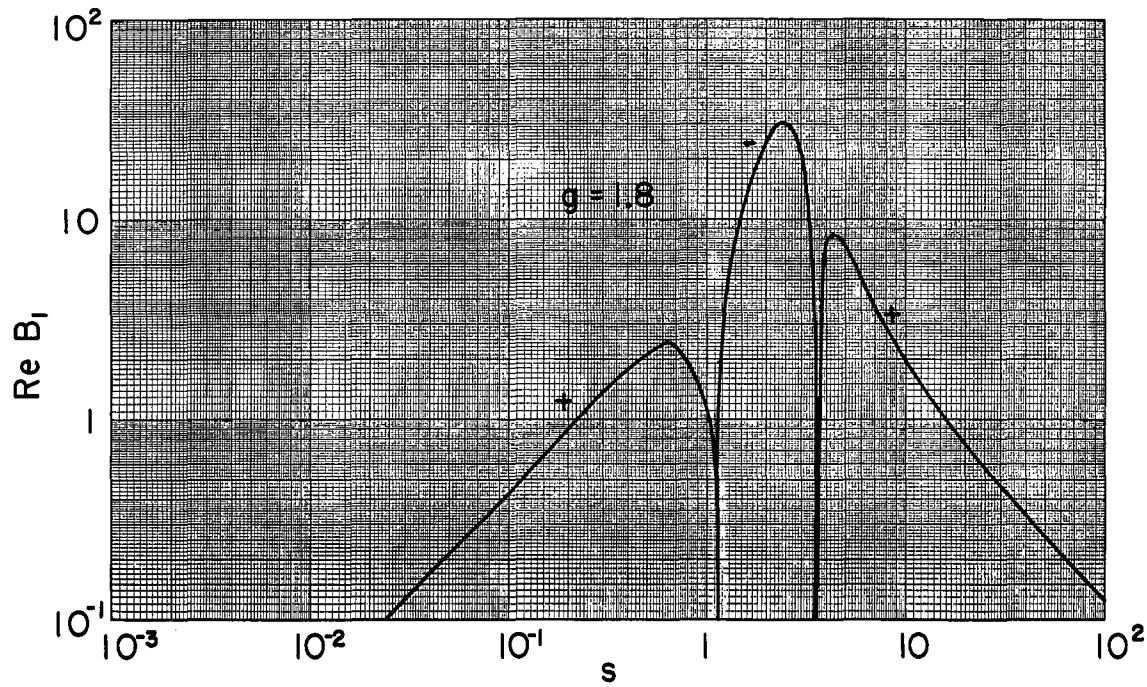

Fig. 70

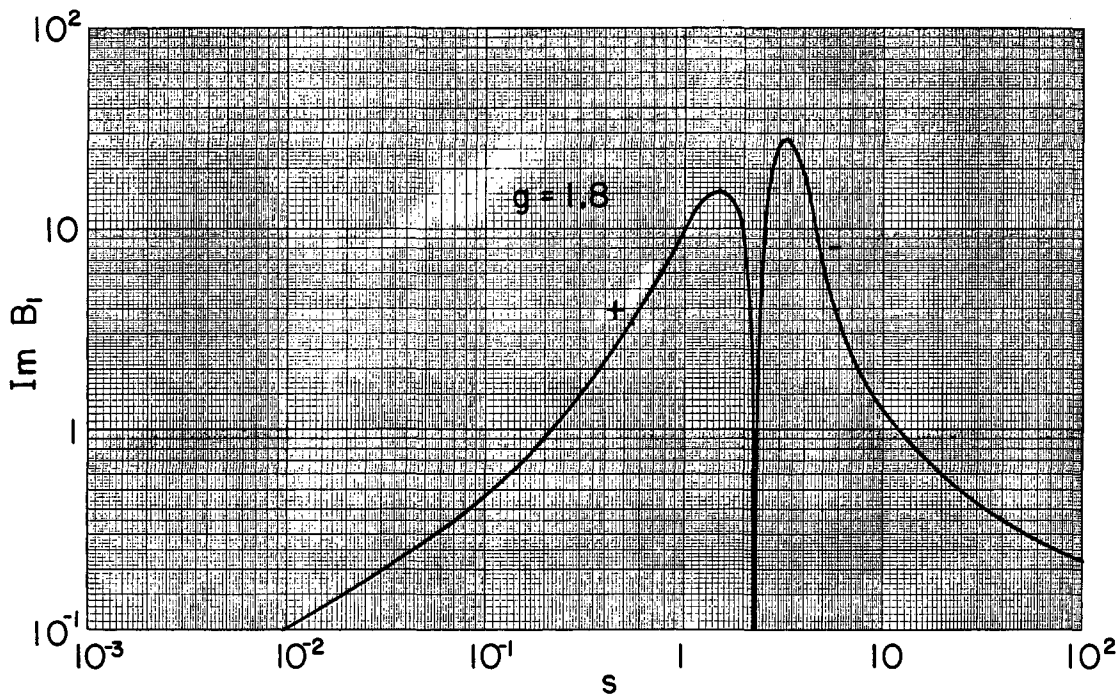

Fig. 71

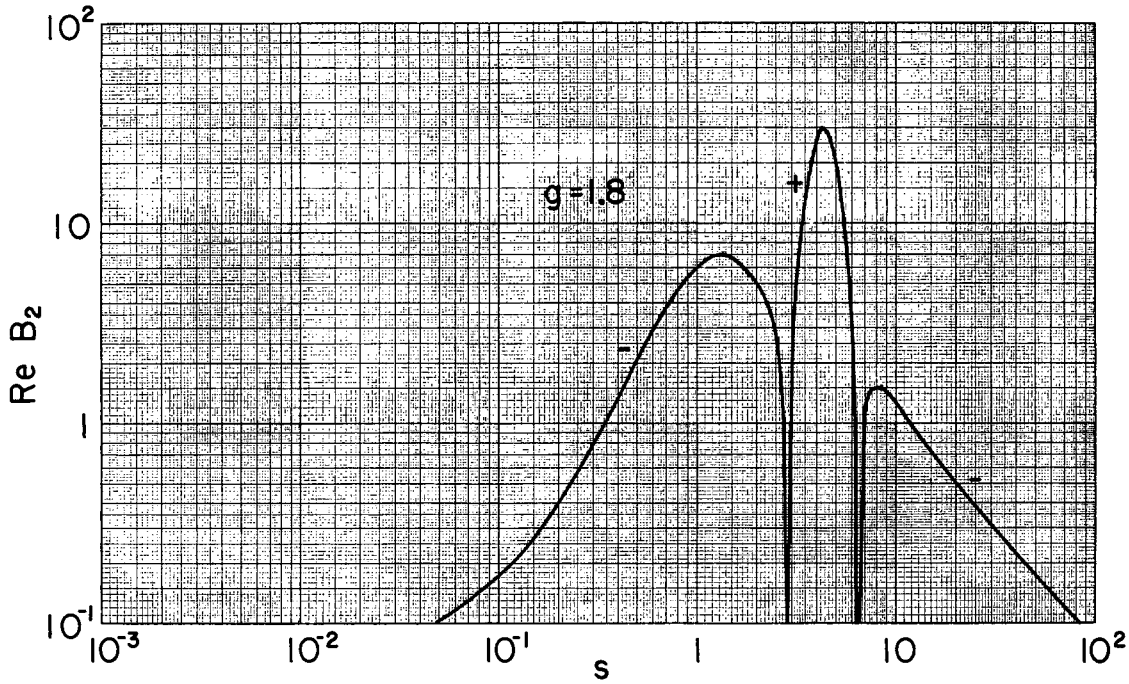

Fig. 72

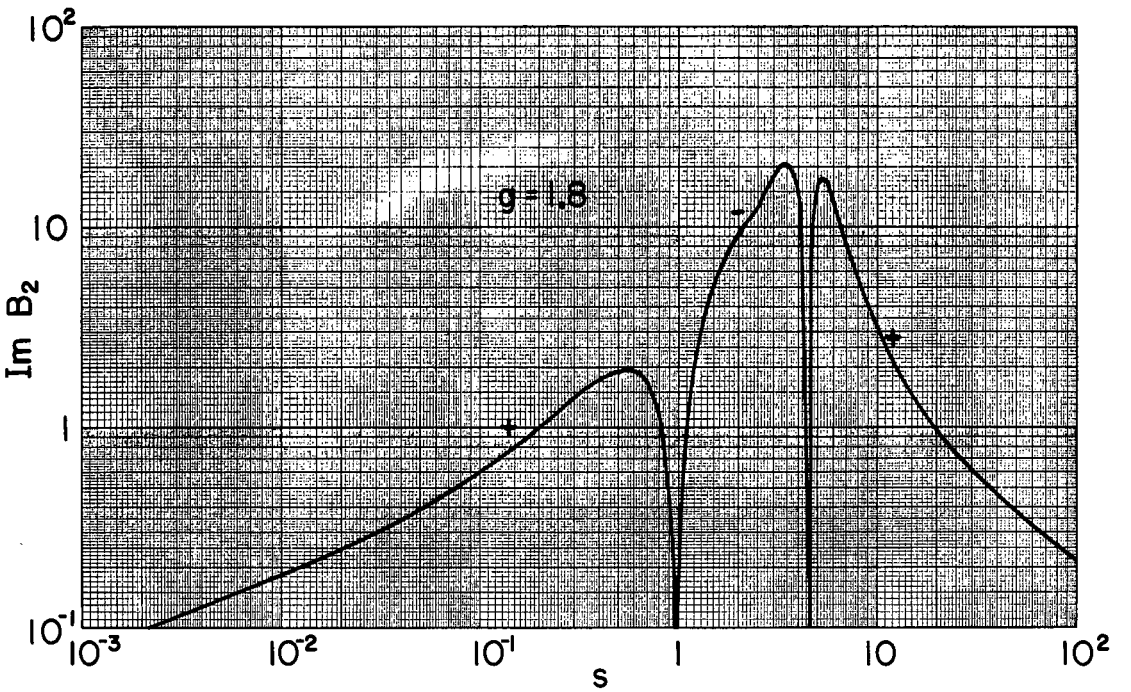

Fig. 73

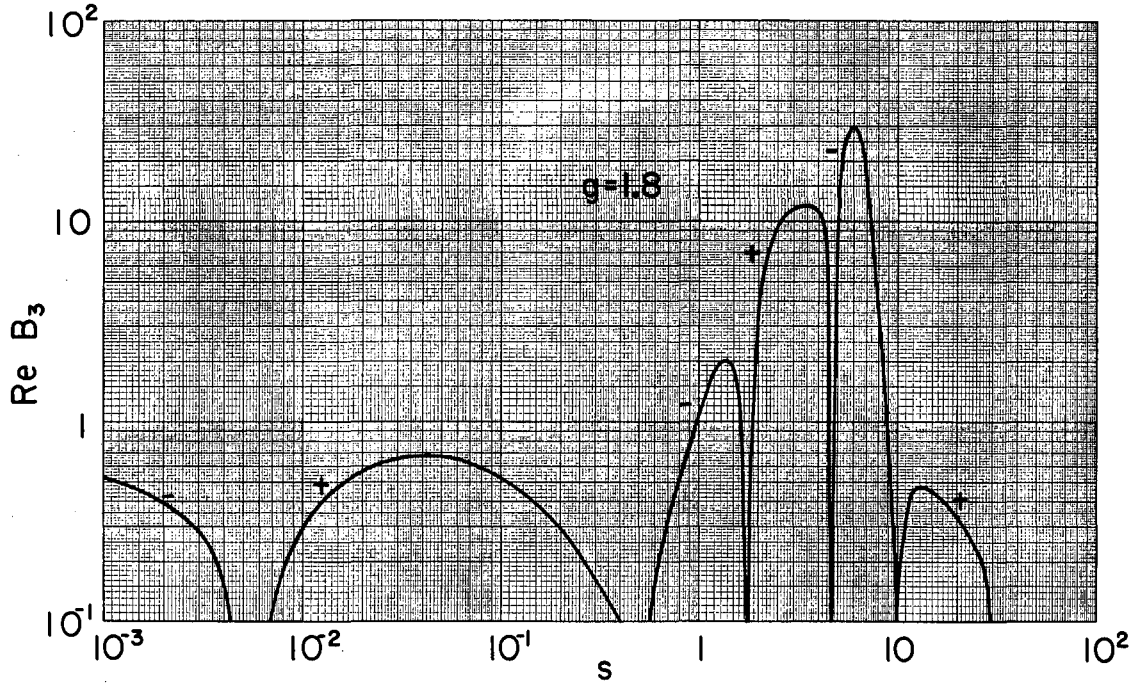

MU-32679

Fig. 74

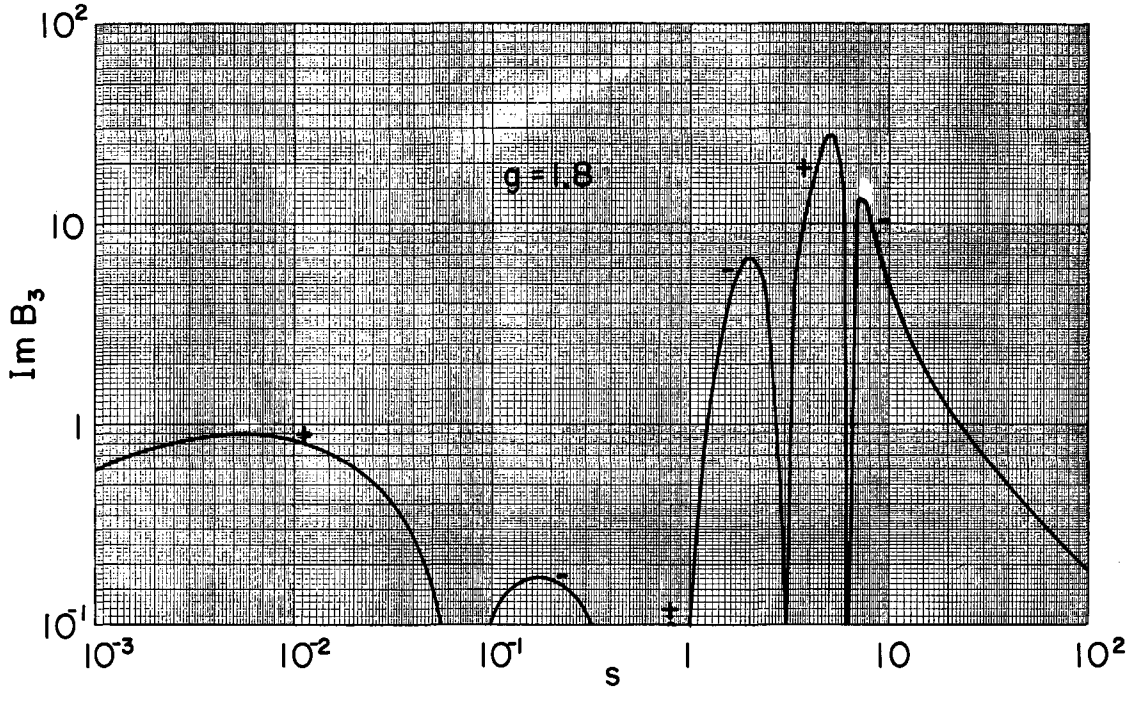

Fig. 75

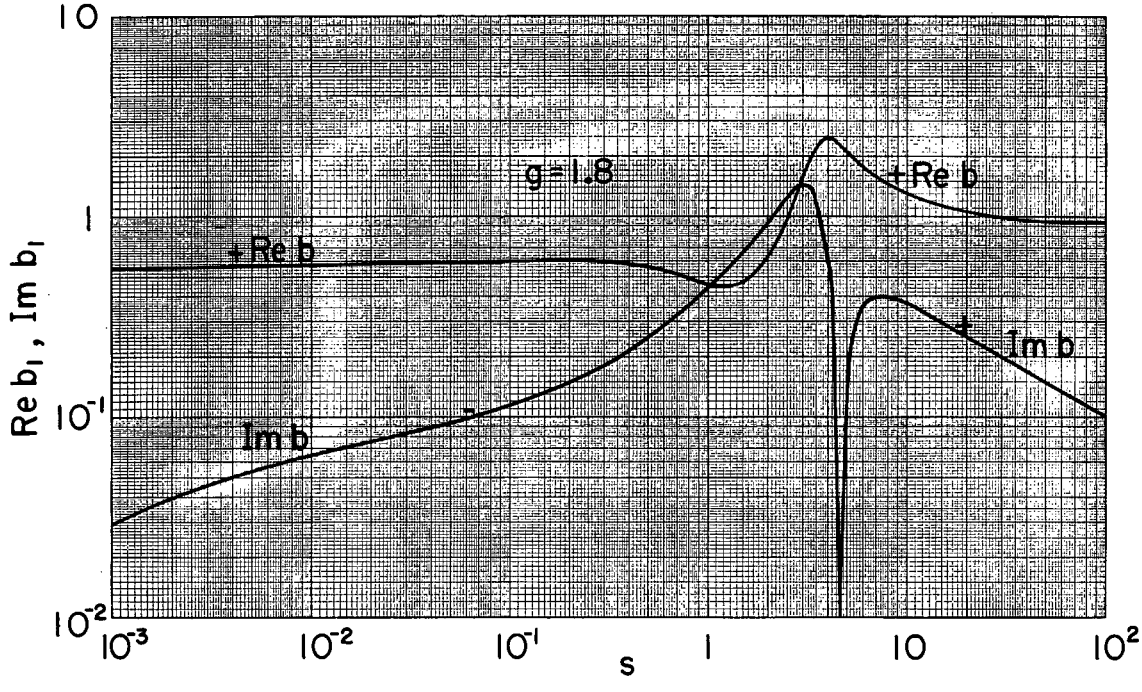
10
1
10^{-1}
10^{-2}
10^{-3}
10^{-2}
10^{-1}
1
10
10^{2}
s
$\mathrm{Re}\, b_1$, $\mathrm{Im}\, b_1$
g = 1.8
+Re b
+Re b
+Im b
Im b
MU-32681

Fig. 76

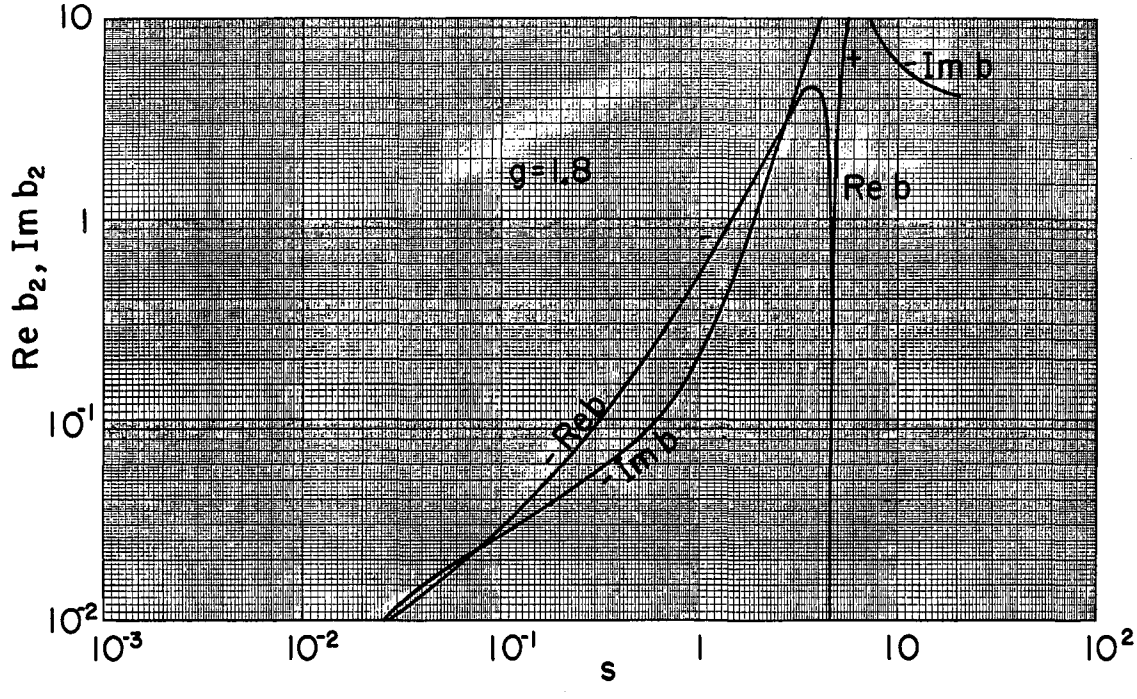
10
1
10^{-1}
10^{-2}
Re b_2, Im b_2
10^{-3}
10^{-2}
10^{-1}
1
10
10^2
s
g=1.8
Re b
Im b
-Re b
-Im b
MU-32682

Fig. 77

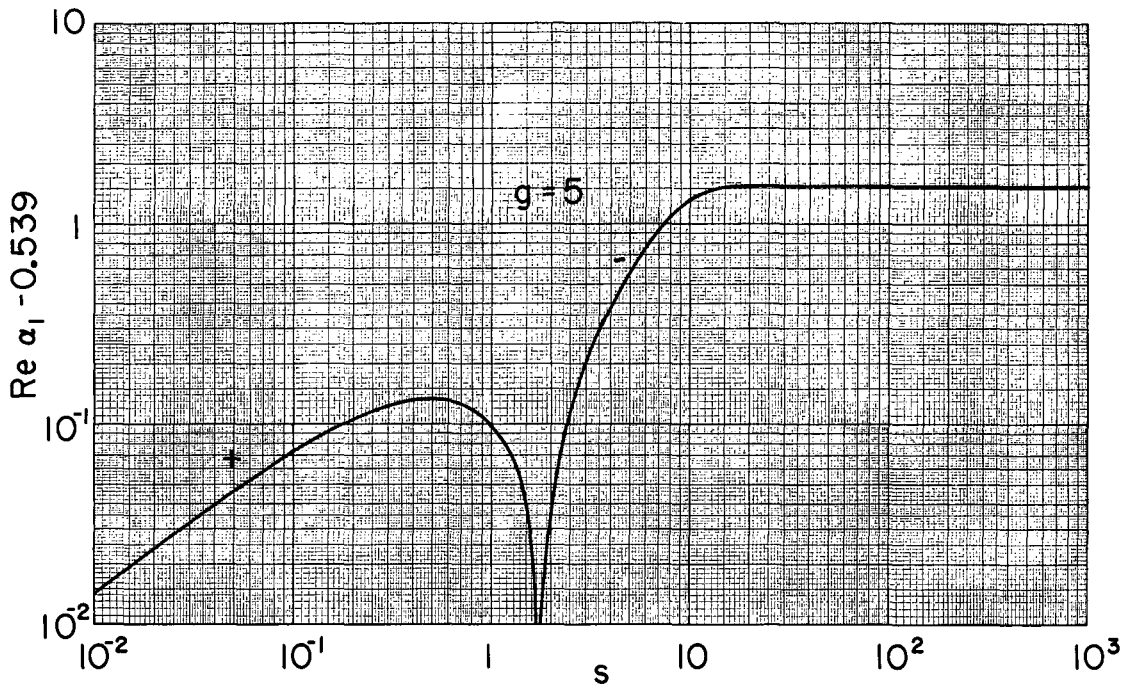

MU-32683

Fig. 78

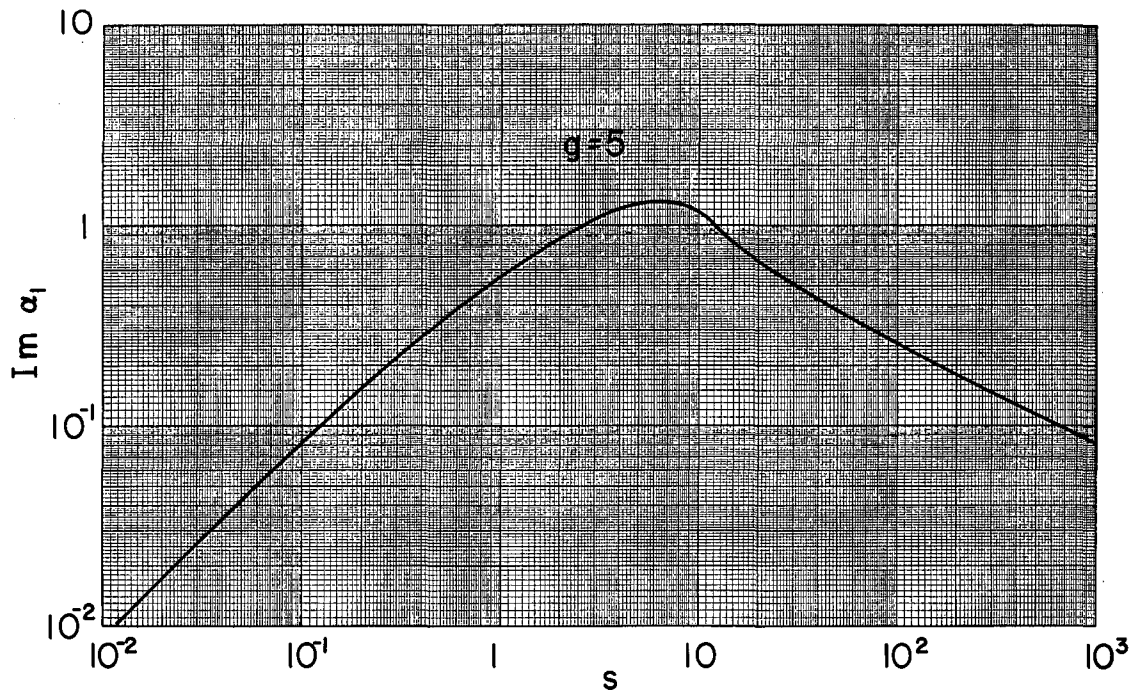

Fig. 79

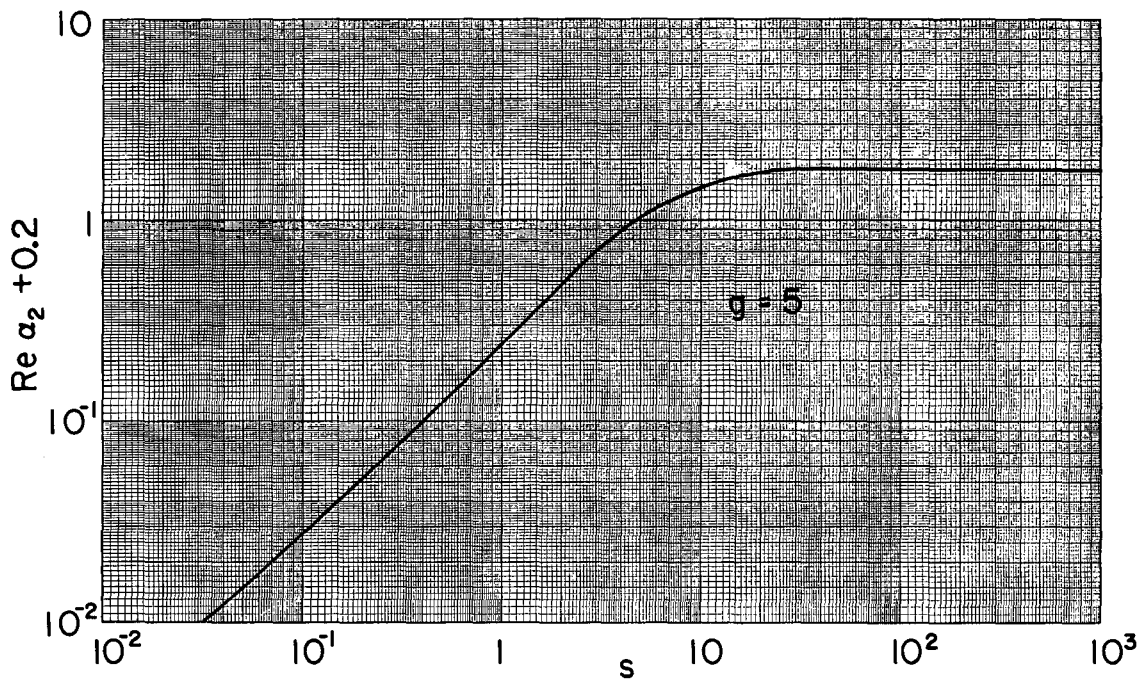

Fig. 80

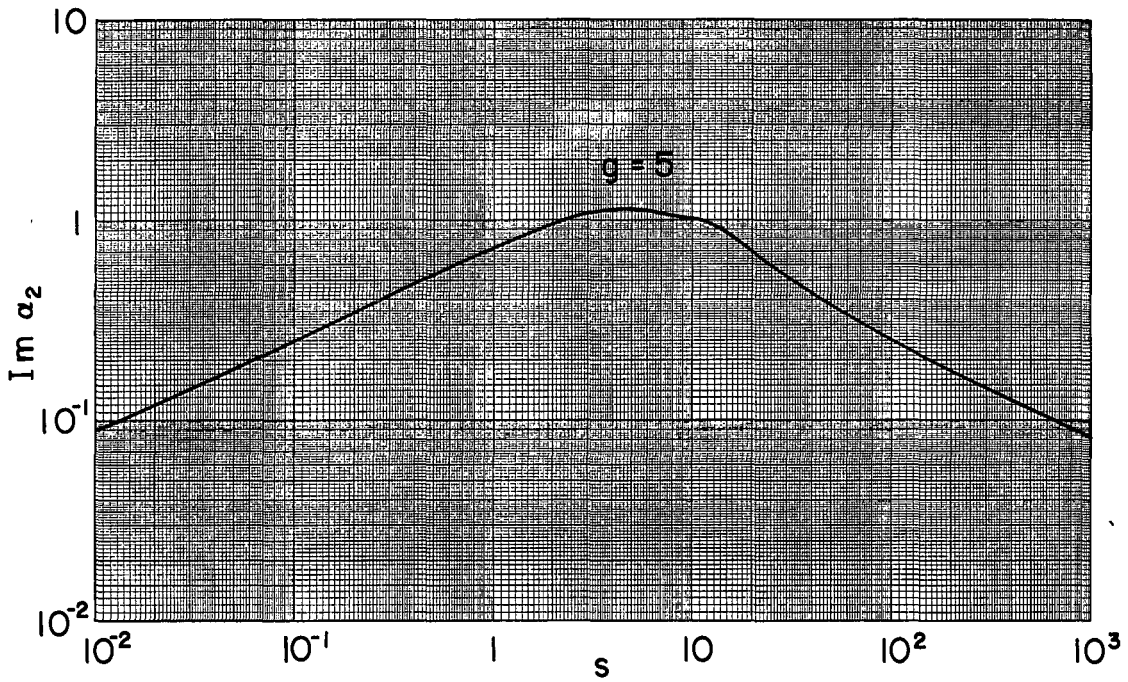

Fig. 81

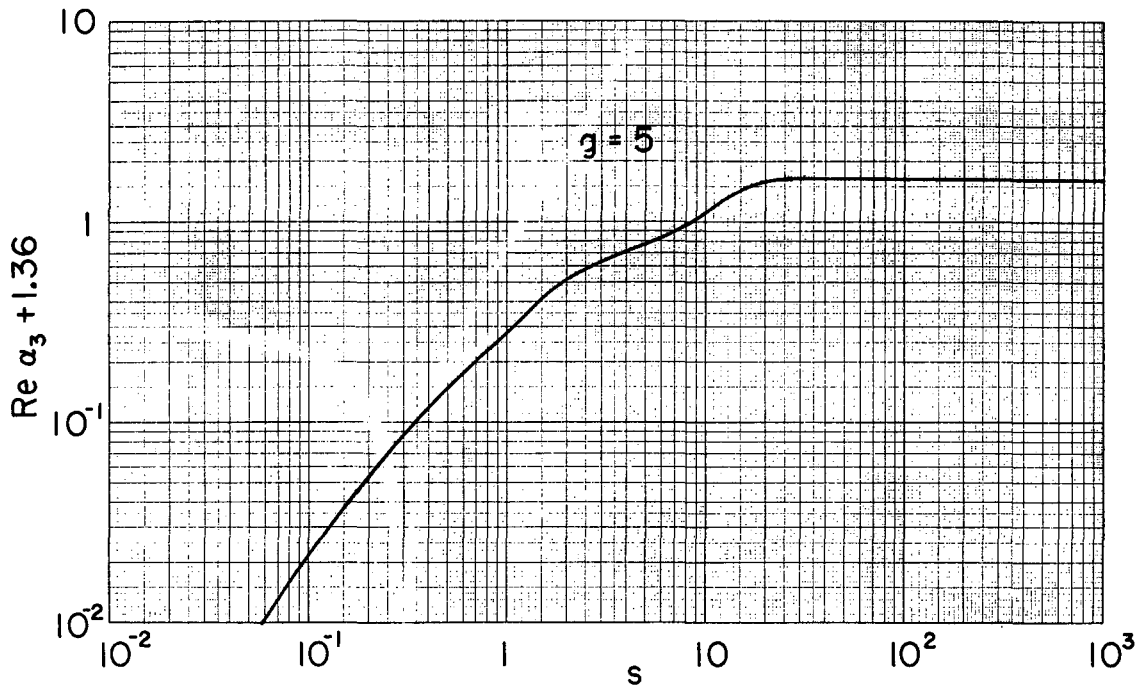

MU-32687

Fig. 82

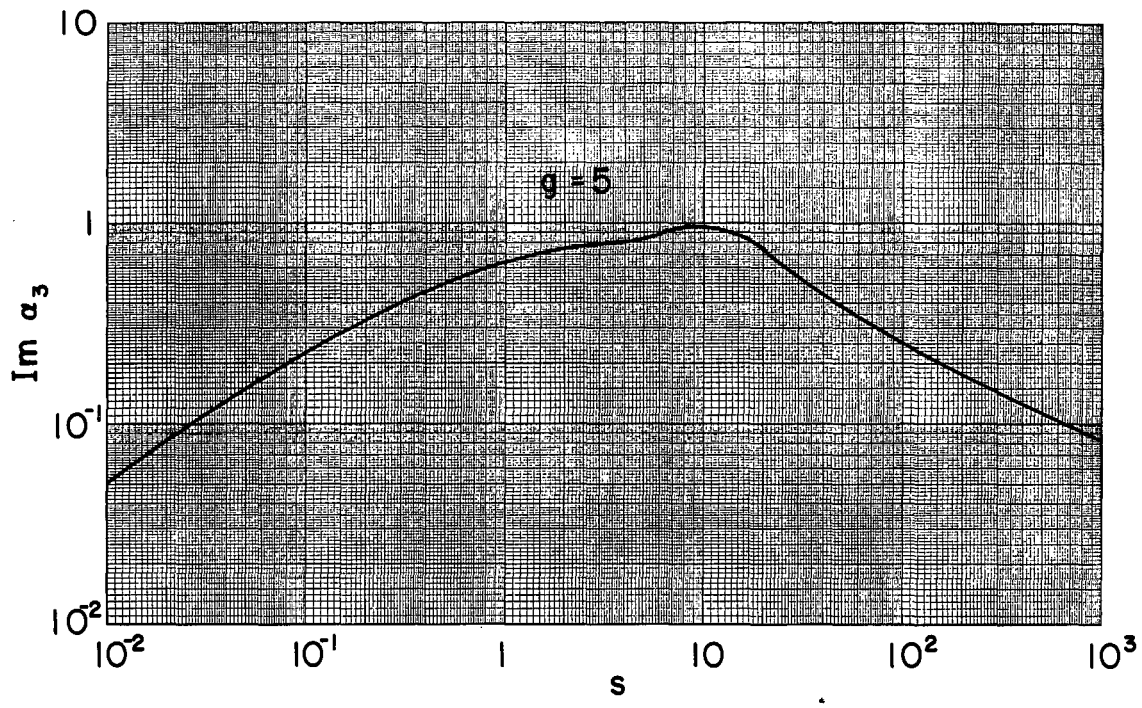

Fig. 83

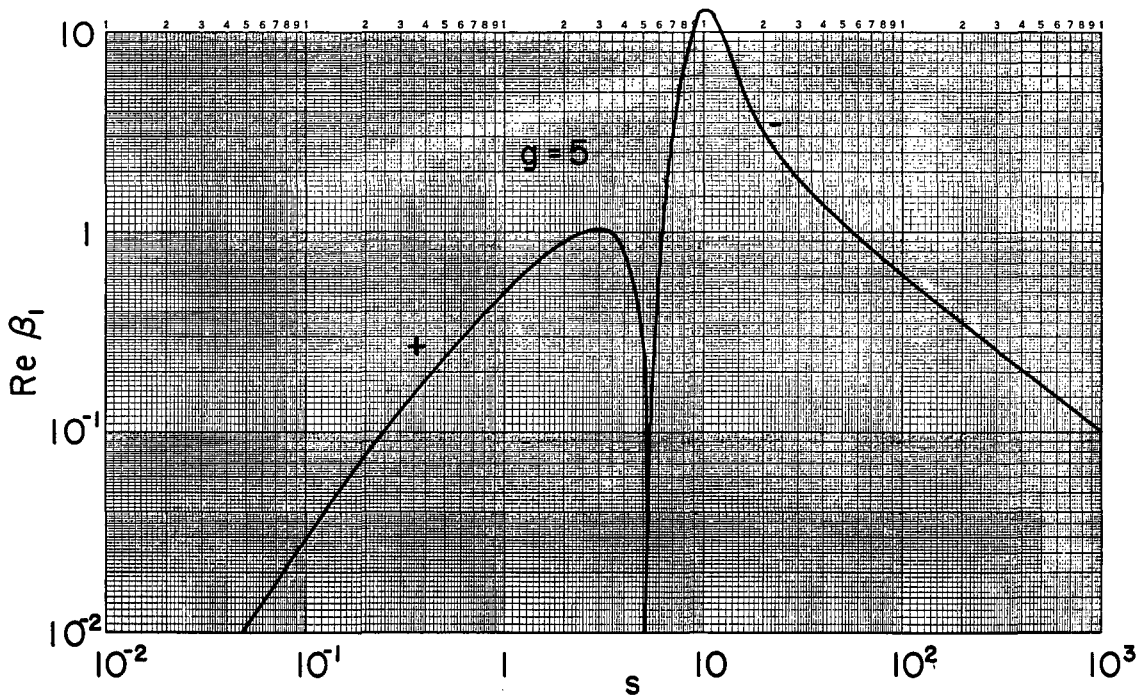

Fig. 84

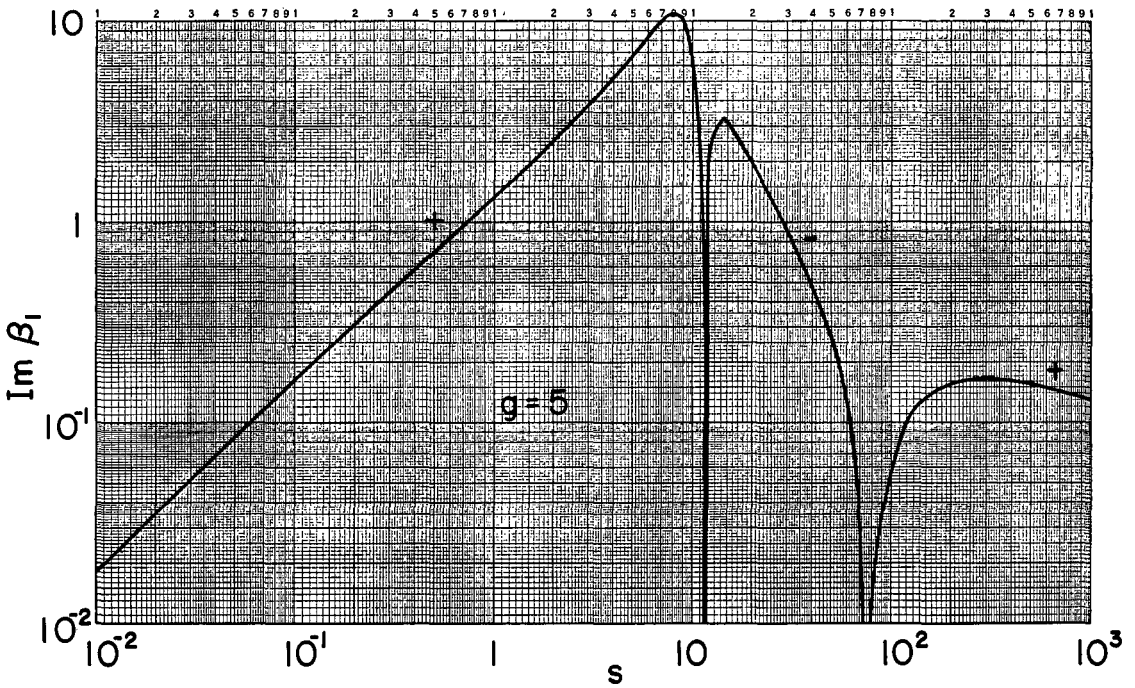

Fig. 85

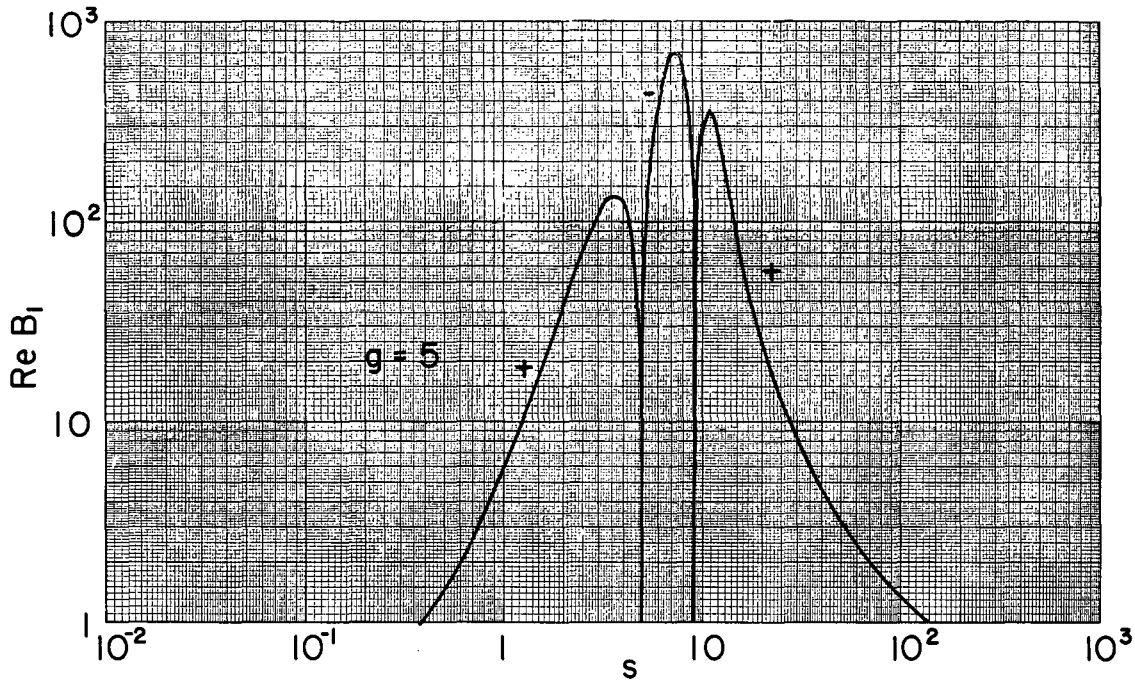

MU-32691

Fig. 86

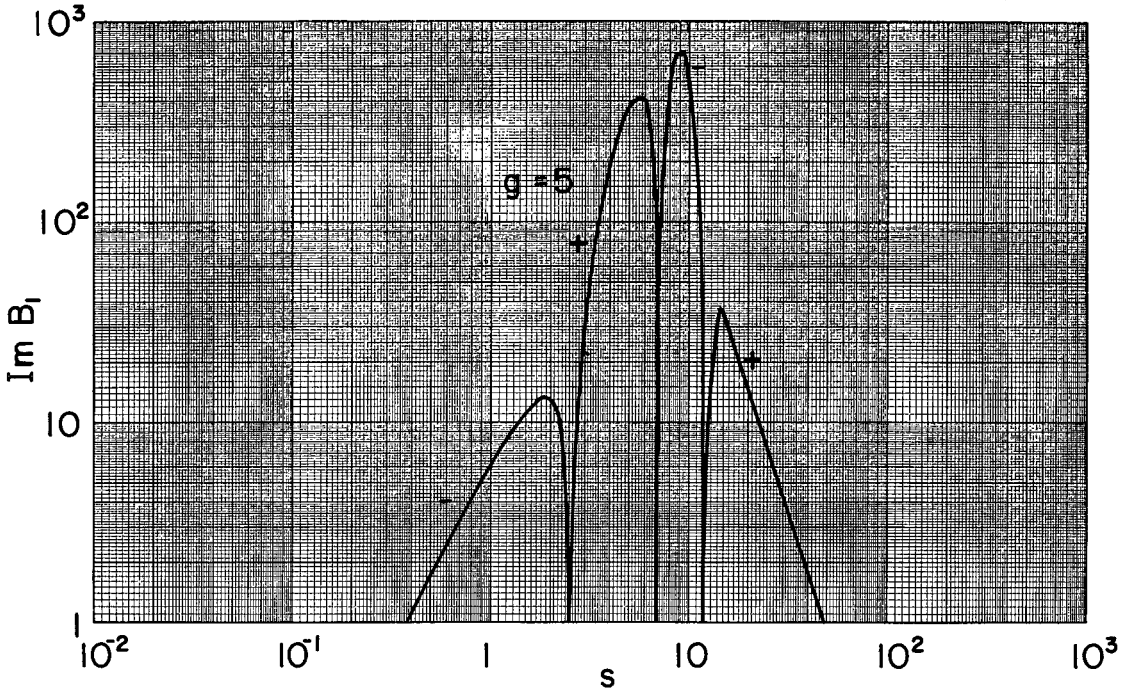

Fig. 87

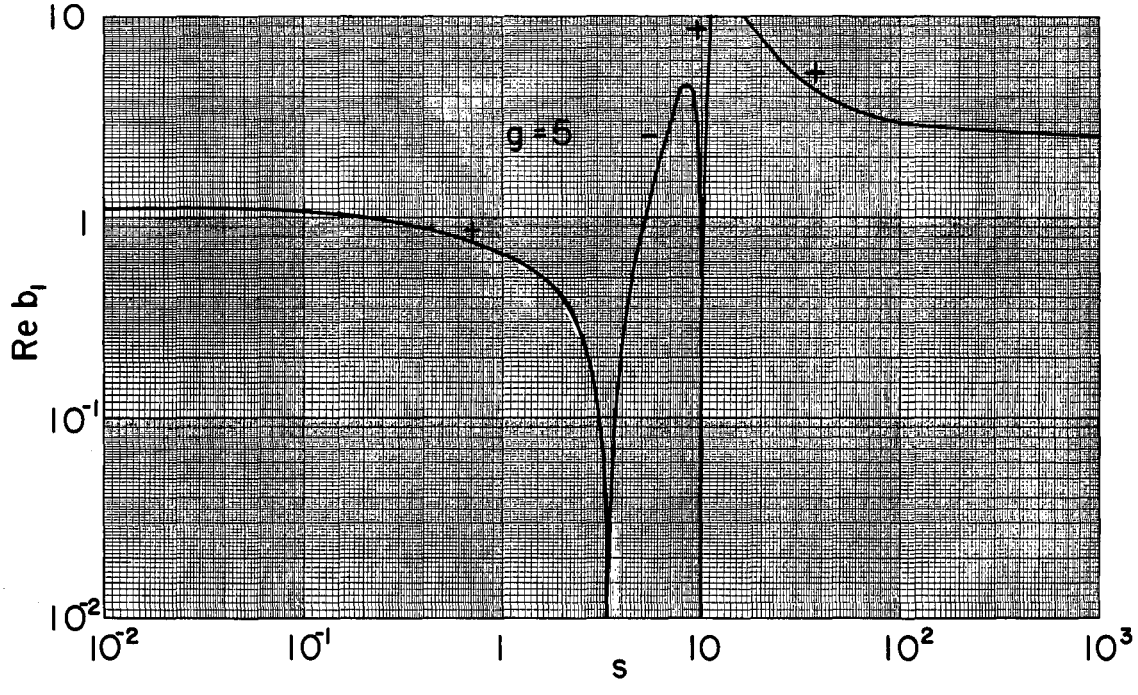

Fig. 88

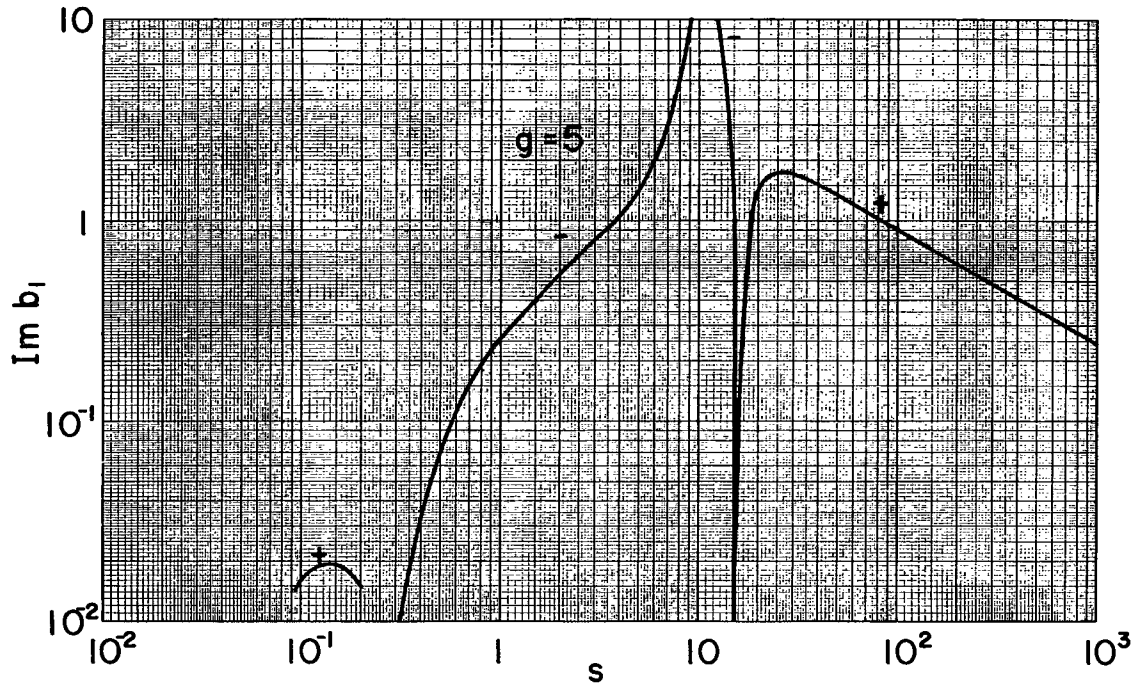

Fig. 89

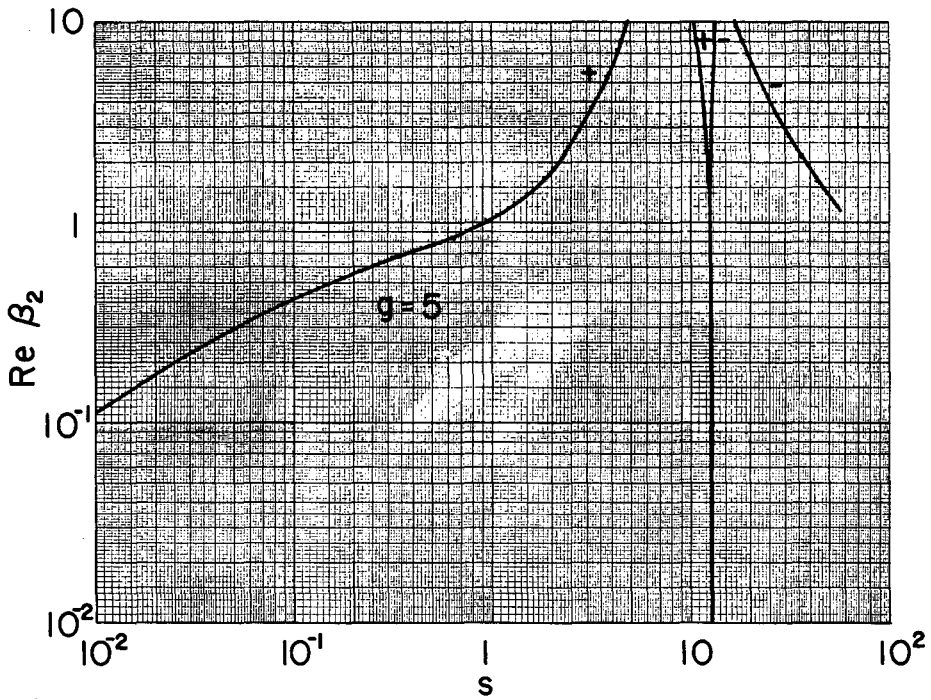

Fig. 90

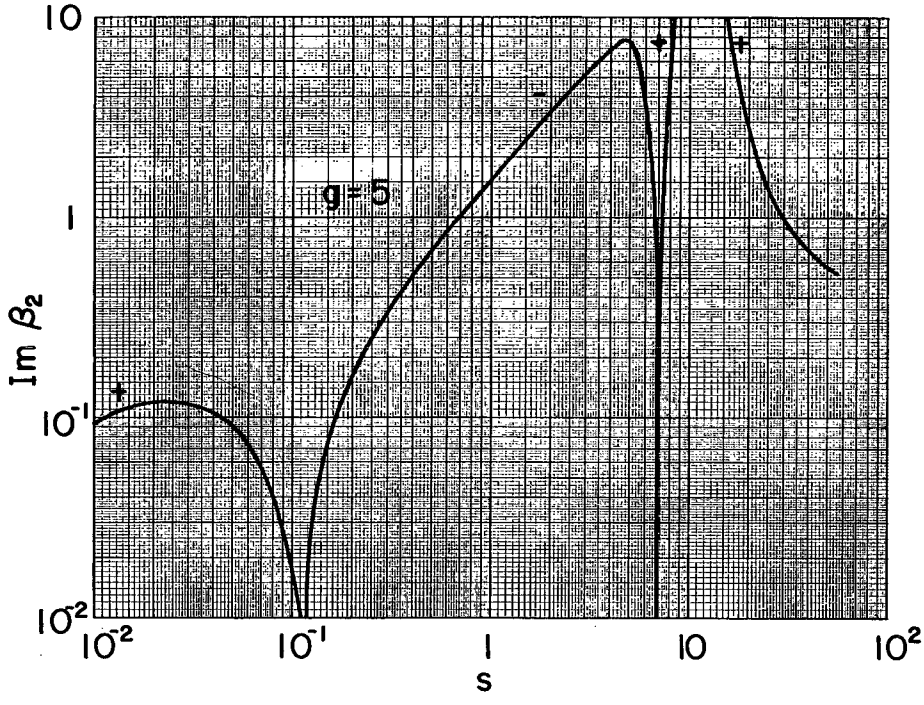

Fig. 91

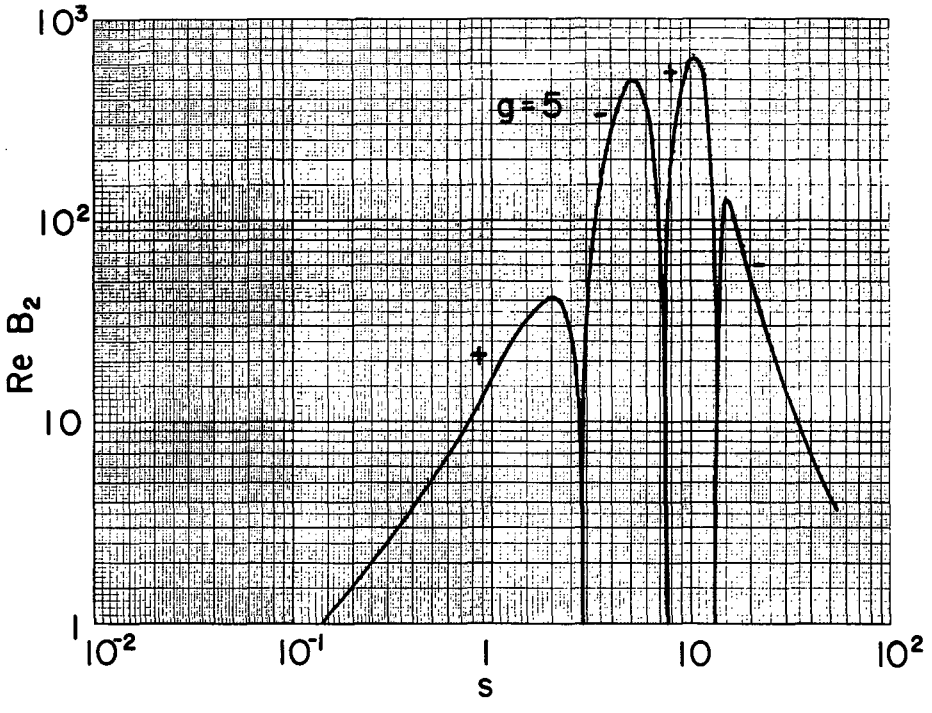

Fig. 92

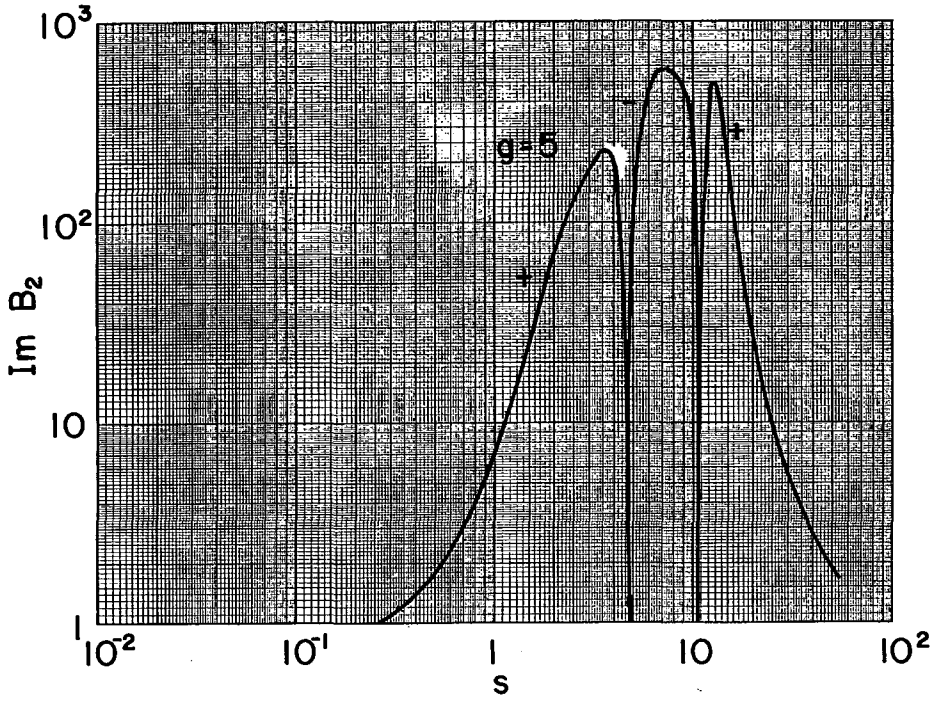

Fig. 93

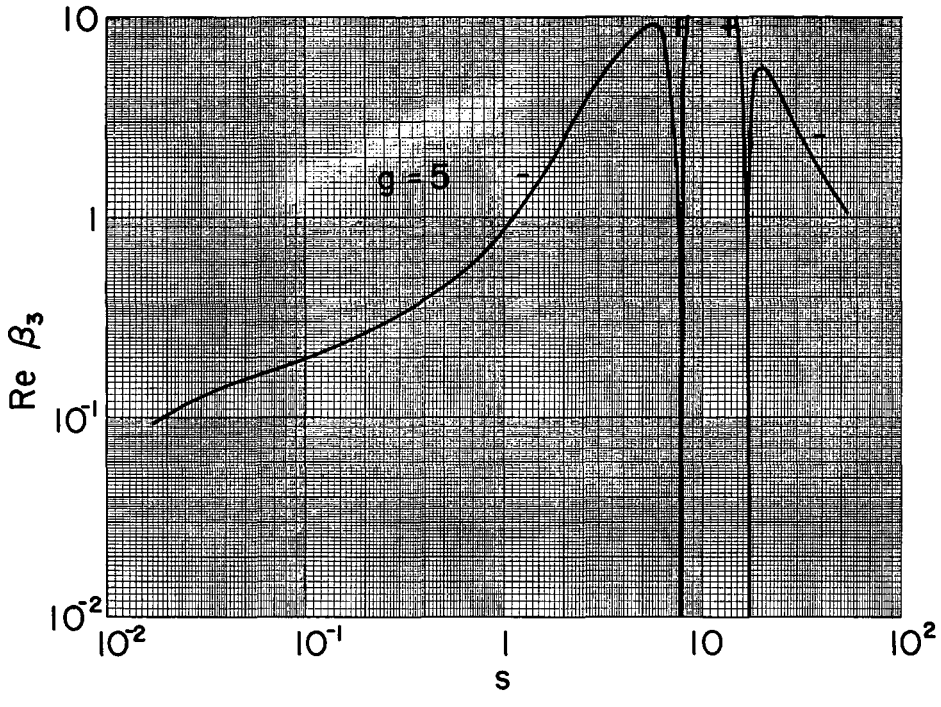

Fig. 94

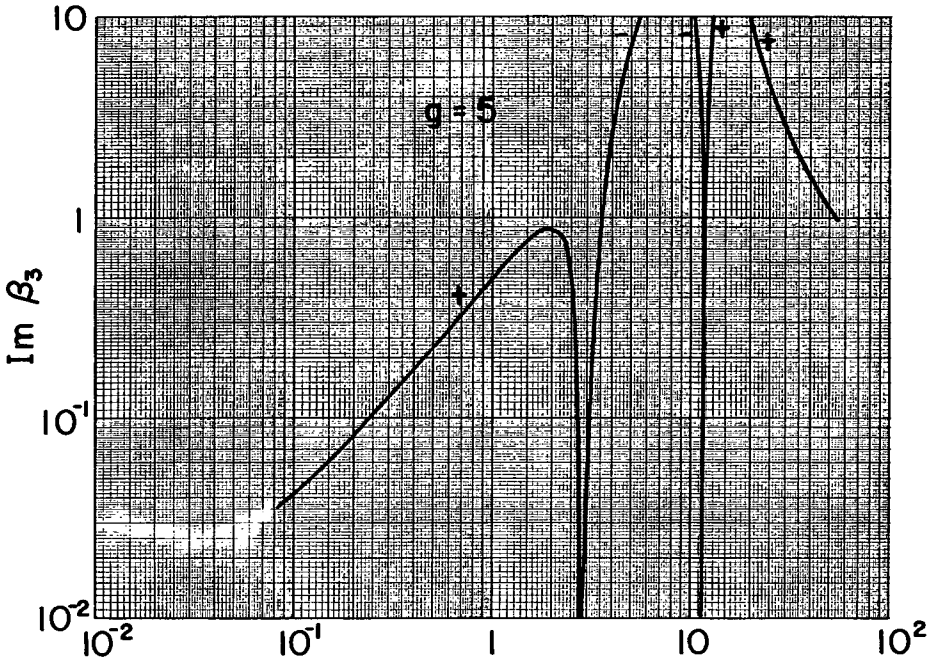

Fig. 95

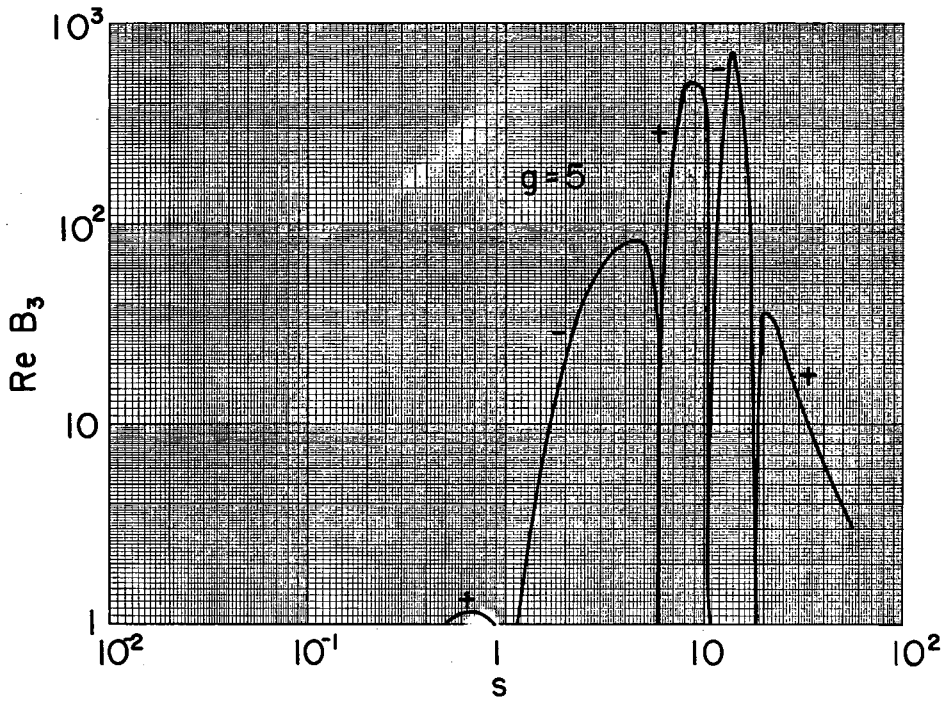

Fig. 96

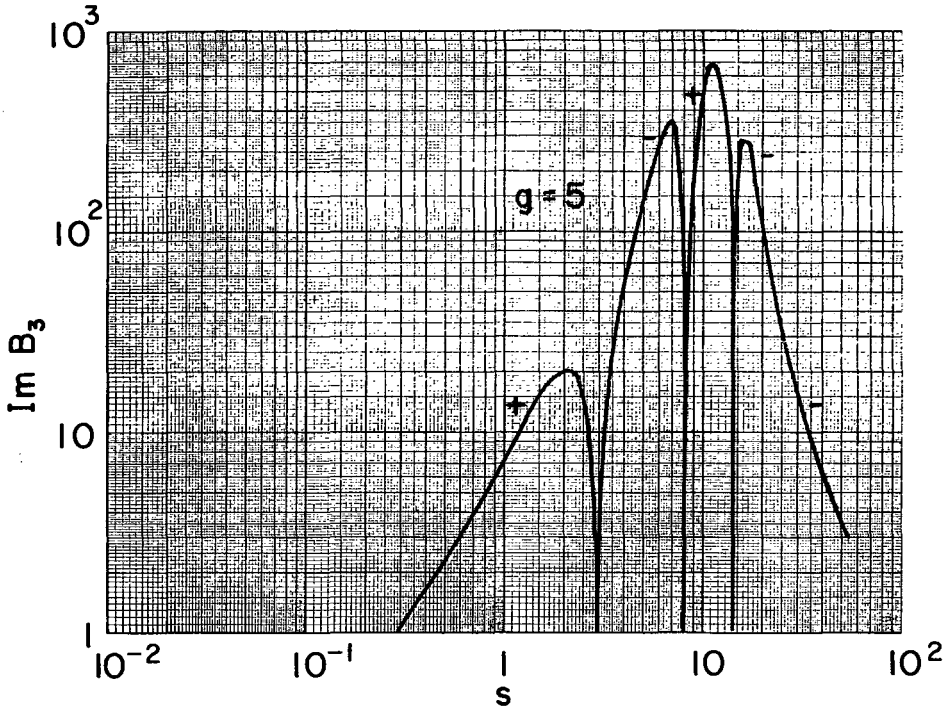

Fig. 97

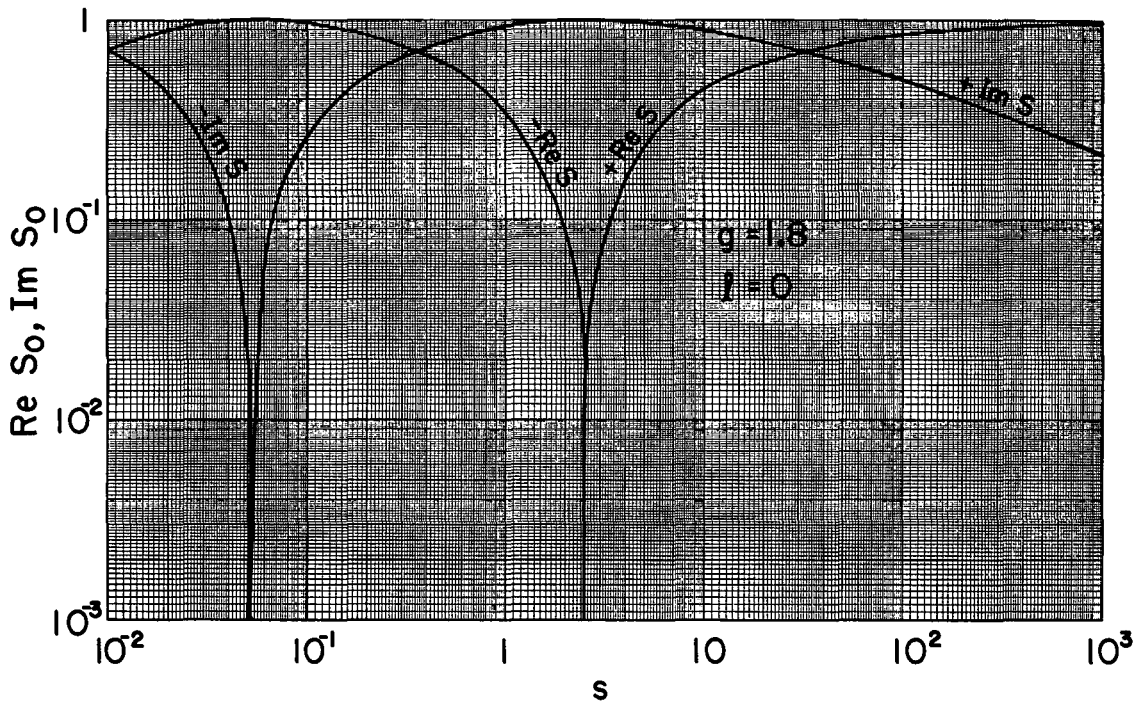
1
10^{-1}
10^{-2}
10^{-3}
Re S_0, Im S_0
10^{-2}
10^{-1}
1
10
10^2
10^3
s
Im s
Re s
Re s
Im s
g=1.8
I=0
MU-32703

Fig. 98

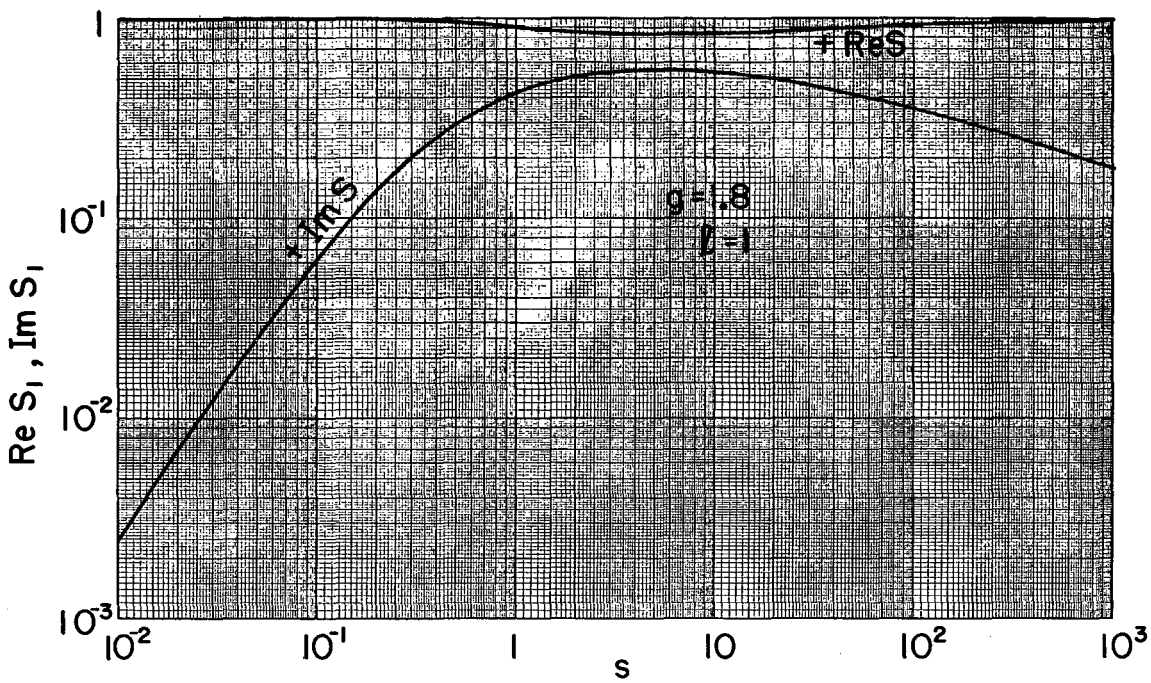
1
10^{-1}
10^{-2}
10^{-3}
Re S_1, Im S_1
+ ReS
× ImS
g=1.8
ℓ=1
10^{-2}
10^{-1}
1
10
10^{2}
10^{3}
s
MU-32704

Fig. 99

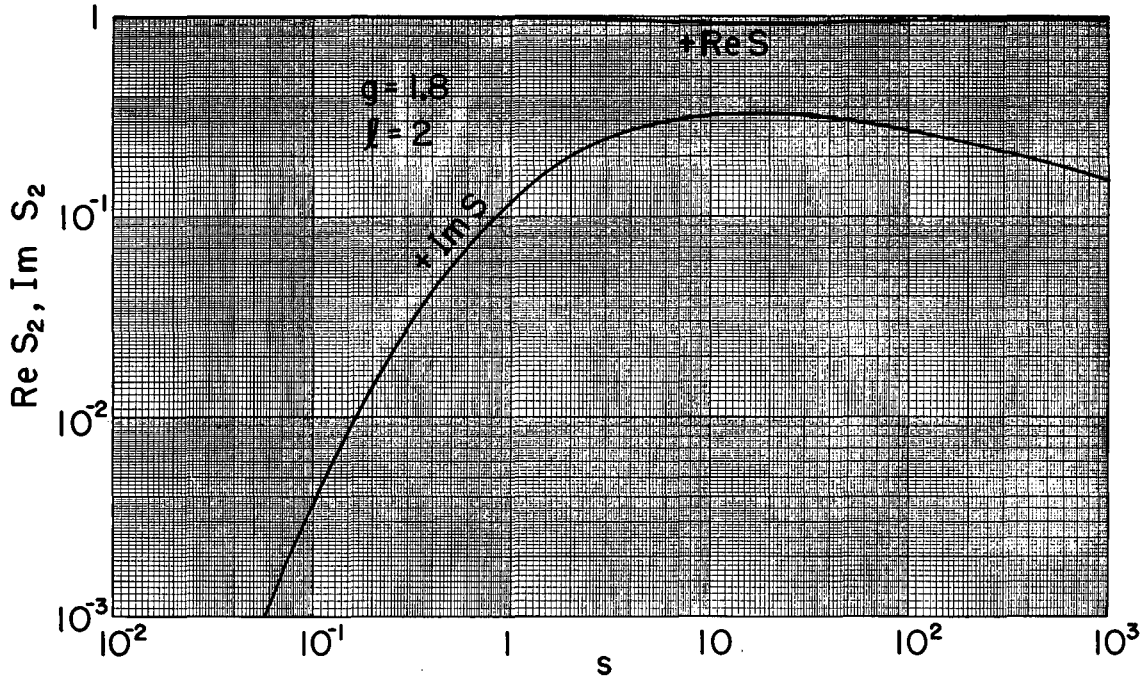
1
10^{-1}
10^{-2}
10^{-3}
Re S_2, Im S_2
+Re S
g=1.8
I=2
×Im S
10^{-2}
10^{-1}
1
10
10^2
10^3
s
MU-32705

Fig. 100

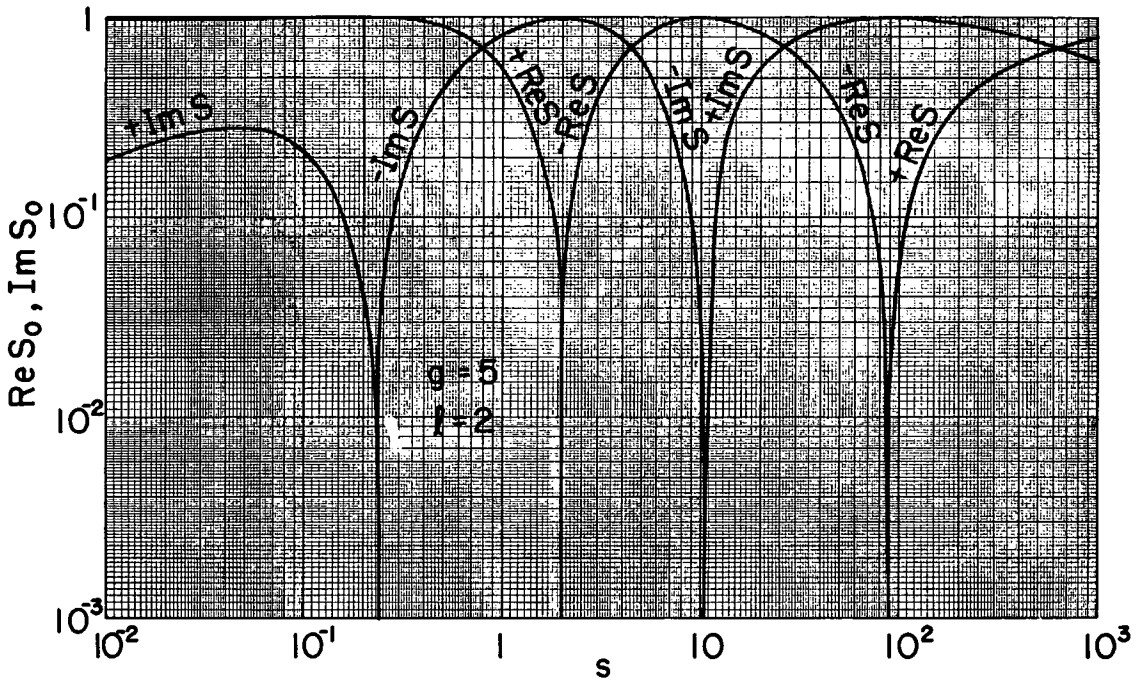
Re S0, Im S0
1
10-1
10-2
10-3
10-2
10-1
1
10
10²
10³
S
+Im S
-Im S
+Re S
-Re S
-Im S
+Im S
-Re S
+Re S
g=5
I=2
MU-32706

Fig. 101

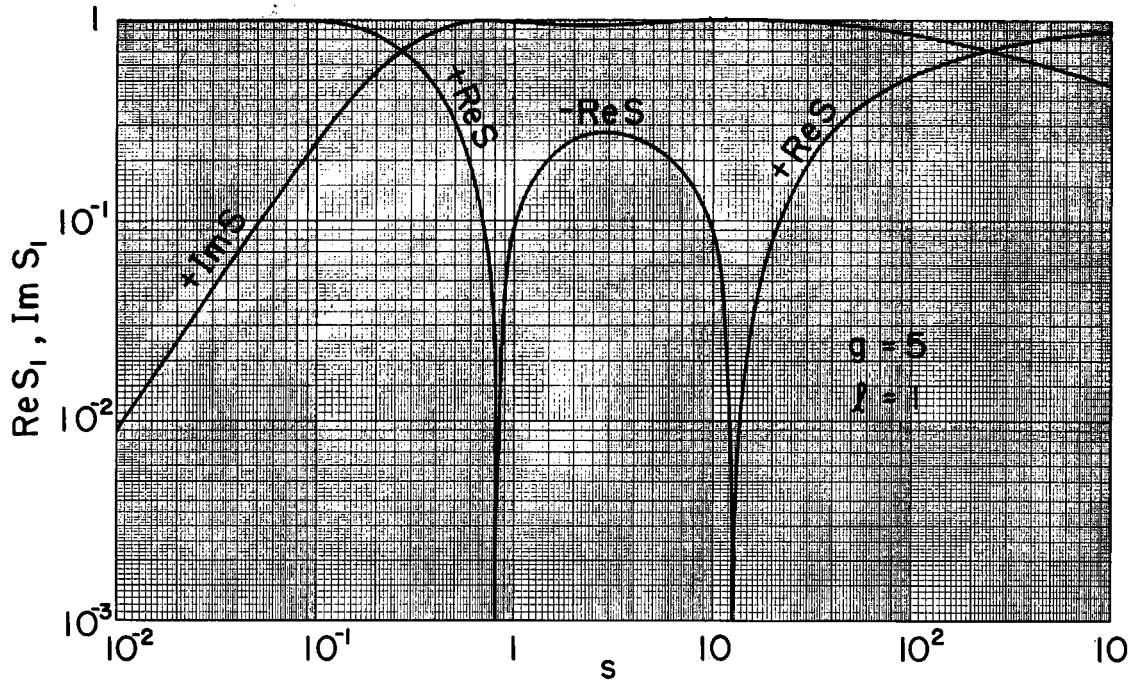
1
10^{-1}
10^{-2}
10^{-3}
$\mathrm{Re}S_l$, $\mathrm{Im}\,S_l$
+ImS
+ReS
-ReS
+ReS
q = 5
l = 1
10^{-2}
10^{-1}
1
10
10^{2}
10^{3}
s
MU-32707

Fig. 102

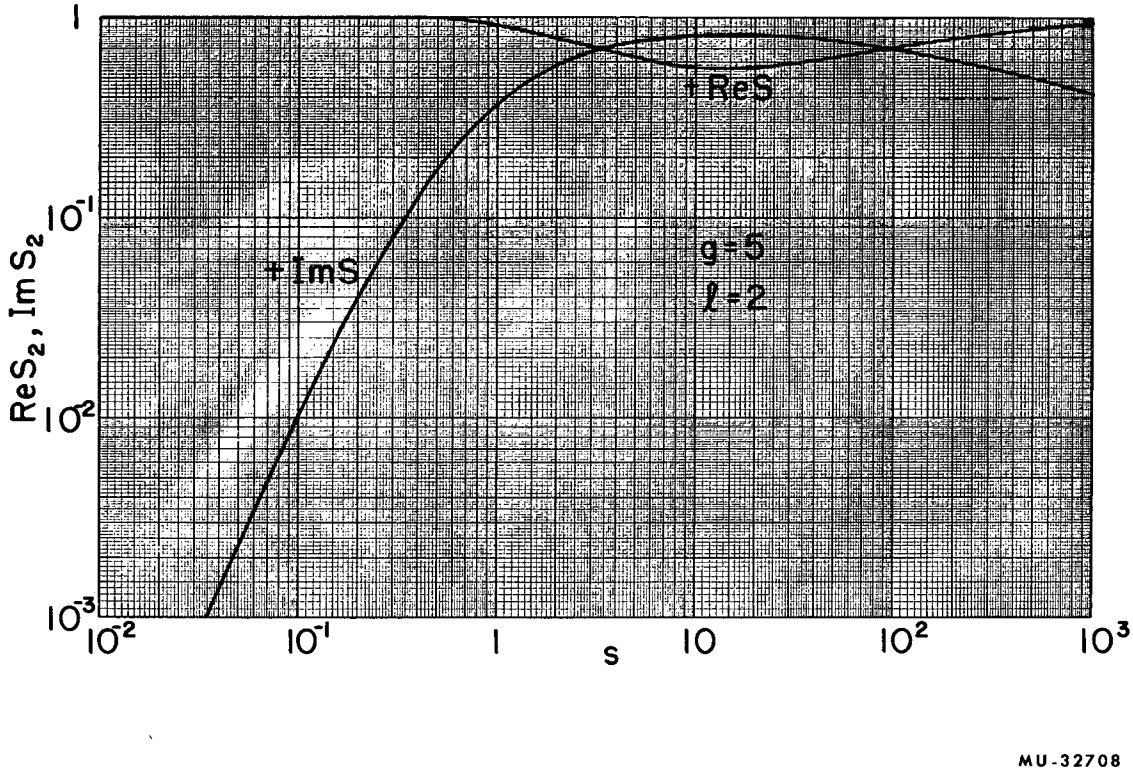
1
10^{-1}
10^{-2}
10^{-3}
ReS_2, ImS_2
+ReS
+ImS
g=5
ℓ=2
10^{-2}
10^{-1}
1
10
10^{2}
10^{3}
s
MU-32708

Fig. 103

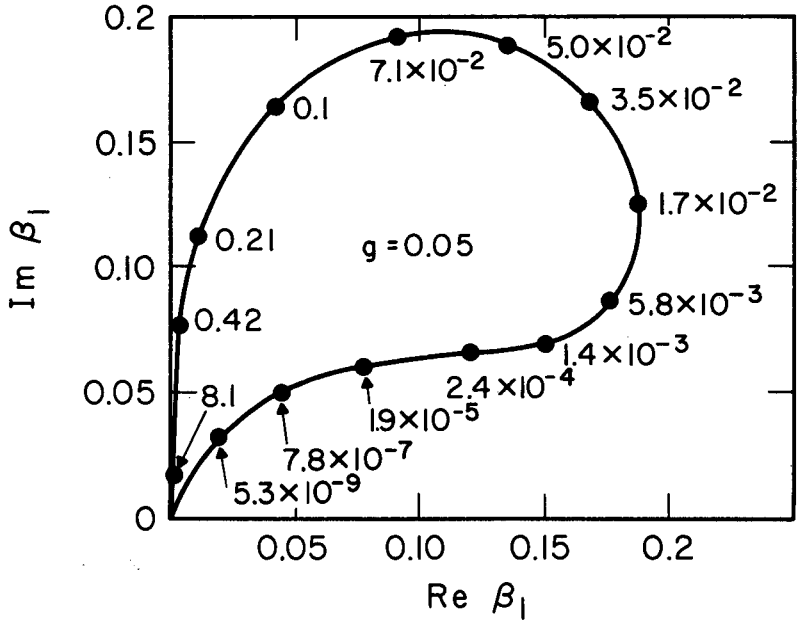
0.2
0.15
0.10
0.05
0
Im β_1
0.05
0.10
0.15
0.2
Re β_1
7.1×10^{-2}
5.0×10^{-2}
3.5×10^{-2}
1.7×10^{-2}
5.8×10^{-3}
1.4×10^{-3}
2.4×10^{-4}
1.9×10^{-5}
7.8×10^{-7}
5.3×10^{-9}
0.1
0.21
0.42
8.1
g = 0.05
MU-32709

Fig. 104

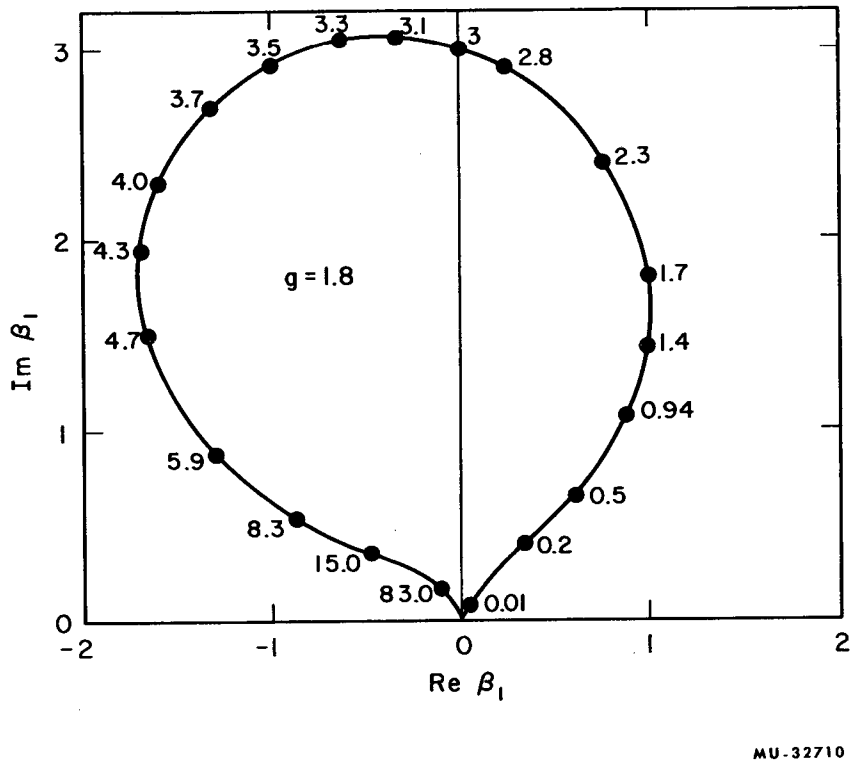
3.3
3.1
3.5
3
3.7
2.8
4.0
2.3
4.3
g = 1.8
1.7
4.7
1.4
0.94
5.9
0.5
8.3
0.2
15.0
83.0
0.01
Im β_1
Re β_1
3
2
1
0
-2
-1
0
1
2
MU-32710

Fig. 105

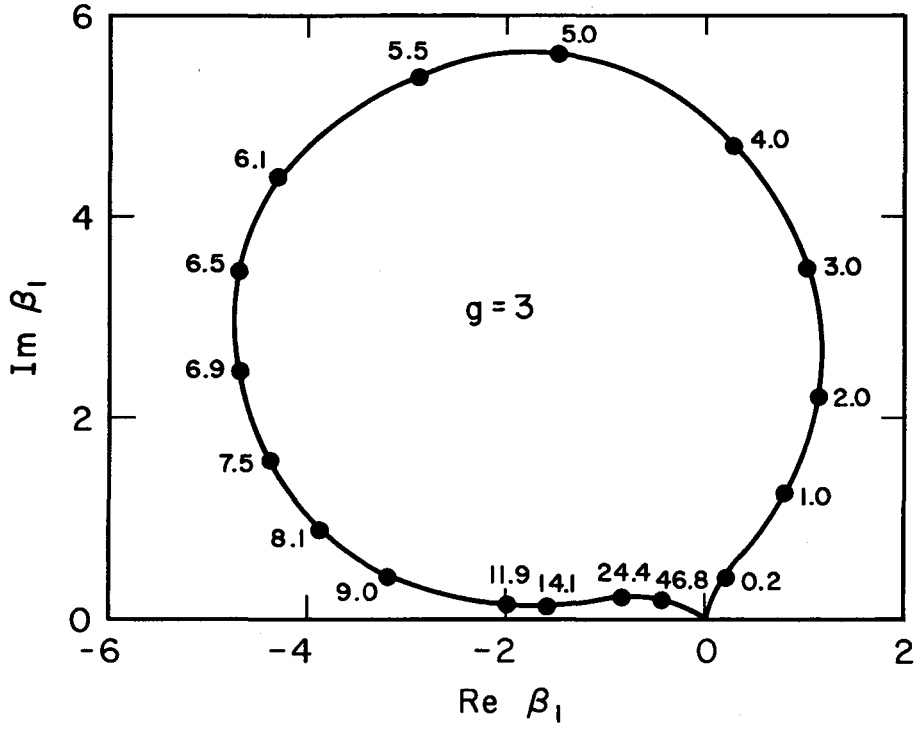
6
4
2
0
-6
-4
-2
0
2
Im β_1
Re β_1
g = 3
5.0
5.5
4.0
6.1
3.0
6.5
2.0
6.9
1.0
7.5
0.2
8.1
46.8
24.4
11.9
14.1
9.0
MU-32711

Fig. 106

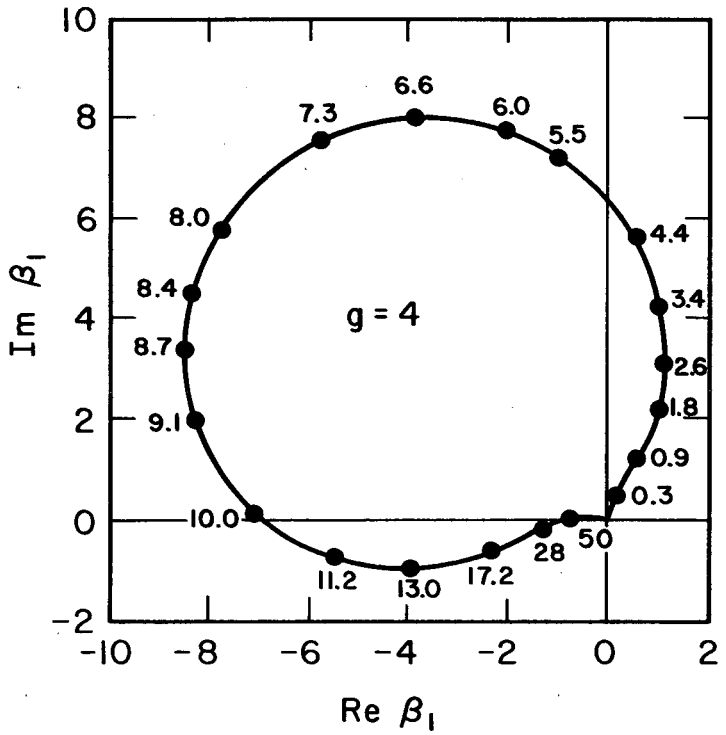

MU-32712

Fig. 107

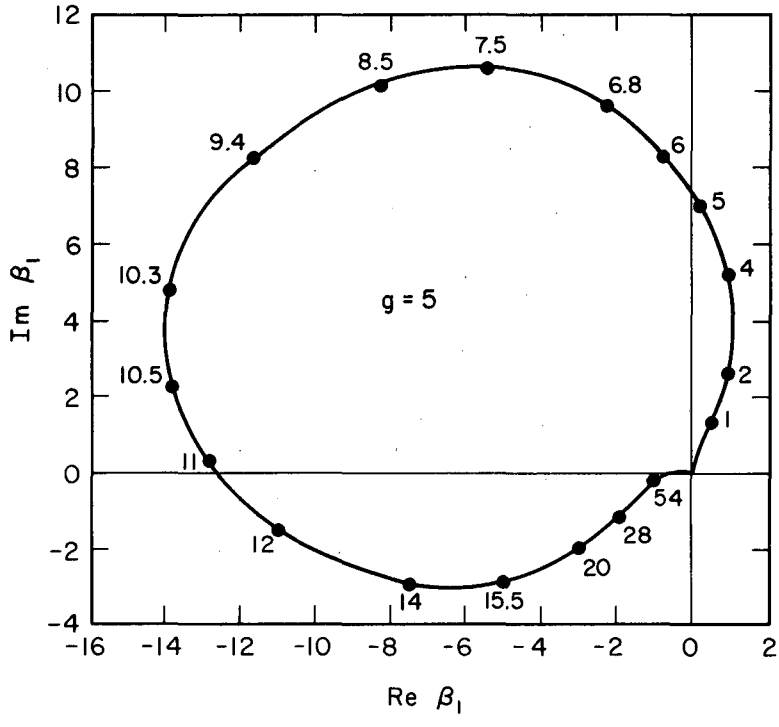
12
10
8
6
4
2
0
-2
-4
-16
-14
-12
-10
-8
-6
-4
-2
0
2
Im β_1
Re β_1
g = 5
7.5
8.5
6.8
9.4
6
5
4
10.3
2
10.5
1
11
54
28
12
20
14
15.5
MU-32713

Fig. 108